Declassified and Approved For Release 2013/02/14 : CIA-RDP10-02196R000100060003-5

Volume 9, No. 3
September, 1961

THE SOVIET JOURNAL OF

ATOMIC ENERGY

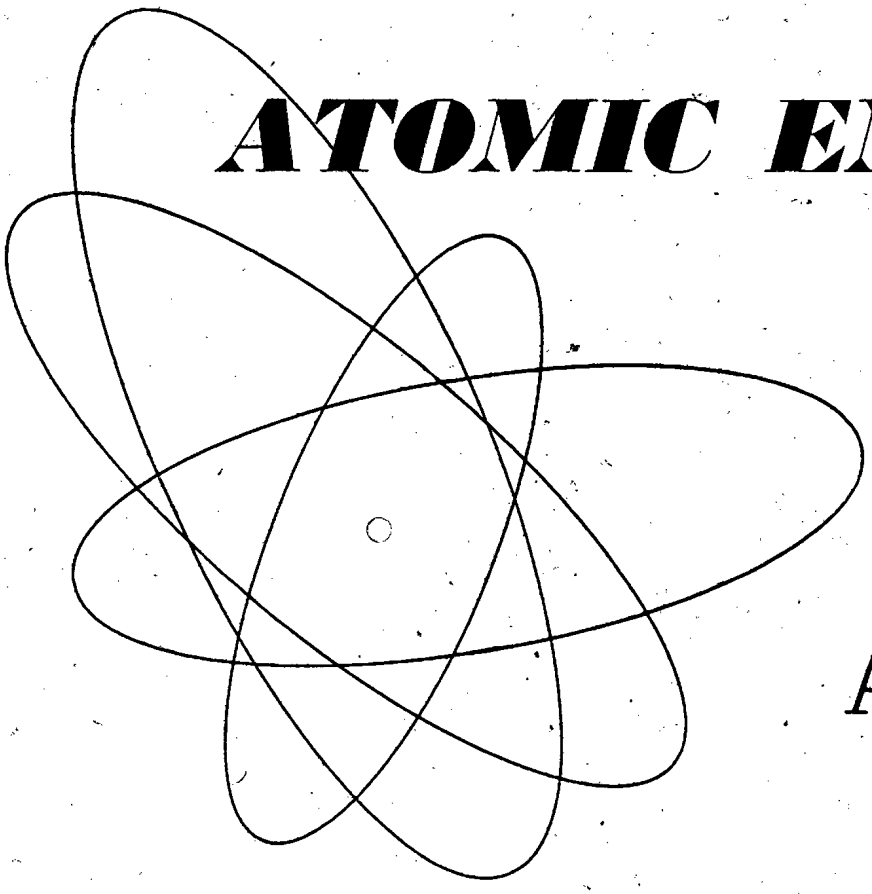

Атомная энергия

TRANSLATED FROM RUSSIAN

CONSULTANTS BUREAU

Declassified and Approved For Release 2013/02/14 : CIA-RDP10-02196R000100060003-5

Declassified and Approved For Release 2013/02/14 : CIA-RDP10-02196R000100060003-5

An important new series published in cooperation with the American Geophysical Union . . .

SOVIET RESEARCH IN GEOPHYSICS

(TRANSACTIONS OF THE GEOPHYSICAL INSTITUTE OF THE USSR ACADEMY OF SCIENCES)

IN ENGLISH TRANSLATION

Volume 1 A COLLECTION OF ARTICLES ON DYNAMIC METEOROLOGY

TRUDY No. 37 edited by I. A. Kibel'

The seven papers presented are the results of original investigations, including a newly proposed theory for the calculation of soil temperature at various depths from a given air temperature; a solution to the problem of the distribution with depth of a steady current in a baroclinic ocean layer; a new method of calculating the advective heat influx, and other reports on recently accumulated data in the field.

cloth 228 pages **$8.00**

Volume 2 ISOSTASY AND ISOSTATIC HYPOTHESES

TRUDY No. 38 by E. N. Lyustikh

The classic theories of Airy, Pratt, Dutton, and others are discussed, criticized, and amplified in the light of new data. The methods of gathering this information, the means of analysis, and the applications of original Soviet research are expounded fully both in the text and on related maps. Present theories related to isostatic rebound, compensation and overcompensation, gravitational anomalies showing concentrations of density, etc., are illustrated with accompanying pertinent data. Designed to produce a clearer and more up-to-date picture of the isostatic status of the earth.

cloth 150 pages **$6.50**

Volume 3 THE MICROSTRUCTURE AND MACROSTRUCTURE OF ELASTIC WAVES IN ONE-DIMENSIONAL CONTINUOUS NONHOMOGENEOUS MEDIA

TRUDY No. 39 by B. N. Ivakin

This book discusses the problems of the structure of waves propagating in continuous nonhomogeneous and generally absorbing media, with a single spatial coordinate, over intervals infinitesimally small or comparable with a wavelength (microstructure) and over intervals larger or appreciably larger than a wavelength (macrostructure). The solutions of the wave problems posed are presented in operator notation, making it possible to study nonsteady-state oscillations, although detailed calculations and graphs are given for steady-state sinusoidal oscillations as well.

cloth 120 pages **$6.00**

Volume 4 INVESTIGATION OF THE MECHANISM OF EARTHQUAKES

TRUDY No. 40 by O. D. Gotsadze

The results of work conducted by the Geophysics Institute of the Academy of Sciences, USSR, since 1948 on the investigation of fault plane displacements are documented in this volume. During this period a method was evolved which makes it possible to determine the mechanical type of fractures at the focus, the dip and strike of the fault plane, and the direction of the displacement and order of the relative intensity of the first shock. Many of the methodological conclusions and results of interpretations are being published for the first time.

cloth 208 pages **$7.50**

CONTENTS UPON REQUEST

You may order on approval from

CONSULTANTS BUREAU

227 West 17th St. • New York 11, N. Y.

Declassified and Approved For Release 2013/02/14 : CIA-RDP10-02196R000100060003-5

Declassified and Approved For Release 2013/02/14 : CIA-RDP10-02196R000100060003-5

EDITORIAL BOARD OF ATOMNAYA ÉNERGIYA
A. I. Alikhanov
A. A. Bochvar
N. A. Dollezhal'
D. V. Efremov
V. S. Emel'yanov
V. S. Fursov
V. F. Kalinin
A. K. Krasin
A. V. Lebedinskii
A. I. Leipunskii
I. I. Novikov
(Editor-in-Chief)
B. V. Semenov
V. I. Veksler
A. P. Vinogradov
N. A. Vlasov
(Assistant Editor)
A. P. Zefirov

THE SOVIET JOURNAL OF

ATOMIC ENERGY

A translation of ATOMNAYA ÉNERGIYA, a publication of the Academy of Sciences of the USSR

(Russian Original dated September, 1960)

Vol. 9, No. 3 September, 1961

CONTENTS

Annual subscription $ 75.00
Single issue 20.00
Single article 12.50

© 1961 Consultants Bureau Enterprises, Inc., 227 West 17th St., New York 11, N. Y.
Note: The sale of photostatic copies of any portion of this copyright translation is expressly prohibited by the copyright owners.

Declassified and Approved For Release 2013/02/14 : CIA-RDP10-02196R000100060003-5

Declassified and Approved For Release 2013/02/14 : CIA-RDP10-02196R000100060003-5

NOTE

The Table of Contents lists all material that appears in Atomnaya Énergiya. Those items that originated in the English language are not included in the translation and are shown enclosed in brackets. Whenever possible, the English-language source containing the omitted reports will be given.

Consultants Bureau Enterprises, Inc.

Declassified and Approved For Release 2013/02/14 : CIA-RDP10-02196R000100060003-5

Declassified and Approved For Release 2013/02/14 : CIA-RDP10-02196R000100060003-5

INSTRUMENTS FOR MEASURING THE PRESSURE, FLOW, AND LEVEL OF FUSED ALKALI METALS

P. L. Krillov, V. D. Kolesnikov, V. A. Kuznetsov, and N. M. Turchin

Translated from Atomnaya Énergiya, Vol. 9, No. 3, pp. 173-181, Sept., 1960
Original article submitted March 22, 1960

The article describes the design, principles of calculation, and operating experience for instruments for measuring the pressure, flow, and level of molten metals. The instruments intended for these purposes are used in reactors with molten metal heat-transfer agents.

Investigations carried out by the authors of the article have shown that the most reliable instruments, simple in design and fairly accurate for practical use, are the double-bellows manometer with an intermediate separating liquid, magnetic flow meter with a permanent magnet, and ultrashort-wave and potentiometric level meters.

In developing methods for using sodium and alloys of sodium with potassium as heat-transfer agents, one of the first problems was to design instruments to measure the pressure, flow, and level of the molten metals. Similar instruments developed for water and gases could not be used because, in the first place, these instruments use materials which are subject to corrosion in these molten metals (brass, tine, etc.) and, in the second place, because of the high melting point of the metal, which requires special devices to heat the detector of the instrument. The purity of the molten metal is very important for the operation of these instruments. The oxides contained in sodium and alloys of sodium with potassium collect in the cold parts of the loop of the instruments; therefore long pipes cannot be used between the place where the pressure is read and the detector. Gas and vacuum pipes, having their open ends over the hot surface of the metal, can be choked by condensed metal.

At the present time there is very little literature on these instruments. The most complete review of them is in a manual on molten metals [1]. In [2] one chapter is devoted to instruments. Most of the methods described in [1, 2] have not found sufficiently wide application in operation with molten metals due to the poor degree of development and the low accuracy or because of the complexity and unreliability of these methods. The present article describes the development and gives results for the operation of some instruments for installations in which molten alkali metals are used.

Manometers

One of the simplest methods of measuring the pressure of a molten metal is to connect an ordinary manometer to a separating tank filled with an inert gas (Fig. 1). The disadvantages of this method are the necessity for checking the level of the metal in the tank and the short life of the device due to the manometric type being choked by condensed metal.

The pressure strain gage described in [2] is too complex for mass production and is not very reliable in operation. The main faults in its operation are the change in properties of the gage wires and the weak fastening of the gages to the membrane.

The "Manometr" factory has designed an induction gage MMS-4 (Fig. 2). A membrane of special steel is pressed between flanges. The bottom flange of the gage is welded directly to the tube of the loop. Due to

Declassified and Approved For Release 2013/02/14 : CIA-RDP10-02196R000100060003-5

Declassified and Approved For Release 2013/02/14 : CIA-RDP10-02196R000100060003-5

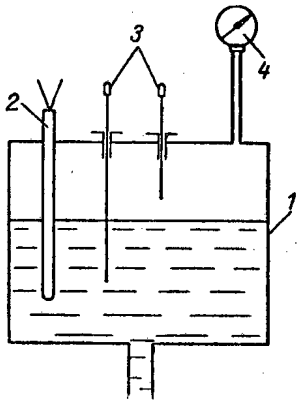

Fig. 1. Diagram of the separating tank for measuring pressure: 1) separating tank; 2) thermocouple; 3) level indicator; 4) manometer.

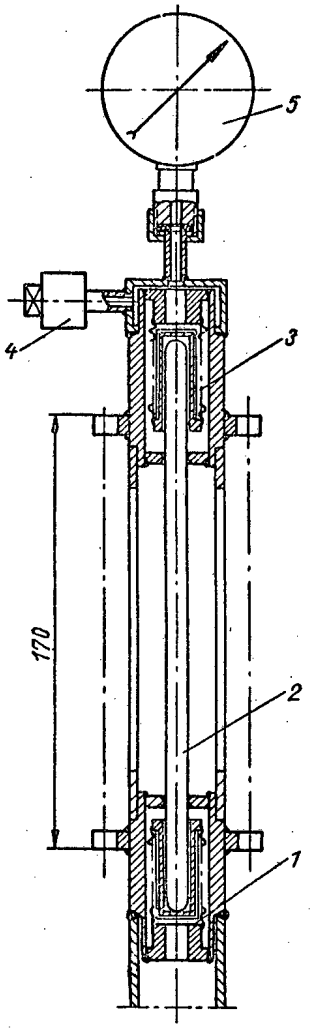

Fig. 3. Double-bellows manometer.

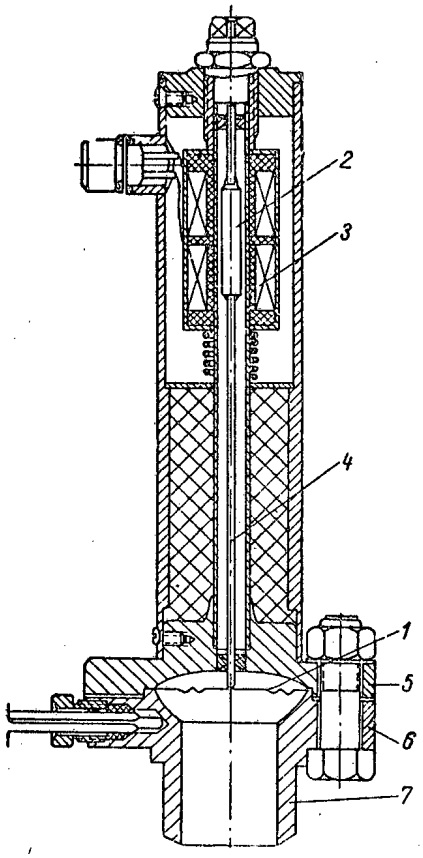

Fig. 2. Membrane type pressure gage with induction coils: 1) membrane; 2) core; 3) induction coil; 4) rod; 5,6) flanges; 7) connecting pipe for welding.

the small distance from the main pipe this instrument does not require special heating. These instruments were used in loops with sodium at temperatures of up to 450°C and pressures up to 10 atm. The weak spot in the instrument is the membrane, which is not protected from overloading and fails due to frequent water hammer in the loop.

The double-bellows manometer (Fig. 3) is fairly simple and reliable for experimental installations. All components of the gage are made of 1Kh18N9T steel. Under the pressure of metal entering the lower chamber 1, the bellows is stretched and moves the rod 2. The movement of the rod is transmitted to the bellows of the upper chamber 3, filled with oil through a connecting pipe 4. Compression of this bellows increases the pressure in the upper chamber, which can be measured by an ordinary manometer 5. The latter should keep its working volume unchanged, since otherwise there would be a large change in the position of the bellows which would introduce errors due to the rigidity of the bellows. The value of this error is directly proportional to the ratio of the bellows rigidity to the area of its transverse cross section.

Declassified and Approved For Release 2013/02/14 : CIA-RDP10-02196R000100060003-5

Declassified and Approved For Release 2013/02/14 : CIA-RDP10-02196R000100060003-5

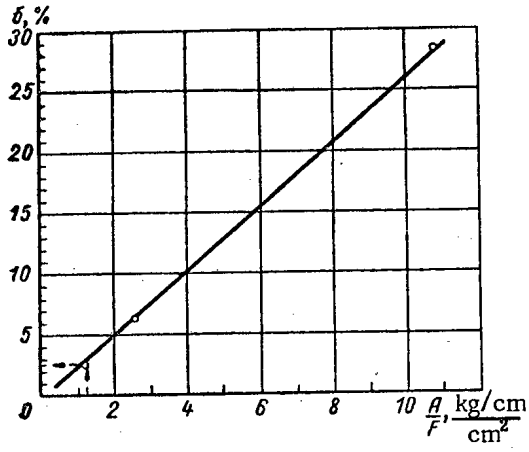

Fig. 4. Change in calibration of the manometer as a function of the ratio of bellows rigidity to the area of its transverse cross section.

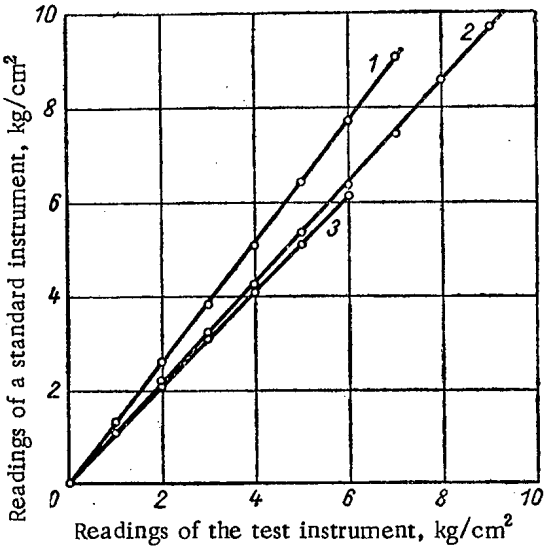

Fig. 5. Calibration of double bellows manometers for different rigidity of the bellows for the following values of A/F (kg/cm³): 1) 10.7; 2) 3.6; 3) 1.25.

Three manometers with bellows of different rigidities and different dimensions were tested in combination with a specimen manometer, class 0.35. From the results of the tests a graph was plotted (Fig. 4) which showed the displacement of the calibration of the instrument δ in percentages for a pressure of 6 atm, depending on the ratio of bellows rigidity to its area of transverse cross section. It can be seen from the graph that with a ratio A/F = 1.25 kg/cm³ the displacement of the calibration is only 2.5%, which means that class 2.5 instruments can be used for technical purposes. When designing these pressure gages special attention should be paid to the temperature error of the instrument. It is mainly due to two factors: in the first place, expansion of the oil in the upper chamber and, in the second place, the different expansion of the rod and coupling bolts. The first component of the temperature error can be calculated from the formula

$$\Delta p_1 = 2A \frac{V\beta\Delta t_1}{F^2}, \qquad (1)$$

where A is the bellows rigidity (kg/cm); V is the volume of the upper chamber (cm³); β is the volumetric coefficient of expansion of oil (1/°C); F is the area of transverse cross section of the bellows (cm²); Δt_1 is the difference in temperatures of the oil during operation of the instrument and during filling of the chamber (°C).

The second component of the temperature error is much less than the first and is calculated from the formula

$$\Delta p_2 = \frac{A\alpha l\Delta t_2}{F}, \qquad (2)$$

where α is the linear coefficient of expansion of the rod (1/°C); l is the length of the rod (cm); Δt_2 is the difference in temperatures of the rod and the connecting bolts (°C).

The calculations and experiments show that it is possible to make a design of this type which gives a 2.5-class gage. Typical calibrations of double-bellows manometers are given in Fig. 5.

Flow Meters

Attempts to use throttle valve flow meters with membrane induction differential manometers to measure the flow of sodium were unsuccessful. The impulse piped of these differential manometers rapidly become choked up with oxide during operation. Rotametric flow meters also failed rapidly due to the pipe with the plunger choking up.

The magnetic flow meter was the simplest and most reliable. The principle of action of this instrument is based on the measurement of the electromotive force which is induced during the movement of a molten metal in a magnetic field. Figure 6 shows the over-all view of this flow meter with a permanent magnet, developed for the main loop of the BR-5 nuclear reactor [3], cooled by liquid sodium.

Declassified and Approved For Release 2013/02/14 : CIA-RDP10-02196R000100060003-5

Declassified and Approved For Release 2013/02/14 : CIA-RDP10-02196R000100060003-5

The electromotive force induced in the flow meter is calculated from the equation

$$E = 0{,}1Bv\,dk_1k_2k_3, \qquad (3)$$

where B is the induction between the poles of the magnet (gauss); v is the average speed of the metal in the pipe (m/sec); d is the pipe diameter (m); k_1 is a coefficient which represents the shunting effect of the walls of the pipe; k_2 is a coefficient representing the limiting dimensions of the magnetic field; k_3 is a coefficient representing the change in induction in the gap due to heating of the magnetic system

$$k_1 = \frac{2\frac{d}{D}}{1+\frac{d^2}{D^2}+\frac{\rho_1}{\rho_w}\left(1-\frac{d^2}{D^2}\right)}; \qquad (4)$$

$$k_3 = \frac{1-\alpha_m(t_m-20)}{1-6{,}95\cdot10^{-6}\frac{b}{a}(t_m-t_b)}. \qquad (5)$$

Where D is the outside diameter of the pipe; d is the inside diameter of the pipe; ρ_1, ρ_w are the specific electrical resistances of the molten metal and the walls of the pipe, respectively; α is the temperature coefficient for the change in induction; t_m, t_b are the temperatures of the poles of the magnet and base, respectively; a, b are the lengths of the gap and armature, respectively.

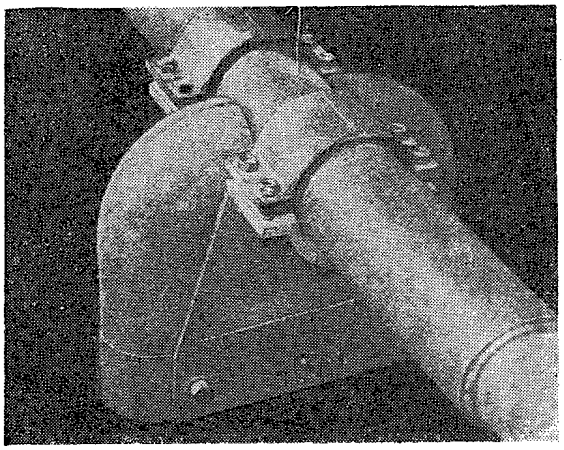

Fig. 6. Magnetic flow meter for up to 200 m^3/hr of sodium.

The stability of the readings of the magnetic flow meter is mainly determined by the quality of the material of the magnet – its ability to retain its properties during a long period of time at high temperature.

We used magnico alloy. Figure 7 shows the temperature dependence of the induction in the gap of a magnet of this alloy from the data of two different investigations. The magnet was placed in a furnace so that the temperature in all of its parts was the same. Under working conditions the distribution of temperature throughout the magnet was uneven. At the poles, which were placed near a pipe containing the molten metals, the temperature of the magnet was higher. Thus, with a temperature of the molten metal of 620°C, the temperature on the surface of the pole facing the pipe was 200-220°C and the temperature of the armature was 80°C. Since the average temperature of the magnet was less than 200°C, the induction changed very little and the coefficient k_3 should be taken equal to unity. This was also confirmed by the calibration of the flow meters (carried out at temperatures of 200 and 450°C) in which no temperature dependence was detected.

Stabilization of operation of the magnets is very important. After assembling and magnetizing they were demagnetized by 5-10% and were heated at 300°C for 24 hr, after which 0.1 kg impacts on the magnet did not cause any noticeable change in induction.

Observations were made on the change in calibration of all three flow meters (working with sodium) for a year with an average sodium temperature of 400°C. The results of the observations showed that during the first seven months the induction in the gap of the magnets decreased by 1% per month and in subsequent months by 0.5% and less.

When the liquid enters the magnetic field near its edges in a plane approximately perpendicular to the field, currents are induced which distort the basic field of the magnet and lead to a reduction in the output signal.

Declassified and Approved For Release 2013/02/14 : CIA-RDP10-02196R000100060003-5

Declassified and Approved For Release 2013/02/14 : CIA-RDP10-02196R000100060003-5

To allow for these edge effects Michel suggested the introduction of a coefficient k_2, depending on the ratio of the length of the pole shoe to the internal diameter of the pipe. Our experiments did not confirm the relationship $k_2 = f(L/d)$; therefore, the influence of edge effects in a magnetic flow meter on its readings requires additional investigation.

In order to determine the effect of inaccuracy in welding the electrodes to the pipe, several pairs of electrodes were welded around its periphery and on its generatrix (Fig. 8). The results of the measurements of the electromotive force between the electrodes are as follows:

Electrodes	Difference in potentials, mv
1 – 1'	32.0
a – a'	34.5
a – 6'	33.5
a' – 6	34.0
6 – 6'	33.5
a' – 7	33.7
6' – 7	33.0
2 – 2'	34.5
3 – 3'	34.0
4 – 4'	33.0
5 – 5'	31.5

As shown by the results of the tests, on a 111 mm diameter pipe a displacement of the electrode by 10 mm in the direction of movement of the metal does not change the readings of the instrument. Moving one of the electrodes along the periphery through 15° reduces the signal by less than 3%.

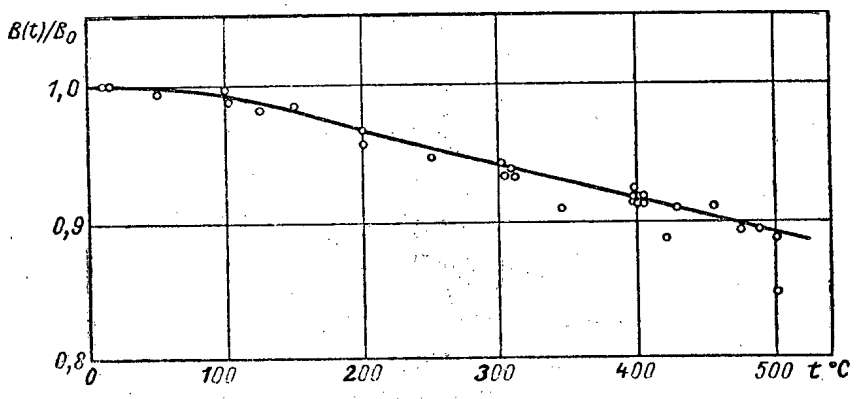

Fig. 7. Temperature dependence of the induction of magnico alloy.

Equation (3) only holds for symmetrical movement of the liquid. Local hydraulic resistances cause a disturbance in the symmetry of the stream and can change the output signal in one direction or another, as shown in [4]. In this work it was also shown that the flow meter should be placed at a distance of not less than 15 diameters of the pipe from the local disturbance of the stream. We have observed that when the flow meter was placed at a distance of seven diameters from a 90° bend of the pipe the signal was reduced by 2.5%.

In the initial period of operation of the magnetic flow meter, the output signal is weak due to the presence of a contact electrical resistance and the absence of wetting on the internal surface of the pipe. With the passage of time and with increase in temperature the contact resistance of the sodium–stainless steel couple decreases and the readings of the flow meter become stable. It can be seen from Fig. 9 that with increase in temperature of the metal for an unchanged flow of heat-transfer agent in it, the readings of the two flow meters change (E_1 and E_2). Therefore, before the start of measurements with the new instruments it is recommended that the section of pipe with metal be heated for 1 hr up to a temperature of 300°C.

Declassified and Approved For Release 2013/02/14 : CIA-RDP10-02196R000100060003-5

Declassified and Approved For Release 2013/02/14 : CIA-RDP10-02196R000100060003-5

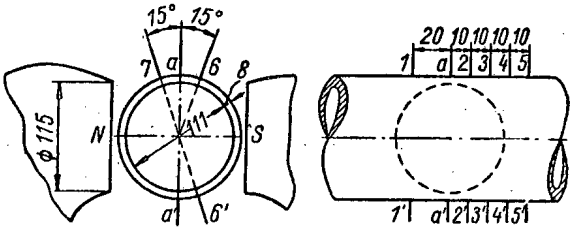

Fig. 8. Diagram showing welding of electrodes to the pipe.

Figure 10 shows calibration characteristics of flow meters designed for a flow Q of 10 and 200 m^3/hr of sodium, constructed for the BR-5 reactor. The calibration of the first flow meter was carried out volumetrically using a measuring tank with electrical contact level indicators. The time for filling the tank was measured with an electrical PV-52 stopwatch. The induction in the gap of the magnet was 1800 gauss; $k_2 = 0.865$; $k_3 = 1$. The flow meter for 200 m^3/hr was calibrated with a Venturi pipe using two differential manometers of a different class of accuracy, connected through separating tanks. The measurements of induction in the gap of the magnet of this flow meter showed its unevenness along the gap (Fig. 11). The calculation of the flow meter was carried out for the average integral induction

$$\overline{B} = \frac{1}{D} \int_{-d/2}^{+d/2} B\, dl.$$

With an average integral induction of 840 gauss its maximum value reached 950 gauss. It follows from Fig. 10 that the calculated characteristics of the flow meters coincide with the experimental characteristics if the values of k_2 and k_3 are taken equal to unity.

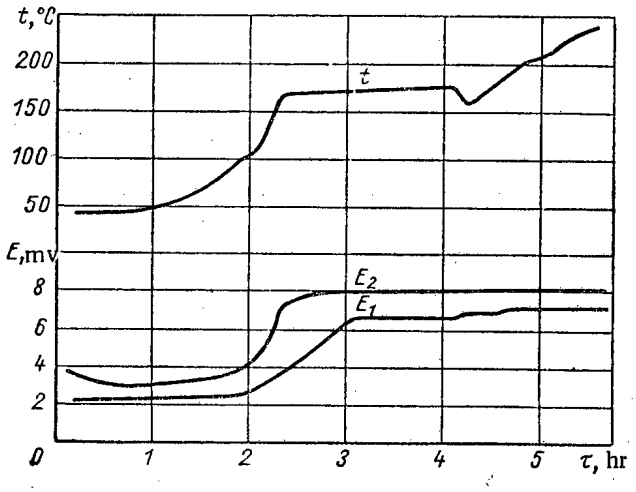

Fig. 9. Changes in the readings of two magnetic flow meters due to the presence of a contact electrical resistance at the internal surface of the pipe.

The calibration of the magnetic flow meter can change due to precipitation of iron and nickel in the pipe between the poles of the magnet. Figure 12 shows a photograph of a pipe of a 27 mm diameter magnetic flow meter after 1000 hr of operation. Accumulations of powder of ferromagnetic materials are clearly visible between the poles of the magnet. A reduction in the cross section led to an increase in the speed of the liquid and increased the output signal by 12.5%.

Operating experience on a large number of magnetic flow meters in loops using sodium and alloys of sodium with potassium showed the high degree of reliability, satisfactory accuracy, and simplicity in servicing of these flow meters. This means that magnetic flow meters can be recommended for use in industrial installations. As secondary instruments for the flow meters, satisfactory results have been obtained for the ordinary laboratory-type potentiometers (PP and PPTN) and also switchboard potentiometers (ĖPV, ĖPP-09, PSR etc.).

Declassified and Approved For Release 2013/02/14 : CIA-RDP10-02196R000100060003-5

Declassified and Approved For Release 2013/02/14 : CIA-RDP10-02196R000100060003-5

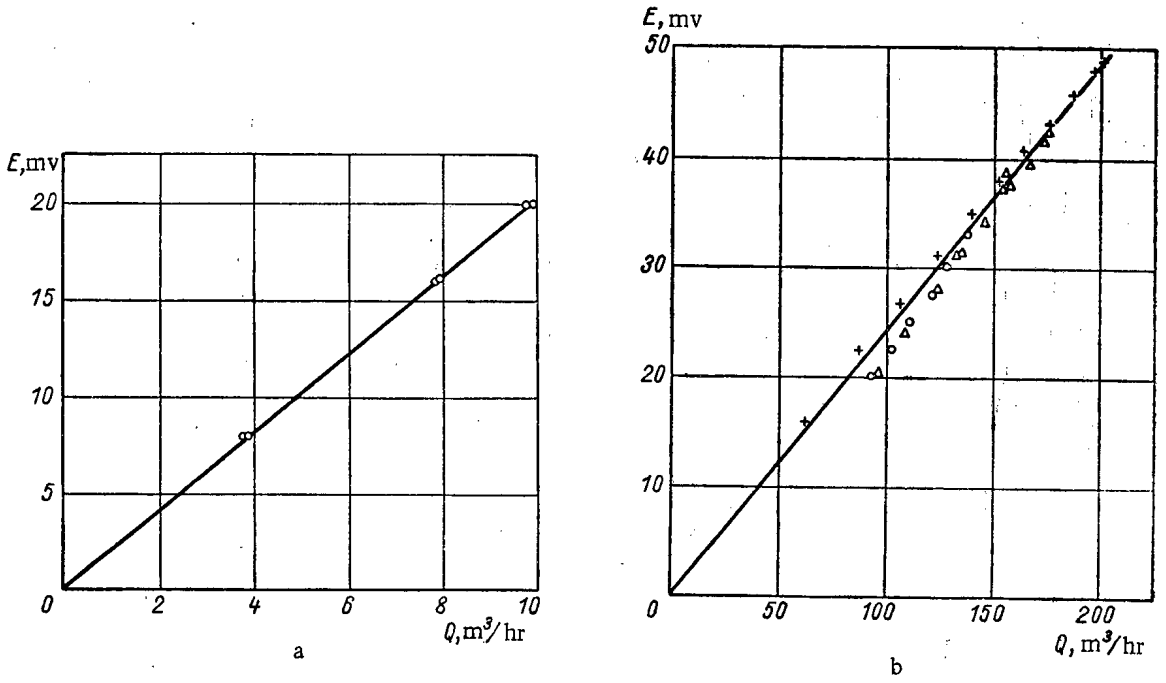

Fig. 10. Calibration of magnetic flow meters. a) Flow of 10 m^3/hr; b) a flow of 200 m^3/hr; o) t = 160°C; +) t = 245°C; △) t = 385°C.

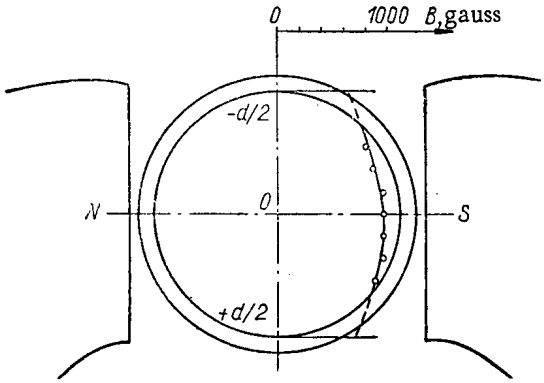

Fig. 11. Distribution of induction in the gap of the magnet.

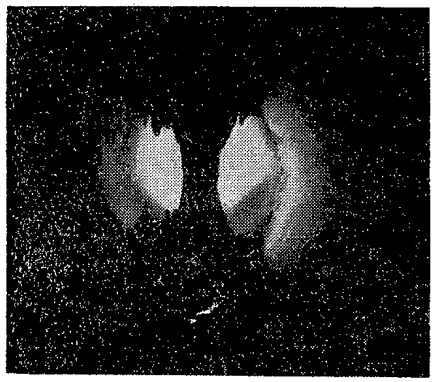

Fig. 12. Deposit of powder of ferromagnetic materials between the poles of the of the magnet in a flow meter.

Level Gages

The simplest level indicator for a molten metal is a bar, insulated from and passing through the cover of the tank containing the molten metal. The bar is sealed in by means of a gland. When the bar contacts the metal surface it closes an electrical circuit and switches on an electrical lamp or ammeter. A serious fault of this type of contact level gage is the short life of the insulator. Vapors of sodium or potassium condense on the surface of the insulator, which is usually at a lower temperature than the metal in the tank, and the level gage gradually fails.

Tests have been carried out on level gages based on the change in resistance of the electrical circuit with change in the level of the metal. Increasing the level of the metal closed a part of the resistance submerged in the tank. By measuring the resistance of the circuit one can determine the level of the metal. The circuit of the instrument is fairly simple. The main fault of this level gage is instability of the readings caused by a

Declassified and Approved For Release 2013/02/14 : CIA-RDP10-02196R000100060003-5

Declassified and Approved For Release 2013/02/14 : CIA-RDP10-02196R000100060003-5

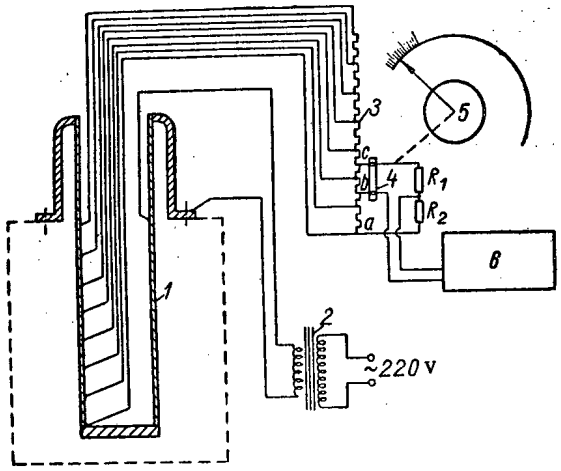

Fig. 13. Circuit of potentiometer level gage.

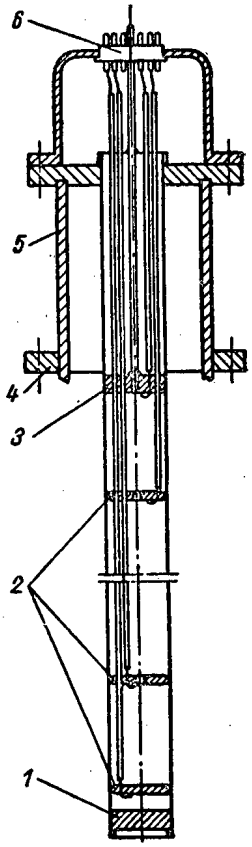

Fig. 14. Design of pick-up for potentiometer level gage.

film of molten metal which remains when the metal is drained. The resistance of the contact depends to a large extent on the contamination by the oxides of sodium or alloy of sodium with potassium. These gages can only operate when using metal freed from oxides.

A radioactive level gage gives a continuous contactless measurement of the level. At the present time Soviet factories are producing the UR-4 instruments covering level changes up to 2 m and diameter of capacity of up to 1.5 m. In this instrument comparisons are made of streams of Co^{60} γ-rays, passing above and below the level of separation of gas and liquid. This level gage can be successfully used in the laboratory and industrial installations. The drawbacks of the instrument are the large measuring columns and the fact that it cannot be used during operation with a radioactive molten metal.

The ultrashort-wave level gage has no moving parts in the detector. Its principle of action is in the reflection of ultrashort electromagnetic waves from the surface of the liquid and the formation of standing waves in a coaxial cable. The detector of the instrument is a continuation of the coaxial cable and is a metal pipe lowered into the molten metal. In the center of the pipe there is an insulated bar. The position of minimum in the standing wave in the cable is measured by the autocompensation method. This instrument can operate for a long time when the temperature of the molten metal does not exceed 200-250°C. At higher temperatures, due to condensation of sodium vapors on the insulator, normal operation of the instrument is disrupted.

If a thin-walled metal tube is lowered into the molten metal and a current is passed through it, the drop in voltage at the section of the tube below the level of the metal will be much less than in the section above the level of metal. A follow-up system can be developed which will automatically determine the place of sharp change in the voltage gradient along the tube. V. D. Kolesnikov suggested a level gage based on this principle and called it a potentiometric level gage. The detector of the level gage (Fig. 13) is a thin-walled tube 1, fed with low-voltage alternating current from a transformer 2. Within the tube of the pickup and uniformly soldered along its length were wires connecting the pickup with a tapped resistor (rheochord) 3 of the secondary instrument. The distribution of potentials on this rheochord will correspond to the distribution of potentials on the measuring tube. The signal is taken by two sliders of a moving carriage 4. The rheochord and two identical resistances R_1 and R_2 form a bridge circuit. With change in level of the molten metal there is a change in the voltage between the points a and b (point b corresponds to the offtake, above the level of the molten metal), which causes an unbalanced signal fed in the corresponding phase at the output of amplifier 6. This makes the servomotor 5 move the carriage 4 along the rheochord 3 in the direction of decrease in unbalance. The detector (Fig. 14)

Declassified and Approved For Release 2013/02/14 : CIA-RDP10-02196R000100060003-5

Declassified and Approved For Release 2013/02/14 : CIA-RDP10-02196R000100060003-5

is in the form of a thin-walled tube of stainless steel 1, inside which discs 2 are soldered at equal distances, and also a bush 3. From the discs and bush, wires are taken out to the plug 6. The upper end of the tube 1 is soldered to the adaptor 5, the height of which is chosen so that the two upper sections of the tube 1 are always above the level of the metal. The level gage is connected to the tank by means of the flange 4. The secondary instrument for the level gage can be any automatic bridge or potentiometer which permits a change in design of the measuring part, consisting of a rheochord, two sliders on a moving carriage, and two constant resistances. The rheochord has 1400 turns of manganin wire in enamel insulation with tappings every 200 turns. The linearity of the instrument scale is ensured by even distances between the sliders and between the tappings from the rheochord.

Tests on the potentiometric level gage were made on a eutectic alloy of sodium and potassium at temperatures of 200, 300, and 450°C. For test purposes a feeler was placed on the flange of the gage under test. During the tests the relationships were obtained between the readings of the level gage and the readings of the inspection feeler with change in the molten metal level. The stability of the readings was checked over a long period of time at a given level. The tests showed that change in temperature over a wide range does not affect the instrument readings. The content of oxygen in the alloy of sodium with potassium reached 0.1 weight%, also having no effect on the characteristics of the instrument. During prolonged operation with molten metal containing a large quantity of oxides floating on the surface, the oxides adhere to the tube of the gage and may cause incorrect readings.

LITERATURE CITED

1. Molten Metal Heat-Transfer Agents, edited by A. E. Sheindlina [Russian translation] (IL, Moscow, 1958).
2. S. S. Kutateladze et al., Molten Metal Heat-Transfer Agents [in Russian] (Atomizdat, Moscow, 1958).
3. A. I. Leipunskii, Proceedings of the Second International Conference on the Peaceful Uses of Atomic Energy, Geneva, 1958 (United Nations, New York, 1960).
4. J. Shercliff, J. Scient. Instrum. 32, 11, 441 (1955).

Declassified and Approved For Release 2013/02/14 : CIA-RDP10-02196R000100060003-5

Declassified and Approved For Release 2013/02/14 : CIA-RDP10-02196R000100060003-5

PULSE METHOD OF MEASURING NEUTRON AGE IN GRAPHITE*

Z. Dlouzy

Institute of Nuclear Problems, Czechoslovakian Academy of Sciences, Prague
Translated from Atomnaya Énergiya, Vol. 9, No. 3, pp. 182-188, Sept., 1960
Original article submitted December 12, 1959

Using a pulse source located within a prism, the age of thermal neutrons from the reactions D–D and D–T in graphite was measured. From the time dependence of the thermal neutron density the author calculated the effective age of D–D neutrons $\tau_{eff} = 355 \pm 9$ cm^2, recalculated for a graphite density equal to 1.6 g/cm^3.

The slowing down of D–T neutrons in graphite can be approximately expressed with the aid of two neutron groups: neutrons suffering but one inelastic collision when slowed down ($\tau_{eff} = 600$ cm^2), and neutrons suffering several inelastic collisions ($\tau_{eff} = 240$ cm^2). In determining the age τ the relative contributions of both groups were assumed equal to 0.65 and 0.25, respectively. A third group is composed of neutrons slowed down only by means of elastic collisions. These neutrons may be neglected in the first approximation, since their contribution is small (about 0.1), while the increase is large.

Introduction

The mean-square distance of neutrons from the source in the slowing-down process plays an important role in the analysis and construction of nuclear reactors. Since the spatial distribution of retarded neutrons is determined by their symbolic age, measurements of the age and diffusion coefficient D would be of significant value.

In the design of reactors for measuring neutron age it is necessary in most instances to make use of a constant source, which is emitting fission neutrons, while the spatial distribution of the retarded neutrons must be determined by means of resonance detectors (e.g., an indium detector having resonance at an energy of 1.44 ev). In the analysis of a reactor with thermal neutrons it appears possible to obtain better results by making use of the value of the age up to thermal energy. The age before thermal energy is clearly determined by measuring the area of migration and calculating from this the square of the diffusion length. It can be measured if we make an appreciable reduction in the effect of diffusion by "poisoning" the medium with an absorbing substance. Such a complex method introduces a certain indeterminateness into the measurement.

It should be borne in mind that the mean lifetime of neutrons in a uranium-graphite reactor (about 1000 μsec) is not very great in comparison with the time required to slow them down and to establish an equilibrium thermal velocity spectrum. A direct determination of the dependence of symbolic age on time is possible by the method of a pulse source. The advantage of this method lies in the fact that it permits us to obtain detailed information concerning the behavior of the neutrons during the interval starting with slowing down and up to the point of steady-state thermal diffusion. Consequently, it becomes possible to observe the gradual transition of thermal neutrons from retardation diffusion during a time interval of significant duration. The intent of the present paper is thus to measure the values of the age and diffusion coefficient in a retarder by means of a pulse neutron source placed in a prism [1]. The experiment was set up so provide for maximum approach to the ideal case of a point source of manoenergetic neutrons in a medium extending infinitely in one direction.

* This work was carried out at the P. N. Lebedev Physics Institute of the Academy of Sciences of the USSR.

Declassified and Approved For Release 2013/02/14 : CIA-RDP10-02196R000100060003-5

Declassified and Approved For Release 2013/02/14 : CIA-RDP10-02196R000100060003-5

Theory

In measuring the age of neutrons obtained from a pulse source, two methods can be used. One method is described in [2], where the age of neutrons in water is determined from the dependence of the initial thermal neutron density on a geometric factor characteristic of the retarder. The dimensions of the retarder were chosen such that after sufficiently large times only the first harmonic of the neutron density distribution function would be significant. The advantage of this method lies in the fact that it requires the application of comparatively small amounts of retarding substance. It cannot, however, give precise information on the diffusion of neutrons in the initial instants of time, since the presence of higher harmonics cloud the diffusion picture. Therefore, as in the constant source method, this method makes it difficult to obtain information on the transition of slowing down to the thermal diffusion process. Another method, which was used in [1], stipulates the application of an infinitely long prism for the purpose of measurement. In the center of the prism is brought about a burst of fast monoenergetic neutrons, which then are slowed down and diffuse inside the prism. This method was applied in our measurements.

The prism was a rectangular parallelepiped with cross section b_0c_0. In order to ensure an infinite system (along the x axis), it was necessary to make use of a prism whose length a_0 was at least four to six times greater than the diffusion length L.

Applying the Fermi age theory, it is not too difficult to obtain the following expression for the density of slow neutrons n(x, y, z, t) created by the pulsed point source of fast monoenergetic neutrons:

$$n(x, y, z, t) = \text{const}\ \frac{1}{\sqrt{\tau(t)}}\, e^{-\frac{x^2}{4\tau(t)}}\ \Phi(y, z, t)\, e^{-\frac{t}{T_c}}, \tag{1}$$

where T_c is the mean lifetime of the neutrons in the retarder as determined by absorption; $\tau(t)$ is the so-called general neutron age.

The factor $\Phi(y, z, t)$ does not depend on the coordinate x. After measuring the neutron density at the points (x_1, y, z) and (x_2, y, z) for a specified time t, we obtain the expression in [1] from Eq. (1) for the generalized age:

$$\tau(t) = \frac{x_2^2 - x_1^2}{4 \ln \frac{n(x_1, y, z, t)}{n(x_2, y, z, t)}}. \tag{2}$$

In the derivation of Eq. (2) no restrictions had to be imposed on the time. This expression remains valid for any time, the only condition being applicability of the age equation.

The generalized age can be written in the form

$$\tau(t) = \int_0^t D(t)\, dt. \tag{3}$$

If the neutrons enter into thermal equilibrium with the medium, the diffusion coefficient D(t) must arrive at a constant value D_T, and for large times the age may be written in the form

$$\tau(t) = \tau_{\text{eff}} + D_\tau t.$$

Consequently, the dependence of generalized age on time for large times becomes linear. Extrapolation of this line to t = 0 gives the effective value of the age. Application of the effective age makes it possible to utilize an ordinary approximation scheme, in which the slowing-down process is assumed instantaneous, and the diffusion coefficient is equal to D_T and does not depend on time.

Declassified and Approved For Release 2013/02/14 : CIA-RDP10-02196R000100060003-5

Declassified and Approved For Release 2013/02/14 : CIA-RDP10-02196R000100060003-5

Description of the Apparatus

To measure the age and diffusion coefficient, a graphite prism was made up with the dimensions 330 × × 120 × 70 cm (Fig. 1). The mean density of the graphite was 1.67 g/cm^3.

The prism was placed in the center of the room; its axis was oriented horizontally. The distance from the surface of the prism to the walls was greater than 180 cm, that from the floor was 100 cm. The prism was set on metal and wood supports and was covered over with a layer of cadmium sheeting with a thickness of 1 mm, for the purpose of eliminating any influence of thermal neutrons scattered outside the prism.

In the center of the prism was a neutron source, a zirconium–tritium or zirconium–deuterium target, on which was aimed a deuteron beam. The deuterons were accelerated in a high-voltage ion tube at the Physics Institute of the Academy of Sciences of the USSR with a constant voltage of 240 kv. In order to get the neutron source inside the prism, a vertical canal 40 cm long was made in the graphite, and into this was snugly fitted the brass tube of the target (diameter 2.8 cm, wall thickness 0.8 mm). The target was situated between two fluoroplast rings.

To obtain a modulated beam, a pulse voltage of 0.8-1.2 kv, 5 μsec in duration, and with a repetition rate of 62-625 cps, was applied to the anode of a Penning-type ion source. The duration of the deuteron current into the target within the pulse amounted to about 8 μsec.

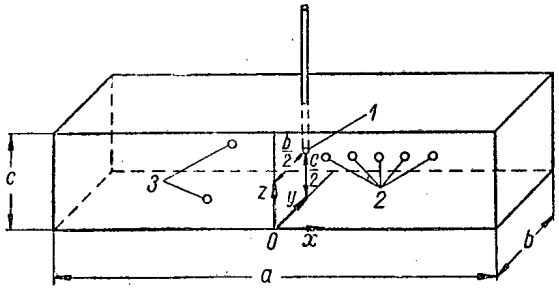

Fig. 1. Geometry of the graphite prism: 1) neutron source (target of the accelerator tube); 2) position of counter used to measure thermal neutron density; 3) monitors.

The deuteron beam was deflected in its path in a magnetic field, making possible the application of a pure beam of atomic ions for the reaction on the target. Here the mean ion current on a 10 mm target was 1.5 μa. Since the mean current on the target was weak, water cooling was not necessary (the presence of water would introduce an additional error into the measurements), which permitted the small target dimensions to be retained. The neutron yield was measured by means of two boron counters (monitors) placed in the graphite and a single proportional counter, which recorded α particles from the D–T reaction.

In order to ensure good resolution and not to greatly disrupt the homogeneity of the irradiated medium, a special small-scale boron proportional counter with a diameter of 10 mm and length of 100 mm, contained in an aluminum tube, was used. After introduction of the counter into the graphite prism the density of one of the graphite bricks was reduced by 0.8%. The distances from the target at which the neutron density was measured were equal to 15, 35, 55, 75, and 95 cm. The counter was introduced into the horizontal canals so that its axis would be perpendicular to the direction toward the source. The canals in which a neutron counter was not placed were filled with graphite rods. The indeterminateness in position of the counter in the x and z coordinates was less than 0.1 cm, in the y coordinate it was about ± 0.2 cm.

The pulses from the counter were amplified by wideband amplifiers and were transmitted to a 100 channel time analyzer developed by I. V. Shtranikh and L. A. Matalin-Slutskii, having a regulatable wide channel (1-80 μsec), where they time-analyzed delays relative to the neutron burst. The principal circuit of this arrangement is similar to the one described in [1]. From a quartz supply generator pulses were delivered to a divider, then to the pulse-forming circuit. From here the identical pulses were sent out through two cathode followers for regulating the neutron burst and triggering the analyzer.

Results of the Measurements

The age of D–D neutrons before thermal energy was calculated from Eq. (2). To do this, the dependence of the thermal neutron density on time was calculated at equal distances from the fast neutron source. Since the thermal neutron density is expressed by Eq. (1), the form of the curves depends on time and distance from the source.

Declassified and Approved For Release 2013/02/14 : CIA-RDP10-02196R000100060003-5

Declassified and Approved For Release 2013/02/14 : CIA-RDP10-02196R000100060003-5

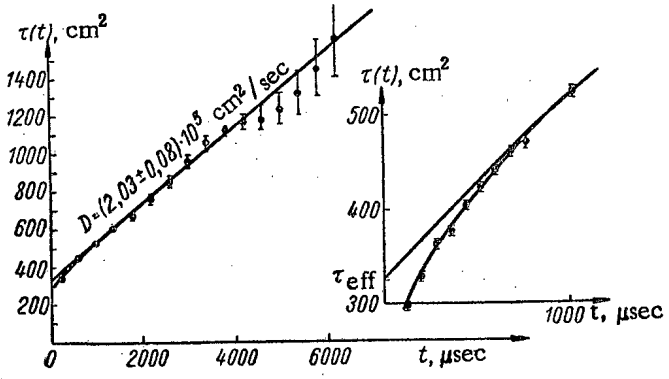

Fig. 2. Time dependence of the age of D–D neutrons. The curve is seen to drop below the extrapolated straight line due to an increase in diffusion coefficient D(t) for small times. The age was measured at distances of 15, 35, and 55 cm from the sources.

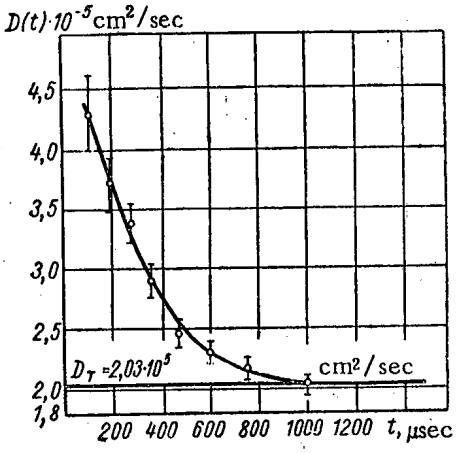

Fig. 3. Time dependence of the diffusion coefficient. $D^2(t)$ approaches D_T^2 exponentially with a relaxation time of $t_s = 195 \pm 35$ μsec.

The time dependence of the age, calculated according to Eq. (2) from the experimental data, is shown in Fig. 2. The initial part of the curve $\tau(t)$ is shown separately on a larger scale on the right side in Fig. 2. From the figure it is evident that the curve $\tau(t)$ at first makes a steep ascent, then asymptotically approaches a straight line. From the equation $D = d\tau/dt$ it follows that the diffusion coefficient falls off with time, approaching a constant value. This constant value is attained after approximately t = = 1000 μsec, where $D_T = (2.03 + 0.08) \cdot 10^5$ cm$^2 \cdot$ sec^{-1} (the time dependence of the diffusion coefficient is shown in Fig. 3). Recalculating it for graphite with a density of 1.6 g/cm^3, we obtain $D_T = (2.12 + 0.08) \cdot 10^5$ cm$^2 \cdot$ sec^{-1}.

It is impossible to determine the diffusion coefficient from the curve of Fig. 2 with any great accuracy because the statistical error, which is small for small times, increases very rapidly, and for 4 msec even it attains 5-10%. Our results may therefore be assumed satisfactory.

Extrapolation of the age curves to t = 0 gives a value of $\tau_{eff} = 325 \pm 8$ cm^2, which corresponds to a value $\tau_{eff} = 355 \pm 9$ cm^2 with a graphite density of 1.6 g/cm^3. Measurement of the age of D–T neutrons is a more complex process than for D–D neutrons. For small times the age curves (Fig. 4), calculated according to Eq. (2) from measurements at various point pairs situated at nonidentical distances from the source, do not coincide with one another. It is therefore not possible to describe uniquely the process of slowing down by means of age alone. A more detailed analysis of the slowing down of D–T neutrons is given below.

Discussion of the Results of Measurements with D–D Neutrons

The processes of retardation and diffusion of neutrons may be conditionally separated into three intervals.

In the first interval corresponding to comparatively high neutron energies (i.e., to small slowing-down times), slowing down occurs in the free nuclei. The mean logarithmic energy decrement for one collision does not depend on the energy. In this energy interval and for retarders of not very low atomic weight, the age of monoenergetic neutrons with an initial energy E_0 which are slowed down to an energy E is determined by the expression

$$\tau(E) = \int_E^{E_0} \frac{\lambda_s(E)}{3\xi(1-\overline{\cos\theta})} \frac{dE}{E}, \qquad (4)$$

Declassified and Approved For Release 2013/02/14 : CIA-RDP10-02196R000100060003-5

Declassified and Approved For Release 2013/02/14 : CIA-RDP10-02196R000100060003-5

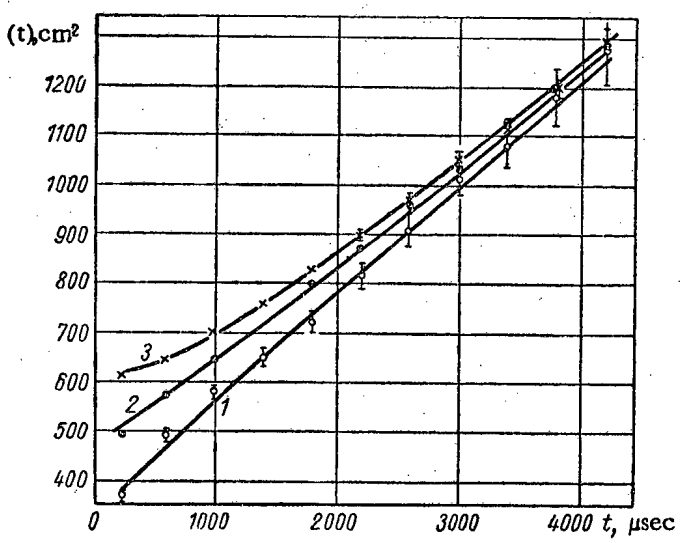

Fig. 4. Time dependence of the age of D–T neutrons. Φ represents the results of measurements at distances of 15 and 35 cm from the source, standing in good agreement with curve 1, which was calculated for these distances taking into account the two groups of neutrons with ages τ_1 and τ_2; • represents points and the analytic curve 2 for distances of 15 and 95 cm; × for the points and analytic curve 3 for distances of 75 and 95 cm.

where λ_S is the mean free path, $\overline{\cos\theta}$ is the mean cosine of the scattering angle in the laboratory system.

However, when the neutron temperature attains a value near the binding energy of the atoms in the crystalline lattice of the retarder (about $5kT_0$), it may be assumed that the neutrons have passed over into another interval. It is difficult to determine theoretically the influence of the binding energy of the atoms in the crystalline lattice of the retarder; but, if we remember that slowing down these atoms proceeds more slowly than the slowing down of free atoms, the assumption may be made that in reality the age of the neutrons exceeds the expected value [according to Eq. (4)], and pure diffusion of thermal neutrons sets in quite a bit later.

If we characterize the mean energy of neutrons not fully slowed down by the temperature T, then it may be assumed [3] that $dT/dt = -\gamma(T - T_0)$, i.e., the rate of decay in temperature is proportional to the difference between T and the temperature of the medium T_0. In this case the excess in temperature of the neutrons over and above the temperature of the medium falls off exponentially as $e^{-\gamma t}$. Here the diffusion coefficient tends to D_T, and the dependence of age on time becomes linear (third interval). The beginning of the curve in Fig. 2 yields the possibility of determining the coefficient γ (see Fig. 3), since the square of the diffusion coefficient is proportional to the instantaneous temperature of the neutrons (on the assumption that in the region from 1 ev to thermal energies λ_{tr} = const). From the experimental data it follows that the temperature of the neutrons T(t) approaches its equilibrium value exponentially with a relaxation time $t_s = 1/\gamma = 195 \pm 35$ μsec. This result agrees with the measurements made in [4, 5], where the process of the approach of the neutron temperature to the equilibrium state was studied by passing neutrons through a silver filter.

In comparing our results with the experimental results obtained by the constant source method, the following must be kept in mind. Data on the age of neutrons with an energy exceeding 0.1 ev, when this data is gathered by means of various resonance detectors, must obey the dependence (4) which, if we represent it on the time scale, will agree with the onset of the curve obtained. But in determining the age of neutrons before thermal energy is reached, the result of measuring [6] the migration area and afterward calculating the square of the diffusion length turned out otherwise. The age thus measured is equal to the value that is obtained on linear extrapolation of the corresponding part of the experimental curve for $\tau(t)$ to zero time. In this way we determine τ_{eff}, the true value of which for small times, obtained, for example, by measurements with resonance detectors, lies below the extrapolated straight line.

Declassified and Approved For Release 2013/02/14 : CIA-RDP10-02196R000100060003-5

Declassified and Approved For Release 2013/02/14 : CIA-RDP10-02196R000100060003-5

Consequently, τ_{eff} as found by measurement of the migration area, ought to be compared with the quantity τ_{eff} as determined by the pulse method. It must be remembered, however, that extrapolation of τ to t = 0 becomes unique only for the linear part of the time dependence of the age, i.e., for t > 1000 μsec, when the diffusion coefficient is constant. Actually, in reactor physics a much smaller time plays the essential role, so that the concept of τ_{eff}, strictly speaking, is not fully defined. Only measurements by the pulse method give us the opportunity to follow the variation in true value of the age with time.

Measurement of the Age of D–T Neutrons

The value of the age of D–T neutrons we tried to calculate in the same manner as for the D–D neutrons. It was noted above that for small times, calculation according to Eq. (2) does not yield a definite value for the age, in that the age curves are obtained differently depending on the distance from source at which the thermal neutron density is measured. This is understandable, for the source of D–T neutrons emits 14.1 Mev neutrons which can lose their energy not only as the result of elastic collisions, but of inelastic as well.

As we know, in slowing down 14.1 Mev neutrons in graphite three different processes can occur: 1) elastic scattering C_6^{12} (n, n')C_6^{12}; 2) inelastic scattering C_6^{12} (n, n')C_6^{12*}, $C_6^{12*} \rightarrow C_6^{12} + \gamma$; 3) inelastic scattering C_6^{12}(n, n') 3α. Both of the inelastic scattering processes strongly influence the magnitude of the age and complicate the slowing-down process. The threshold of the process 2) lies in the energy region of 4.41 Mev [7], for the process 3) in the region of 7.7 Mev.

If we take into account the fact that in the slowing-down process not all of the neutrons undergo the same number of inelastic processes, and the energy losses in the inelastic process 3) so far exceed the energy loss in the inelastic process 2), then it becomes clear that for the exact description of the slowing-down of D–T neutrons it is not possible to use only one age, rather it is necessary to consider at least two groups of neutrons, assigning different ages to these.

In this case the density of thermal neutrons from the D–T source must obey the relation

$$n(x, y, z, t) = \text{const}\, e^{-\frac{t}{T_c}} \left[\frac{a_1}{\sqrt{\tau_1}} e^{-\frac{x^2}{4\tau_1}} \Phi_{\tau_1}(y, z, t) + \frac{a_2}{\sqrt{\tau_2}} e^{-\frac{x^2}{4\tau_2}} \Phi_{\tau_2}(y, z, t) \right], \quad (5)$$

where $\Phi_{\tau_i}(y, z, t)$ are terms which do not depend on the coordinate $\underline{x}$. It is evident that from Eq. (5) it is impossible to obtain an expression similar to (3) for determining the age. It may be assumed that the age τ_1 determines the behavior of neutrons suffering but one inelastic collision in the course of slowing-down; then the lower age τ_2 should, on the average, characterize the behavior of all the remaining singly inelastically scattered neutrons. It is troublesome to segregate exactly into two such groups, but it is clear that at small distances from the source the distribution of thermal neutrons in the initial period of time (up to 1000 μsec) must be determined primarily by the age τ_2, while at very large distances the age τ_1 plays the greater role. This permits us to find approximate values for τ_1 and τ_2.

However, for a more precise determination of the ages τ_1 and τ_2 it is necessary to know the contribution of the corresponding terms in (5), i.e., the ratio $a_1\Phi\tau_1(y,z)t / a_2\Phi\tau_2(y,z)t$. Since the terms $\Phi\tau_1(y,z,t)$ may be assumed proportional to $e^{-\omega^2\tau i}$, where $\omega^2 = \pi^2 (1/b^2 + 1/c^2)$ (we take only the first term of the sum of harmonics describing decay in the $\underline{y}$ and $\underline{z}$ directions), the main problem consists in determining a^1/a^2 ($b = b_0 + 2 \cdot 0.71 \lambda_{tr}$; $c = c_0 + 2 \cdot 0.71 \lambda_{tr}$). We tried to determine the ratio a_1/a_2 from the dependence of the effective scattering cross sections of the processes 1), 2), 3) on the energy [8]. Since the dependence of these cross sections on energy and the inelastic scattering spectrum of the neutrons were not measured with sufficient accuracy, the ratio a_1/a_2 can be determined with a relatively high error. If we make use of the approximate value $a_1/a_2 = 0.65/0.25$ thus obtained, comparison of Eq. (5) and the measured age curves provides the opportunity for approximately evaluating the value of the ages τ_1 and τ_2. The values $\tau_{1eff} = 600$ cm^2 and $\tau_{2eff} = 240$ cm^2 thus found can only be treated as empirical constants. Qualitatively they correspond to the energies of the groups of inelastically scattered neutrons that should appear upon scattering of 14.1 Mev neutrons in graphite [9, 10].

Declassified and Approved For Release 2013/02/14 : CIA-RDP10-02196R000100060003-5

Declassified and Approved For Release 2013/02/14 : CIA-RDP10-02196R000100060003-5

A more precise examination shows that, in addition to the two groups of neutrons with ages τ_1 and τ_2, another, third, term should be used in (5), this term describing a group of neutrons with age τ_3. This group should determine the behavior of those neutrons which are slowed down only by elastic collisions. The age of these neutrons is very great ($\tau_3 \simeq 900$ cm^2) and they are of no great significance, since their contribution comes to only about 10%, and because of the large value of τ_3 the quantity $\Phi\tau_3(y, z, t)$ is small. Therefore, it seemed to us nearly sufficient to express the behavior of the neutrons in graphite from a D–T source by two ages.

In conclusion, the author expresses his gratitude to Corresponding Member of the Acad. of Sci. of the USSR I. M. Frank for suggesting the research topic, for his steadfast interest in the work, and for valuable remarks during the course of discussion.

LITERATURE CITED

1. I. M. Frank, Report of the FIAN SSSR [in Russian] (1955); Antonov et al., Proceedings of the First International Conference on the Peaceful Uses of Atomic Energy, Geneva, 1955 (United Nations, New York, 1956).
2. Romanna et al., Proceedings of the First International Conference on the Peaceful Uses of Atomic Energy, Geneva, 1955 (United Nations, New York, 1956).
3. G. Dardel, Trans. Roy. Inst. Technol. No. 75 (1954).
4. A. V. Antonov et al., Physics and Heat Technology of Reactors, supplement No. 1 to the journal Atomnaya énergiya [English translation] (Consultants Bureau, New York, 1959).
5. K. Beckurts, Nucl. Sci. and Eng. , No. 4 (1957).
6. Daggal and Martelli, Proceedings of the First International Conference on the Peaceful Uses of Atomic Energy, Geneva, 1955 (United Nations, New York, 1956).
7. J. Anderson et al., Phys. Rev. 111, 572 (1958).
8. M. McGregor and R. Booth, Phys. Rev. 112, 486 (1958).
9. B. Whitemore, Phys. Rev. 92, 654 (1953).
10. E. Graves and L. Rosen, Phys. Rev. 89, 343 (1953).

Declassified and Approved For Release 2013/02/14 : CIA-RDP10-02196R000100060003-5

Declassified and Approved For Release 2013/02/14 : CIA-RDP10-02196R000100060003-5

HIGH-FREQUENCY STORAGE OF A BEAM IN CYCLICAL ACCELERATORS*

A. N. Lebedev

Translated from Atomnaya Énergiya, Vol. 9, No. 3, pp. 189-193, Sept., 1960
Original article submitted February 10, 1960

In the theory of high-frequency storage of a beam in accelerators with a constant magnetic field, it is important to take into account the disturbances of the already stored beam by successive cycles of acceleration. Such a disturbance leads, on the whole, to an increase in the energy spread of the stored particles and to a change of their mean energy. The general formulation of the problem and its solution for some special cases are presented in this article.

1. Equations of Motion

The change in energy of the particles is conveniently considered in the dimensionless variables

$$z=\frac{2\pi Q}{eV}\int_{E_0}^{E}\frac{dE}{\Omega(E)};\ \varphi;\ Q=\left|\frac{q\cdot\Omega_0\Omega_0' eV}{2\pi}\right|^{1/2}, \tag{1.1}$$

where Ω (E) is the frequency of revolution of the particles of energy E; $\Omega' = d\Omega/dE$; q is the multiplicity; and V is the amplitude of the accelerating voltage. The subscript 0 refers to quantities corresponding to the storage energy. We denote by φ the phase of the accelerating field of frequency $\omega(t)$ in which the particle is traveling:

$$\varphi = q\Omega - \omega(t). \tag{1.2}$$

We assume that the energy of the particles in the stored beam differs little from the storage energy E_0, i.e., it is possible to make the linearization

$$\Omega(E)=\Omega_0+\frac{\Omega_0' eV\Omega_0}{2\pi Q}z. \tag{1.3}$$

Later on it will be seen that this assumption holds for the great majority of particles. Furthermore, in the neighborhood of the storage energy, let the frequency of the accelerating field change in accordance with a linear law, increasing or decreasing with time.

Under the assumptions that have been made, the equations of motion have the simple form [1]

$$\begin{gathered}\dot{z}=\cos\varphi=-\frac{\partial H}{\partial\varphi};\ H=-\sin\varphi+\frac{\Omega_0'}{|\Omega_0'|}\frac{z^2}{2}-\tau z\cos\varphi_s;\\ \dot{\varphi}=\frac{\Omega_0'}{|\Omega_0'|}z-\tau\cos\varphi_s=\frac{\partial H}{\partial z};\ \cos\varphi_s=\frac{d\omega}{dt}\left(\frac{2\pi}{q\Omega_0\Omega_0' eV}\right).\end{gathered} \tag{1.4}$$

* This work was performed in 1958.

Declassified and Approved For Release 2013/02/14 : CIA-RDP10-02196R000100060003-5

Declassified and Approved For Release 2013/02/14 : CIA-RDP10-02196R000100060003-5

Here and in what follows we shall use as the independent variable the dimensionless time

$$\tau = Qt. \tag{1.5}$$

The beginning of the time scale is chosen is such a way that $\omega(0) = q\Omega_0$.

It is seen from expressions (1.4) that the variables z and φ are canonically conjugate variables, which permit us at once to draw some general conclusions on the behavior of the beam on the basis of Liouville's theorem [1, 2]. In fact, as long as the frequency depends linearly on the time, there will exist on the phase cylinder (z, φ) a region of closed phase trajectories (for $|\cos\varphi_s| < 1$) traveling with a velocity equal to $\cos\varphi_s$. We denote the area of this stable region by S and assume that it is filled with accelerated particles of mean density ρ. At the end of each storage cycle, the frequency rapidly returns to its initial value, so that the particles remain close to the storage energy. According to Liouville's theorem, the mean density of the stored beam in phase space cannot be greater than ρ, and therefore we obtain for its energy width the estimate

$$\delta_n z \geqslant \frac{Sn}{2\pi}, \tag{1.6}$$

where n is the number of cycles of storage. Inequality (1.6) goes over into an equality only if the entire phase space in the storage energy region is uniformly filled with particles of density ρ, or, as we shall express it, only for a "dense arrangement" of the separatrices. A deviation from the equality is considered in the following sections.

In what follows, we shall need the equation of the phase trajectories. From Eqs. (1.4) it follows that in the canonical variables $y = \Omega_0'/|\Omega_0'|\, z - \tau\cos\varphi_s$ and φ we have

$$y^2 - 2(\sin\varphi - \varphi\cos\varphi_s) = \text{const}. \tag{1.7}$$

2. Change in the Energy of Particles in One Storage Cycle

After one cycle of storage, all particles experience displacements of the z coordinates, where the value of the displacement Δ depends on the final coordinate z_f and on the phase ψ at which the particle should pass the separatrix (at $y = 0$). At the point ψ the condition $q\Omega(z) = \omega(\tau)$ is fulfilled, after which the sign of $\dot{\varphi}$ reverses, since $\dot{\varphi}(\psi) = 0$.* It is readily noted that the quantity ψ cannot take on any values in the interval $0-2\pi$. This is demonstrated in the figure, where the rising separatrix and phase trajectories in the unstable region are shown schematically. The region of values which can be taken on by ψ is shown shaded, and is bounded on one side by the quantity $2\pi - \varphi_s$, and on the other by the point φ_1 determined from the equation

$$\sin\varphi_1 - \varphi_1\cos\varphi_s = -\sin\varphi_s + \varphi_s\cos\varphi_s. \tag{2.1}$$

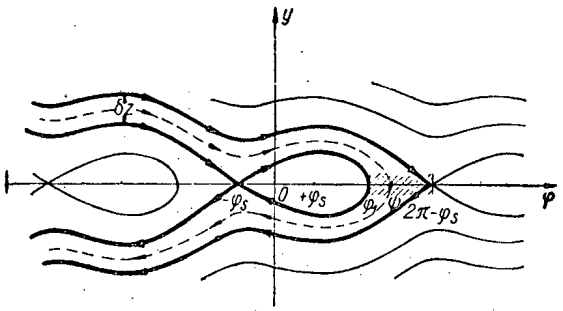

Phase trajectories of stored-beam particles.

Using Eq. (1.7) we express the displacement of the coordinate Δ as a function of the final phase φ_f and ψ:

$$\Delta = \int_{\varphi_i}^{\varphi_f} \frac{2^{-1/2}\cos\xi\, d\xi}{[\sin\xi - \sin\psi - (\xi-\psi)\cos\varphi_s]^{1/2}} + \begin{cases} 2^{1/2}\displaystyle\int_{\varphi_f}^{\psi} \frac{\cos\xi\, d\xi}{[\sin\xi - \sin\psi - (\xi-\psi)\cos\varphi_s]^{1/2}}; \\ 0, \end{cases} \tag{2.2}$$

*Since for $\tau = 0$, the frequency can return to its initial value, not all particles pass through the phase ψ.

Declassified and Approved For Release 2013/02/14 : CIA-RDP10-02196R000100060003-5

Declassified and Approved For Release 2013/02/14 : CIA-RDP10-02196R000100060003-5

where the choice of the upper or lower value depends on whether or not the particle attains the phase ψ. Since at the initial instant the separatrix is far from the stored beam, the initial phase φ_1 in the lower limit of the integral (2.2) can be replaced by $-\infty$ (for $\cos\varphi_s < 0$, by $+\infty$).

In case the separatrix does not vanish when the storage energy is attained, but moves past the beam, expression (2.2) goes over into

$$\Delta = \Delta_\infty = \sqrt{2}\int_{\mp\infty}^{\psi} \frac{\cos\xi\, d\xi}{[\sin\xi - \sin\psi - (\xi-\psi)\cos\varphi_s]^{1/2}} \quad (\cos\varphi_s \gtrless 0), \tag{2.3}$$

i.e., the quantity Δ turns out to be independent of z_f.

We shall now find the probability that the phase trajectory moves past the separatrix at the phase ψ.* For this, we shall consider the phase trajectories contained in the strip between two limiting trajectories passing through singular points of the phase cylinder (indicated in the figure by thick lines). The vertical dimension of this strip for large $|\varphi|$ (at the beginning of the storage cycle) is

$$\delta_0 z = 2\pi\left|\frac{\cos\varphi_s}{z-\tau\cos\varphi_s}\right|. \tag{2.4}$$

Since the closed region of phase space for large $|z-\tau\cos\varphi_s|$ has practically no effect on the phase trajectories in the neighborhood of the storage energy, it may be assumed that the density of the trajectories is constant in the interval $\delta_0 z$. Therefore the probability that the phase trajectory passes through the interval between z and z + dz is

$$F(z)\,dz = \left|\frac{dz}{\delta_0 z}\right| = \frac{dz}{2\pi}\left|\frac{z-\tau\cos\varphi_s}{\cos\varphi_s}\right|. \tag{2.5}$$

It is readily noted, however, that some value of ψ corresponds to each point of the strip $\delta_0 z$; from relation (1.7) we obtain

$$|z-\tau\cos\varphi_s|\,dz = |\cos\varphi_s - \cos\psi|\,d\psi. \tag{2.6}$$

(We note that for particles in the unstable region, it always follows that $\cos\varphi_s \gtrless \cos\psi$ for $\cos\varphi_s \lessgtr 0$). From expressions (2.5) and (2.6) we find that the probability that a phase trajectory passes through point ψ is different from zero in the interval $(\varphi_1, 2\pi - \varphi_s)$ and

$$F(\psi)\,d\psi = \frac{d\psi}{2\pi}\left|\frac{\cos\varphi_s - \cos\psi}{\cos\varphi_s}\right|. \tag{2.7}$$

It is readily shown that this probability is normalized to unity.

In what follows, we shall need the asymptotic expression for Δ at large values of $|\varphi_f|$. After simple calculations, we obtain from Eq. (2.2) for $\cos\varphi_s \lessgtr 0$

$$\Delta \approx \mp\frac{1}{[2|\cos\varphi_s|]^{1/2}}\frac{\sin|\varphi_f|}{\sqrt{|\varphi_f|}} \approx 0; \tag{2.8a}$$

$$\Delta \approx \Delta_\infty(\psi) \pm \frac{1}{[2|\cos\varphi_s|]^{1/2}}\frac{\sin|\varphi_f|}{\sqrt{|\varphi_f|}} \approx \Delta_\infty(\psi) \tag{2.8b}$$

depending on whether or not the particle passed through the phase ψ.

* A similar treatment is given in [2].

Declassified and Approved For Release 2013/02/14 : CIA-RDP10-02196R000100060003-5

Declassified and Approved For Release 2013/02/14 : CIA-RDP10-02196R000100060003-5

3. Equations for the Distribution Function for a Large Number of Storage Cycles

A general equation describing the variation of the distribution function is given by the difference equation relating two successive cycles:

$$P(z, n) = \int_0^{2\pi} P(z-\Delta, n-1) F d\psi - \alpha P(z, n-1) + \Phi(z). \tag{3.1}$$

In formula (3.1), the probability $F(\psi)$ is given by expression (2.7), and $\Phi(z)$ describes the appearance of new particles from the rising separatrices. If all the cycles are exactly the same, then $\Phi(z)$ does not depend on n. The quantity Δ should be expressed as a function of z and ψ (hereafter, we omit the subscripts). In the general case of arbitrary z, this can, in principle, be done by expressing φ by means of Eq. (1.7) in terms of z and φ and inserting the obtained value in Eq. (2.2). In some cases, one can simply use the asymptotic expressions (2.8). This approach is justified by the fact that in practice it is necessary only that the spread does not exceed some values much larger than unity.* In this connection, the behavior of the distribution function at small $|z|$ is of no particular interest, and it is sufficient to know how the function $P(z)$ behaves for $|z| \gg 1$.

The quantity α in Eq. (3.1) describes the probability of beam losses during one cycle of acceleration due to scattering on residual gas and other processes:

$$\alpha = \frac{T}{\tau_0} \ll 1, \tag{3.2}$$

where τ_0 is the mean lifetime of the beam, and T is the duration of one storage cycle.

The usual method of obtaining the Fokker-Plank differential equation from expression (3.1) is inexpedient in the given case for a number of reasons. It will be seen later on that the basic features of the behavior of $P(z)$ can be obtained directly from Eq. (3.1).

4. Disturbance of the Beam by Traveling Separatrices

We shall first consider the behavior of the stored beam when the separatrices pass through the beam toward infinity. It is physically obvious that the mean energy of the beam should then decrease with at the rate $S/2\pi T$. In fact, each traveling separatrix decreases the area of the phase cylinder located under the beam by the quantity S, equal to the mean energy of beam multiplied by 2π. When $\cos\varphi_s < 0$, i.e., when the separatrix travels through the beam from top to bottom, it follows, for the same reason, that the mean energy of the beam should increase.

The problem can be solved by means of Eq. (3.1), where, of course, we should set $\Phi(z) = 0$ and $\Delta = \Delta_\infty$. The fact that the quantity Δ_∞ does not depend on z considerably simplifies the problem and allows it to be solved to the end.

Applying a Fourier transformation to Eq. (3.1), we obtain the solution in the form

$$P(z, n) = \int_{-\infty}^{+\infty} \exp\{i\lambda z - n \ln[1+f(\lambda)]\} p(\lambda) d\lambda, \tag{4.1}$$

where

$$p(\lambda) = \frac{1}{2\pi} \int_{-\infty}^{+\infty} P(z, 0) e^{i\lambda z} dz, \tag{4.2}$$

*We note that the spread $\delta z \approx 1$ corresponds approximately to the maximum amplitude of the phase oscillations.

Declassified and Approved For Release 2013/02/14 : CIA-RDP10-02196R000100060003-5

Declassified and Approved For Release 2013/02/14 : CIA-RDP10-02196R000100060003-5

and

$$f(\lambda) = \int_0^{2\pi} (1 - e^{i\lambda\Delta_\infty})\, F\, d\psi. \tag{4.3}$$

The obtaining of numerical results from Eq. (4.1) requires cumbersome calculations. One can, however, draw some conclusions as regards the asymptotic behavior of the function P(z,n) for large n. To do this, we note that the value of R(f) is always positive, and, generally speaking, of the order of unity. Calculating the integral (4.1) by the method of steepest descent, we obtain the asymptotic formula

$$P(z,\ n) \simeq \frac{N_0 e^{-n\alpha}}{\sqrt{2\pi n\,(\bar{\Delta}_\infty^2 - \bar{\Delta}_\infty^2)}}\ \exp\left[-\frac{(z - n\bar{\Delta}_\infty)^2}{2n\,(\bar{\Delta}_\infty^2 - \bar{\Delta}_\infty^2)}\right], \tag{4.4}$$

where N_0 is the total initial number of particles.

Hence, regardless of the initial distribution, the beam center at large n is displaced with a velocity $\bar{\Delta}_\infty/T$. The distribution then tends to a Gaussian one, where its dispersion increases in accordance with the law

$$D^2 = (\overline{\Delta_\infty^2} - \bar{\Delta}_\infty^2)\, n. \tag{4.5}$$

Using formulas (2.2) and (2.7), we can show, by direct integration, that for $\cos\varphi_s \gtrless 0$, we have $\bar{\Delta}_\infty = \mp (S/2\pi)$. Thus the estimate made at the beginning of this section on the basis of Liouville's theorem is fully applicable to the motion of the center of the beam. At the same time, the traveling separatrices "spread" the beam in accordance with formula (4.5).

The obtained result permits one to estimate the disturbance of the stored beam caused by parasitic separatrices traveling through the beam in the case of multiple-cascade storage schemes, and also by separatrices moving from top to bottom (in the case of an accelerator with a transition through the critical energy).

5. Energy Spread of the Stored Beam

We shall now consider the behavior of a beam approached from below by separatices filled with particles. It is assumed that, upon reaching the energy E_0, the separatrix vanishes and the particles inside the separatrix infuse into the stored beam, after which the cycle is repeated.

We shall consider only the stationary state of the beam and not interest ourselves in the transient processes. The initial equation is, of course,

$$P(z) = \int_0^{2\pi} P(z - \Delta)\, F\, d\psi - \alpha P + \Phi(z). \tag{5.1}$$

As was mentioned in Sec. 3, the behavior of P(z) for large $|z|$ is of greatest interest. Then, in Eq. (5.1), we can set $\Phi(z) = 0$, since, according to its physical sense, $\Phi(z)$ drops to zero already for $|z| \approx 1$. By using the asymptotic formulas (2.8), for large positive z, we then obtain

$$P(z) \equiv 0. \tag{5.2}$$

The physical sense of this result is fully understandable if it is recalled that the separatrix approaches only the storage energy, since the phase trajectories for $z \gg 1$ are practically undisturbed and are close to the curve $z = \text{const}$. This means that the energy of the particles does not change for large z, and since the source function is concentrated in the region of $|z| \lesssim 1$, the particles cannot, in general, reach the region of large z. For large negative values of z, past which the separatrices travel, the particles are in a different situation. In analogy with the considerations in Sec. 4, one may expect that the particles will move downward with the velocity $\bar{\Delta}_\infty/T$, and in the stationary state the lower boundary of the beam will have the value $\bar{\Delta}_\infty/\alpha$. This value is also obtained if we employ Liouville's theorem and assume that the separatrices are "densely arranged."

Declassified and Approved For Release 2013/02/14 : CIA-RDP10-02196R000100060003-5

Declassified and Approved For Release 2013/02/14 : CIA-RDP10-02196R000100060003-5

We shall seek the solution for large negative $\underline{z}$ in the form

$$P(z) = \text{const} \cdot e^{\lambda z}, \tag{5.3}$$

where $\lambda > 0$. Inserting expression (5.3) into (5.1) and assuming that $\alpha \ll 1$, we find, after some simple calculations, that

$$\frac{1}{\lambda} = \frac{|\bar{\Delta}_\infty|}{\alpha}\left(1 + \frac{\alpha\bar{\Delta}_\infty^2}{2\bar{\Delta}_\infty^2}\right). \tag{5.4}$$

The first term of this expression coincides exactly with that calculated from Liouville's theorem. The corrections are small and are of the order α.

Since $1/\lambda \gg 1$, the basic quantity of particles is concentrated in the region in which the asymptotic expression (5.3) is applicable. In fact, according to Liouville's theorem, the function P(z), for any $\underline{z}$, is bounded from above, so that at small $|z|$ there are a small number of particles ($< |z| 2\pi\rho$). Without introducing any essential error, we can therefore use the asymptotic expressions

$$P(z) = \begin{cases} 0; \\ \dfrac{S\varrho\lambda}{\alpha} e^{\lambda z}, \end{cases} \tag{5.5}$$

where $z \gtrless 0$ over the entire region of variation of $\underline{z}$.

In conclusion, the author expresses his deep gratitude to A. A. Kolomenskii for discussion of a number of basic questions.

LITERATURE CITED

1. K. Symon and A. Sessler, CERN, Symposium (1956).
2. N. Vogt-Nilsen, Report CERN (1958).

Declassified and Approved For Release 2013/02/14 : CIA-RDP10-02196R000100060003-5

Declassified and Approved For Release 2013/02/14 : CIA-RDP10-02196R000100060003-5

RELAXATION OF ELASTIC STRESSES UNDER THE ACTION OF NEUTRON IRRADIATION

S. T. Konobeevskii

Translated from Atomnaya Énergiya, Vol. 9, No. 3, pp. 194-200, Sept., 1960
Original article submitted September 9, 1960

In the article, the author discusses the results of investigations on the influence of neutron irradiation on the relaxation of elastic stresses in flat springs made of uranium alloyed with molybdenum and on the relaxation of microstresses caused by broadening of the x-ray lines of drawn uranium. The theoretical notions appearing in [1] are developed further, and the results of analysis are compared with the experimental data.

Brief Review of Experimental Research

In order to evaluate more readily the ability of fuel materials to resist creep under the action of a neutron flux, it was decided to use relaxation as a test. It was assumed that between creep (deformation rate under constant load) and relaxation (loss of elasticity for a specific deformation) there exists some correspondence. We will make the necessary clarifications for the experimental part and present the most significant results obtained in [1].

Flat springs made from alloy of uranium with molybdenum and having the dimensions 30 x 1.5 x 0.1 mm were pressed between bushings, imparting an arc form to the springs, and in this form they were annealed at a temperature of 570°C for one hour. As a result of such heat-treatment, the specimens, after being freed from the restraints, retained their concave form. These specimens were then placed between two flat bushings and a part of them were irradiated in a reactor with a flux density of $1.5 \cdot 10^{13}$ neutrons/cm^2 · sec, the other part being subjected to prolonged control heating (200°C). Before and after the irradiation, the camber of the spring was measured. Alloys of uranium with 0.91 and 9.0% molybdenum were irradiated. The uranium was in the α phase, the molybdenum alloy in the γ phase. As a result of irradiation, the camber of both the alloy with 0.91% and that with 9.0% molybdenum diminished, the greatest change occurring after the first 1-2 hours of irradiation, which corresponded to an integral flux of $0.5 \cdot 10^{17} - 1.0 \cdot 10^{17}$ neutrons/cm^2. Although the first downward jump in elastic stress for the α- and γ-uranium specimens occured at approximately the same time, for the α-uranium specimen the initial magnitude of the jump was greater and in the succeeding relaxation proceeded more rapidly and went further, reducing the level of the maximum stresses after 10 hours of irradiation (integral flux $\sim 5 \cdot 10^{17}$ neutrons/cm^2) from 24 to 2-3 kg/mm^2. In the γ uranium, the second stage of relaxation proceeds much more slowly, the level of maximum stresses after 100 hours dropping by no more than 25-30% (Fig. 1).

In conducting these experiments it was noted that a great part of the change in shape taking place under irradiation proved to be reversible. A spring, when taken out from under plane compression, gradually increases its curvature once again, and this restoration can be easily accelerated by annealing. The change in form with short-lived irradiation of γ-uranium foil proves to be especially reversible. This can be well seen from the table, where the values of the camber of two specimens of uranium alloyed with 9.0% molybdenum (UM-9) after irradiation, holding at normal temperature and then annealed, as shown.

Declassified and Approved For Release 2013/02/14 : CIA-RDP10-02196R000100060003-5

Declassified and Approved For Release 2013/02/14 : CIA-RDP10-02196R000100060003-5

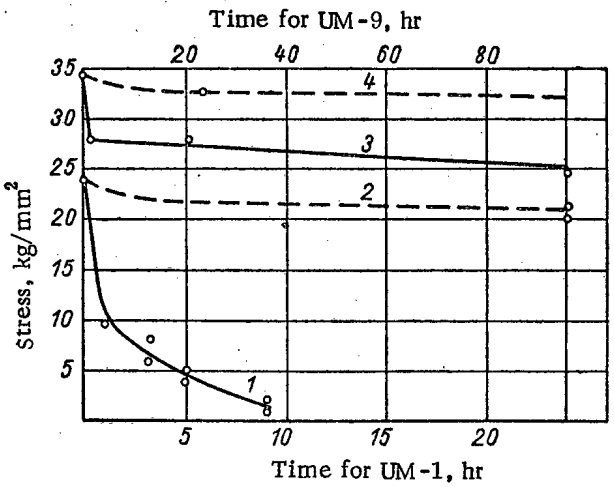

Fig. 1. Stresses in flat springs made from uranium alloyed with molybdenum as a function of neutron irradiation time: 1,3) 0.91 and 9.0% molybdenum, respectively; 2,4) control curves for anneal of the same alloys at 200°C.

TABLE

After-Effect in Flat Springs made from UM-9 Alloy (camber measured to ± 0.02 mm accuracy)

Treatment	Camber, mm	
	Specimen No. 1	Specimen No. 2
Before irradiation	6.87	6.85
Irradiation (flux $1.9 \cdot 10^{17}$ neutrons/cm^2)	5.22	5.22
Holding at normal temperature (21 days)	6.29	6.28
Annealed at:		
220° C (2 hr)	6.49	–
320° C (2 hr)	6.67	–
400° C (1 hr)	6.72	–
Specimens placed in a flat press; held at normal temperature:*		
75 hr	6.71	6.25
167 hr	6.72	6.21
Holding at 210° C* (5 hr)	6.70	6.16

* Experimental data described below.

The experimental results on relaxation of flat springs made from uranium alloys correspond to data obtained measuring the width of the x-ray lines of cold-cathode foils of uranium and UM-9 alloy subjected to neutron irradiation in a reactor [1, 2]. Analysis of the form of the lines according to the Warren-Averbach method [3] showed that as the result of irradiation, the microstresses responsible for part of the broadening of the lines of the cold-deformed metal decrease, the rate of decrease corresponding approximately to the relaxation rate of the elastic stresses in the springs. Curves are shown in Figs. 2 and 3 for the time variation (neutron flux density $2 \cdot 10^{13}$ neutrons/cm^2 · sec) of the line width B and relative values of the microstresses σ for the α- and γ-uranium samples. Relieving of the stresses giving rise to broadening of the lines at the beginning of irradiation proceeds quite rapidly, so that 60-70% of all the change is observed after just the first 1-1.5 hours of irradiation. In α uranium, immediately after a drop in level of the stresses to almost zero, the width of the

Declassified and Approved For Release 2013/02/14 : CIA-RDP10-02196R000100060003-5

Declassified and Approved For Release 2013/02/14 : CIA-RDP10-02196R000100060003-5

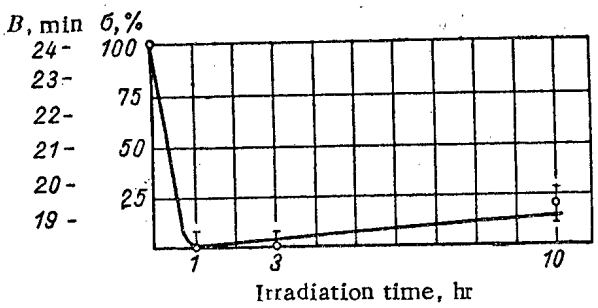

Fig. 2. Change in width of the line 114 in the x-ray photogram (B) and value of the residual microstresses σ (in percents of the initial value) of a cold-cathode specimen of α uranium as a function of irradiation time (flux density $2 \cdot 10^{13}$ neutrons/cm^2 · sec).

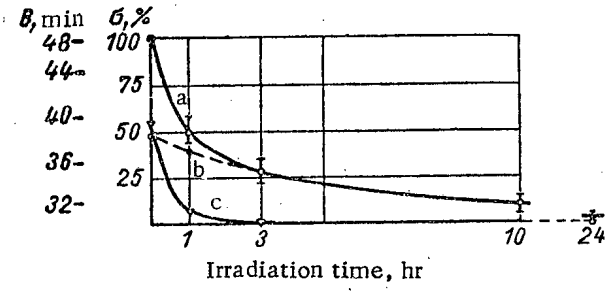

Fig. 3. The same as in Fig. 2 for the line 222 of γ uranium (UM-9 alloy). The plastic deformation is 90%.

lines during the process of further irradiation begins slowly to increase, which for polycrystalline uranium is clearly connected with magnification of the pressure of the grains bearing on one another due to radiation "growth."

It is interesting that the change in line width due to short-duration irradiation turns out to be reversible, just as the curvature of the irradiated springs was reversible in the relaxation tests. A light anneal (200-300°C) of the irradiated specimens of both α and γ uranium leads to a paradoxical result: The line width does not decrease; quite on the contrary, it increases slightly, tending to return to its position prior to irradiation.

As is evident from what has been said, the features of the variation in relaxation of elastic stresses (reduction in stress with constant deformation) under the action of a neutron flux reproduces to a certain extent the effect of accelerated creep (deformation under constant load). Thus, the existence of anomalous accelerated relaxation in α uranium undoubtedly corresponds to the accelerated creep of this same substance; but, relaxation exists, even if to a lesser degree, in the cubic γ uranium as well. The rate of change of relaxation in uranium testifies to the fact that in every case the first, rapid, stage of this effect must be assumed a primary radiation effect created directly by the fission events themselves, not a secondary effect elicited by radiation growth of the α uranium, as Roberts and Cottrell have suggested on the basis of their theory of radiation creep [4]. Consequently, the relaxation effects require special attention. Their mechanism naturally relates to the primary event of radiation action on the fissioning material (with the existence of fission peaks or thermal peaks).

In [1] it was assumed that fission events created mobile defects in the crystalline lattice, which facilitated transition of the atoms in the stress field. Migration of point defects to the stress sites should reduce the level of the stressed state. It turns out in this case that defects of different sign (interstitial atoms and vacancies) diffuse predominantly into regions with the total principal stresses of corresponding sign. For the reverse motion of the defects an increased activation energy is required; in this way they fall into "traps." With the indicated distribution of the point defects, only partial and temporary liquidation of the stresses takes place. A more stable state will be obtained when the defects are reinforced, forming complexes, being connected in one way or another with dislocations present in the crystal. We will try to expand on this notion and make it specific.

Theoretical Part

Near a point with coordinate r (Fig. 4) let a fission event take place. Without looking in detail into all of the atomic transitions which might take place near this point, let us assume, as before [1], that there exists some region v, inside which there occurs a complete shuffling of the atoms. After cooling and crystallization, the former crystalline lattice will be retained, but at each atom inside and near this region there will arise $10^3 - 10^4$ elementary defects of the interstitial atom and vacancy type.

If the lattice in the irradiated metal is deformed, then as a result of the metal passing through the state of a thermal peak the following changes take place. First of all, it must be imagined that in the space of the thermal peak the mean atomic concentration, i.e., the number of atoms per unit volume, becomes equalized, since this is connected with an over-all reduction in elastic energy. Such an equalization in concentration may be interpreted as a mass flow in the direction from a compression site to an extension site. Secondly, in the

Declassified and Approved For Release 2013/02/14 : CIA-RDP10-02196R000100060003-5

Declassified and Approved For Release 2013/02/14 : CIA-RDP10-02196R000100060003-5

elastically deformed layer the number of defects of either sign, i. e., the number of interstitial atoms or, correspondingly, vacancies remaining after passing through the thermal peak in the volume v can in general be nonidentical.

Both factors, as we will see below, should lead to a reduction in elastic energy. Let us consider their roles in turn.

For a model of the elastic state we choose a simple cylindrical bend (see Fig. 4) in a layer of thickness D along the radius of curvature ρ .

In the case of a cylindrical bend, the mean atomic concentration is $n = n_0 (\rho/r_0)$ where n_0 is the atomic concentration in the unstressed body, ρ the radius of curvature, and r the thickness coordinate in the layer. Equalization of this concentration in a thermal peak region of volume $\cong d^3$ denotes the existence of an atomic flux in the direction from a compression region to an extension region. This flux is*

$$\varphi = \frac{n_0 \varrho d^2}{2}\left(2\int_{r-d/2}^{r}\frac{dr}{r} - \int_{r-d/2}^{r+d/2}\frac{dr}{r}\right) \cong \frac{v n_0 \varrho d}{8r^2}. \tag{1}$$

Let the number of thermal peaks per unit time per cm^2 be equal to N. Then the mass-flow density, or number of atoms passing through 1 cm^2 in the flexed layer will be

$$\Phi = Nv\,\frac{n_0}{8}\,\frac{\varrho d}{r^2} = \frac{Nv}{4}\,\frac{d}{D}\,\frac{\sigma_m}{E}\,n_0. \tag{2}$$

On the convex boundary, this flow is equal to the temporary increase in concentration of atoms, which in turn stipulates the reduction in stress:

$$-\Delta\sigma_m = \frac{\Phi}{n_0}E.$$

Consequently, we obtain, finally,

$$\left.\begin{aligned} &\frac{d}{dt}\ln\sigma_m = -\frac{Nv}{4}\,\frac{d}{D}, \\ \text{or}\quad &\sigma_m = \sigma_{m_0} e^{-\frac{Nv}{4}\frac{d}{D}t}. \end{aligned}\right\} \tag{3}$$

The expression obtained determines the timewise behavior of the stress in terms of the relaxation time:

$$\tau = \frac{4D}{d}\,\frac{1}{Nv}. \tag{4}$$

The quantity Nv indicates what part of the volume passes through the thermal-peak state per unit time. If we take one hour as the unit, then for under ordinary operational conditions Nv is near unity. The relaxation time thus depends considerably on the ratio D/d, i.e., on how inhomogeneously distributed the stresses are.

The quantity τ is not extremely large only for cases when the region D differs little from the linear dimensions of the thermal peak. Evidently, the mechanism described here is a slow process, and its role is essential only in the case of a concentration of bends in the crystalline lattice near the face, particularly if in the latter there is inherent a large anisotropy in elastic properties.

Let us turn now to the second possible mechanism for relaxation under the influence of fission events.

After slowing down of the fission fragments in the volume of the thermal peak, at the same time as the

*Equation (1) is valid if $d/2 \ll 1$. Otherwise it should be multiplied by the factor $-(1/x^2)\ln(1-x^2)$, where $x = d/2r$. However, in all practically conceivable instances the correction does not exceed 10%.

Declassified and Approved For Release 2013/02/14 : CIA-RDP10-02196R000100060003-5

Declassified and Approved For Release 2013/02/14 : CIA-RDP10-02196R000100060003-5

abrupt rise in mean temperature in this region, there arises a large number of displaced atoms and vacancies. The greater part of these vanishes immediately following hardening of this region. This occurs either as the result of counter-displaced atoms with vacancies or as the result of formation of complexes, coordinated in some way or other in the lattice, or, finally, due to adsorption of the defects by dislocations and other inhomogeneities. This process normally leads to the over-all concentration of defects of either sign (interstitial atoms and vacancies) becoming the same throughout the volume of the irradiated body.

However, in an elastically stressed body, the probability of defects disappearing by formation of complexes or adherence to dislocations will depend substantially on whether the elastic energy increases or decreases in this case. Consequently, also the concentration of the remaining defects of either sign should be functions of the coordinates of the corresponding original distribution of elastic deformations. Because the mean atomic volume is not the same in different parts of the elastic field, part of the elastic deformation goes over to inelastic deformation, and this will mean an over-all reduction in elastic energy, i.e., relaxation will occur.

Let the number of defects created by a single fission event, referred to the total number of atoms in the thermal peak volume be

$$n_v + n_i = 2n.$$

Here the subscript v refers to vacancies, i to interstitial atoms. If α_v and α_i are the increments in volume upon appearance of a single vacancy and interstitial atom, respectively, expressed in units of the mean atomic volume, then the total relative change in volume of the thermal peak region due to the formation of defects is $n_v\alpha_v + n_i\alpha_i$, where the difference $n_v - n_i = 2n'$ in the curved region depends on the coordinate (e.g., is a negative quantity on the convex side and positive on the concave). The difference between the total change in volume at the given point and mean value $n(\alpha_v + \alpha_i)$ will be equal to $n'(\alpha_v - \alpha_i)$. This relative change in volume due to traversal of a thermal peak should be compared with the change in volume by the linear elastic deformation ϵ. The ratio

$$\frac{n'(\alpha_v - \alpha_i)}{\varepsilon(1-2\mu)} \tag{5}$$

typifies the attenuation in elastic deformation during the time necessary for the entire volume of irradiated material to pass through the thermal peak state (approximately 1/Nv). Hence, we may write

$$-Nv\frac{n'(\alpha_v-\alpha_i)}{\varepsilon(1-2\mu)} = \frac{d\varepsilon}{\varepsilon\, dt},$$

or

$$-\frac{1}{n'}\frac{d\varepsilon}{dt} = \frac{Nv(\alpha_v-\alpha_i)}{1-2\mu} \tag{6}$$

where n' obviously must be a function of the direction or density of the elastic energy at the point. By analogy with the corresponding dependence for thermally activated processes, we obtain

$$n' = n\left(1 - e^{-(\sigma/\sigma')^2}\right), \tag{7}$$

where n is the mean number of defects created by the peaks. Substituting this into Eq. (6) and making use of a more general notation, we have

$$\frac{d(\sigma/\sigma')}{1-e^{-(\sigma/\sigma')^2}} = -\frac{dt}{\tau}, \tag{8}$$

where

$$\tau = \frac{1}{Nv}\frac{(1-2\mu)\,\sigma'}{E}\frac{1}{n\Delta\alpha}. \tag{9}$$

Declassified and Approved For Release 2013/02/14 : CIA-RDP10-02196R000100060003-5

Declassified and Approved For Release 2013/02/14 : CIA-RDP10-02196R000100060003-5

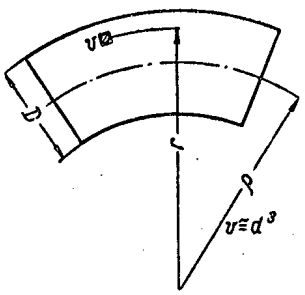

Fig. 4. Explanatory diagram showing effect of thermal peaks on relaxation.

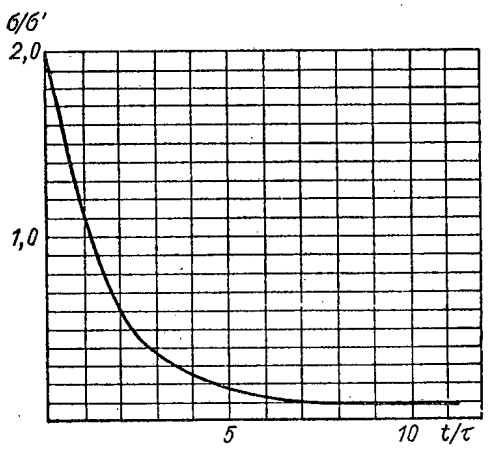

Fig. 5. Dependence of stress on time, expressed in terms of the dimensionless quantities σ/σ' and t/τ, calculated from Eq.(6). The curve is drawn for a value of $\sigma' = \sigma_m/2$.

Here, E is Young's modulus, $\Delta\alpha = \alpha_v - \alpha_i$, σ' is the energy parameter introduced above and determines the probability of the defects remaining assymetric, μ is the Poisson ratio, τ the relaxation time. According to (8), the dependence of σ on t is divided into two intervals. For large values of σ/σ'

$$\sigma = \sigma_m - \frac{t}{\tau}\sigma', \qquad (10)$$

whereas for small values of σ/σ' this relation is expressed approximately as

$$\sigma t = \sigma'\tau. \qquad (11)$$

In other words, in the beginning of the relaxation process the stress falls off sharply, following a descending straight line whose slope relative to the time axis is determined by the relaxation time τ. Further along, the rate of decrease in stress becomes less, following a hyperbolic dependence. A graph of σ/σ' as a function of t/τ, given the value $\sigma' = \sigma_m/2$, is shown in Fig. 5. The relaxation time τ can be determined if we proceed from the fact that n must be a quantity of the order $10^3 - 10^4$, while $\Delta\alpha$ is in all probability equal to one or a few [5].

The factor $(1-2\mu)\sigma'/E$ is not known and should be determined from experimental data. In any case, it should be of the order of the mean bending deformation, which in the experiments on relaxation of springs was $\sim 10^{-3}$. Consequently, $\tau \leq 1/Nv$ (τ expressed in hours). Substituting $-\sigma_m/2$ in place of σ in (10), we find that half the reduction in maximum stresses can be expected during a time of order τ, i.e., during the time necessary for the entire volume of irradiated material to fall at least one time in the thermal peak state. This is observed in the relaxation of springs made from α uranium, as well as in the relief of microstresses as computed from the width of the x-ray lines of the deformed uranium under irradiation.

The mechanism described qualitatively here represents a rapid process, attributed directly to the appearance of an excess number of defects of one sign or the other, depending on the magnitude and sign (extension or compression) of the deformation at the given point. The rapid relief of the stresses that takes place still is not a stable change, since it is not directly connected with atomic displacements which would be necessary for an irreversible change in shape. The defects which cancel out the elastic deformations act as if they exist in traps, from which they can emerge with a change in the stressed state created by external forces. This part of the relaxation must therefore be reversible, as shown by experiment. In order for the change in shape to be fixed, an actual displacement of the atoms, corresponding to a deformation gradient, is necessary; i.e., it is necessary that the diffusion process leading to irreversible changes proceed in their own way. Such a process in fissioning materials is possible as the result of recrystallization in the thermal peak region, as described above. The process is considerably slower and depends on the disperseness of the distributed stresses. However, for somewhat elevated temperatures the usual, thermically activated process of diffusion of the atoms via vacancies or by a mechanism of mobility of interstitial atoms, which also leads to irreversible change in form, is likely to be possible.

The role of an increased concentration of defects, caused by irradiation in the acceleration of relaxation effects, is demonstrated in the following experiment, conducted by K. P. Dubrovin.

Declassified and Approved For Release 2013/02/14 : CIA-RDP10-02196R000100060003-5

Declassified and Approved For Release 2013/02/14 : CIA-RDP10-02196R000100060003-5

Two bent flat springs of γ uranium (UM-9 alloy), whose curvature was fixed by annealing in the upper temperature interval, were irradiated in the unbent state in a press, after which the camber was reduced from 6.87 (6.85) to 5.22 mm. The No. 1 specimen was subjected to additional heat-treatment – annealing in the interval 200-400°C (see table). After this, its curvature decreased (after-effect); the No. 2 specimen suffered only partial restoration in due to leaching out at room temperature. Both specimens were then placed in a flat press and held in it under the conditions described in the table. It can be seen that the No. 1 specimen did not change its curvature, whereas in the No. 2 specimen it underwent a marked decrease; i.e., there was a partial occurrence of the relaxation which first took place under the action of irradiation.

These results can be easily explained as follows. After irradiation, a certain surplus of defects held within the traps exists in the relaxing specimens. Their escape from these traps causes the after-effect. A part of the defects freed from the traps during the after-effect period are retained for a long time if this is allowed to happen at room temperature. With an increase in temperature to 400°C, almost complete annihilation of the radiation defects takes place. Consequently, if the defect-containing specimen (No. 2) undergoes deformation, as a result of displacement of the residual defects and their secondary adsorption in the traps, the deformation becomes inelastic and relaxation takes place. In the specimen where there are no surplus defects, relaxation no longer happens.

SUMMARY

The experiments described in the article and the calculations made show that the main cause of relaxation of both the acting and residual stresses, which takes place under irradiation, is the appearance and displacement of atomic defects (interstitial atoms and vacancies). There is no doubt that the principal part of the relaxation takes place during a short period of radiation, when the radiation growth is only slight. This does not enable one to see the reason for relaxation in internal shear processes caused by compounding of the acting stresses with growth stresses, as this is assumed in [4] and [6] for the effects of anomalous creep of α uranium under irradiation. In the present paper, the accelerated relaxation is interpreted as a primary radiation effect. The fission events creating the thermal peaks in uranium and its alloys play a double role now. First of all, the thermal peaks cause generation of a large number of point defects, which are connected with a change in specific volume in the region of the defect and which are also a condition for increase in intensity of self-diffusion of atoms of the material irradiated. Secondly, the liberation of heat in the thermal peak region increases the mobility of the atoms and in this way serves as a medium for the radiation activation of atomic displacement processes. The fact that in the region of reversible relaxation the accumulation of point defects and their selective capture by traps play a fundamental role is demonstrated by the described experiments on magnification of the relaxation capacity of preliminarily irradiated γ uranium. However, irreversible relaxation changes in α uranium subjected to a somewhat longer irradiation (integral flux $5 \cdot 10^{17}$ neutrons/cm^2) calls for another explanation and appears to be connected with the radiation activation mechanism of self-diffusion of defects in the stress field. Finally, in the relaxation effects in α uranium, some participation of the Cottrell–Robert mechanism is not to be excluded; but the intervals of the relaxation and growth effects are evidently separate, as seen even in Fig. 2.

From the above, it follows that relaxation effects do not entirely lead to radiation creep effects in uranium, although they do to a certain extent correlate with them. The converse issue also arises: Does radiation relaxation play some role in uranium creep under irradiation, does anomalous creep in uranium, even though only partially, lead to anomalous relaxation? It is, in the present state of things, difficult to come up with the answer to this question. Since we are assuming that radiation relaxation occurs on account of diffusion processes, it may be concluded that it is related to the Nabbarro–Herring theory of diffusion creep [7], and in this sense can be included in it. However, even though radiation acceleration of creep in α uranium is specifically connected with the region of diffusion (steady-state) creep, the notions indicated have not yet found application in this region. The possible role of this mechanism of creep can be explained better as the result of more careful tests on creep in γ uranium and other fissioning materials with a regular crystalline structure, as well as by investigations of creep in α-uranium monocrystals. Carrying out such experiments would be desirable, since the question of creep and stability of uranium and other fissioning materials under irradiation is of great practical importance.

Declassified and Approved For Release 2013/02/14 : CIA-RDP10-02196R000100060003-5

Declassified and Approved For Release 2013/02/14 : CIA-RDP10-02196R000100060003-5

LITERATURE CITED

1. S. T. Konobeevskii et al., Proceedings of the Second International Conference on the Peaceful Uses of Atomic Energy, Geneva 1958 (United Nations, New York, 1960).
2. S. T. Konobeevskii , N. F. Pravdyuk, and V. I. Kutaitsev, Proceedings of the First International Conference on the Peaceful Uses of Atomic Energy, Geneva 1955 (United Nations, New York, 1956).
3. B. Warren and B. Averbach, J. Appl. Phys. 21, 595 (1950).
4. A. Roberts and A. Cottrell, Philos. Mag. 1, 711 (1956).
5. D. Holmes et al., Proceedings of the Second International Conference on the Peaceful Uses of Atomic Energy, Geneva, 1958 (United Nations, New York, 1960).
6. A. S. Zaimovskii et al., Atomnaya énergiya 5, 4, 412 (1958).*
7. C. Herring, J. Appl. Phys. 21, 437 (1950).

* Original Russian pagination. See C. B. translation.

Declassified and Approved For Release 2013/02/14 : CIA-RDP10-02196R000100060003-5

Declassified and Approved For Release 2013/02/14 : CIA-RDP10-02196R000100060003-5

PRINCIPLES OF CLASSIFICATION OF INDUSTRIAL URANIUM ORES

P. V. Pribytkov

Translated from Atomnaya Énergiya, Vol. 9, No. 3, pp. 201-207, Sept., 1960
Original article submitted April 4, 1960

Principles are proposed for the classification of industrial uranium ores according to the criteria by which they are processed: nature of the uranium mineralization, composition of the lode, uranium content, the presence of concomitant precious components, and according to their textural and structural characteristics. Practical application of the proposed classifications will greatly facilitate the technological evaluation of uranium ores and their processing.

The composition of uranium ores has a considerable effect on their processing technology. In this connection, the classification of ores according to their technological properties would be of utmost value.

A classification of industrial uranium ores was first proposed in 1954 [1, 2]. In [1],27 ore types are broken down according to the nature of uranium mineralization, content of carbonates and vanadium, and their effect on the technological process. The classification was further developed for ore from the Colorado Plateau (USA). In [2],ten mineralogical types of uranium were discriminated according to the nature of uranium mineralization, and their behavior in the processes of dressing and hydrometallurgical treatment was investigated. In [3],industrial ores are broken down according to the nature of uranium mineralization, association of elements, size of the mineral aggregates, grain size of the minerals, and other criteria.

The indicated classifications were developed only in a most general form and cannot completely satisfy the requirements of industry in evaluating the technological properties of industrial uranium ores.

The present article represents a proposal for a classification drawn up on a more extensive basis and satisfying more fully the practical problems of studying the composition, evaluating technological properties, and typing uranium ores. The classification is based on a number of criteria defining the technique of processing of ore, to wit: nature of uranium mineralization, mineral and chemical composition of the lode, uranium content in the ore, presence in the ore of concomitant useful components, size of the mineral aggregates, textural-structural properties of the uranium alloys, and contrast of the lode. Industrial uranium ores are broken down by type, variety, and grade on the basis of the above criteria.

Nature of Uranium Mineralization

At the present time about 190 uranium and uranium-containing minerals are known to us. Of uranium minerals proper,the following are of principal industrial value: the endogenous minerals (in decreasing order of practical value) – pitchblende, uraninite, brannerite, nenadkevite; the exogenic minerals – uranium black ores, pitchblende, coffinite, * carnotite, tyuyamunite, hydropitchblende, uranophane, beta-uranotyl, kasolite, soddyite, autunite, torbernite, metatorbernite, uranospinite, zeunerite [5, 6, 4].

Among the uranium-bearing minerals (in the majority of cases magmatogenous in origin) having industrial value are monazite, davidite, cyrtolite, betafite, euxenite, fergusonite, wiikite, and others [2, 6]. In

* In the paper quoted [4],coffinite was formed under exogenous conditions at the Ambrosia Lake site.

Declassified and Approved For Release 2013/02/14 : CIA-RDP10-02196R000100060003-5

Declassified and Approved For Release 2013/02/14 : CIA-RDP10-02196R000100060003-5

TABLE 1

Classification of Ores According to Nature of Uranium Mineralization

Ore group	Ore type according to uranium mineralization	Base minerals	Possible methods of mechanical dressing	Possible methods of hydrometallurgical processing	Remarks
Endogenous (primary ores)	Pitchblende	Pitchblende	A, B	E[a], F	–
	Uraninite	Uraninite	A, B	F, G[a]	–
	Brannerite	Brannerite	A, B	G	–
	Ores with uranium-bearing titanium, zirconium, niobium, tantalum, thorium, and rare-earth minerals	Monazite	B, C	G	Firing and melting down required before hydrometallurgical processing
Exogenous (secondary ores)	Pitchblende	Pitchblende	A	E[a], F	–
	Coffinite	Coffinite	–	F	–
	Black ores	Uranium black ore	A	E, F	–
	Hydroxides	Simple and complex uranium hydroxides	A, B	E[a], F	–
	Uranophane-kasolite	Uranophane, beta-uranophane, kasolite, soddyite, etc.	A	E, F	–
	Otenite-torbernite	Autunite, torbernite, uranocircite, metatorbernite	A, C	E, F	–
	Uranospinite-zeurnerite	Uranospinite, zeunerite, metazeunerite	A, C	E, F	–
	Carnotite-tyuyamunite	Carnotite, tyuyamunite	A	E, F	Firing and melting down required before hydrometallurgical processing
	Undetermined form of uranium mineralization	Calcium phosphate, organic compounds, argillaceous minerals, hydroxides of iron, manganese, etc.	A, B[a] C, D	F, G	Firing and melting down required before hydrometallurgical processing
Mixed ores	Pitchblende-black ore	–	A, B	F	–
	Pitchblende-hydroxide	–	A, B	F	–
	Pitchblende-uranophane-kasolite	Endogenous and exogenous uranium minerals	A	E[a], F	–

Declassified and Approved For Release 2013/02/14 : CIA-RDP10-02196R000100060003-5

Declassified and Approved For Release 2013/02/14 : CIA-RDP10-02196R000100060003-5

TABLE 1 (continued)

Ore group	Ore type according to uranium mineralization	Base minerals	Possible methods of mechanical dressing	Possible methods of hydrometallurgical processing	Remarks
Mixed ores	Pitchblende-carnotite-tyuyamunite	–	A	E[a], F	Firing and melting down required before hydrometallurgical processing

Note. In Tables 1-3 the following conditional notation is made: A) radiometric dressing; B) gravitational dressing; C) flotation dressing; D) multistage classification on hydrocyclones; E) carbonate leaching; F) leaching with dilute acids; G) leaching with strong acids; F, G) (boldface) acid leaching with application of oxidizers; [a]Rarely employed.

sedimentary formations, uranium is concentrated in calcium phosphate, organic compounds, argillaceous minerals, limonite, opal, hyalite, and others. In most instances the form in which the uranium is found is not established.

Proceeding from the composition of uranium and uranium-bearing minerals, and those physical-chemical properties which govern the behavior of the minerals in the dressing process and hydrometallurgical processing (crushing, solubility in mineral acids and soda solutions in the natural state, after firing, etc.), uranium ores can be classified according to the scheme in Table 1.

As seen in Table 1, ores containing endogenous minerals are usually dressed radiometrically or by gravitation methods, but the leaching of uranium from them in many cases, particularly in the processing of uranium-bearing minerals, requires the application of high-concentration acid solutions [1, 2]. Ores containing exogenous minerals withstand dressing much more poorly, but the leaching of uranium from them can be accomplished with weak solutions of acid and soda.

Mineral and Chemical Composition of the Lode

In choosing a technological scheme for processing the ores, it is in many instances of decided value to have the physical and chemical properties of nonuranium minerals in the ore-bearing powders and vein, since it is these materials that determine the composition and over-all yield of reagents during hydrometallurgical processing.

The greatest influence is exerted on the technological properties of ores by carbonates, sulfides, phosphates, iron oxides, and organic substances. On the basis of the data published [1, 3, 5, 7, 8] (though by no means complete), it is possible to come forth with a scheme for classification of the uranium ores according to composition of the lode (Table 2).

Silicate and sulfide ores are processed mainly by the method of acid leaching. Ores with high and medium carbonate contents, but with a low content of uranium, are usually leached with soda solutions [1]. Ores with low and medium carbonate contents and with a high content of uranium are in many cases, as far as is economically permissible, processed by the methods of acid leaching out. Uranium is taken out from phosphate ores as a by-product in the acid preparation of these for phosphate fertilizer [9]. In the processing of iron oxide and caustobiolithic ores, the application of specific processes (melting, firing, etc.) is required in some cases.

Uranium Content in the Ore

The most important criterion of ore quality is its content of uranium. The lower limit of uranium content in ores is usually set for each formation individually, depending on a series of geological and technical-economical factors.

Declassified and Approved For Release 2013/02/14 : CIA-RDP10-02196R000100060003-5

Declassified and Approved For Release 2013/02/14 : CIA-RDP10-02196R000100060003-5

TABLE 2

Classification of Uranium Ores According to Mineral and Chemical Composition of the Lode

Ore type	Variety	Contents of components governing ore type	Possible methods of mechanical dressing*	Possible methods of hydrometallurgical processing*	Remarks
Silicate and alumosilicate	–	More than 95% silicate and alumosilicate minerals	D*	E*, F	–
Carbonate	With low carbonate content	6-12% carbonates	–	E, F	–
	With medium carbonate content	12-25% "	C	E, F*	–
	With high carbonate content	> 25% "	C	E	–
Sulfide	With low sulfide content	3-10% sulfides	B, C	(B)E*, F	–
	With medium sulfide content	10-25% "	B, C	F	–
	With high sulfide content	> 25% "	B, C	F	–
Iron oxide	–	Industrial iron ores		E	Preliminary firing and melting required before hydrometallurgical processing
Phosphate	With low phosphate content	3-10% P_2O_5	B, C	F	–
	With medium phosphate content	10-20% P_2O_5	B, C	G	–
	With high phosphate content	> 20% P_2O_5	B, C	G	–
Caustobiolithic	Uranium-bearing coals and hard bitumens	–	B	E, F	Preliminary firing and melting required before hydrometallurgical processing
	Coal and bituminous shales, sandstone, and other powders	–	C, D	E, F	The same

* In the table are shown processing methods whose application is stipulated by the composition of the ore-bearing powders and of the vein.

Prior to World War II, ores with a high uranium content (from 1.5 to 10% and higher) were mined at the formations of the upper Belgian Congo, Great Bear Lake (Canada), the Colorado Plateau. In more recent years, and particularly during the last decade, ores with a lower uranium content have been mined. This is because of the discovery of new formations with large deposits and low uranium content in the ore (Ambrosia Lake, Blind River, etc.), the greater demand for uranium, and the improvement of techniques for processing the raw material.

Declassified and Approved For Release 2013/02/14 : CIA-RDP10-02196R000100060003-5

Declassified and Approved For Release 2013/02/14 : CIA-RDP10-02196R000100060003-5

TABLE 3

Classification of Ores According to Uranium Content (for explanation of notation see the note at bottom of Table 1)

Ore group	Uranium content, %	Possible methods of mechanical dressing	Possible methods of hydrometallurgical processing
First (very rich)	> 1	A, B	F, G
Second (rich)	1-0.5	A, B	F, G*
Third (medium)	0.5-0.25	A, B	F
Fourth (mediocre)	0.25-0.09	A, B	E*, F
Fifth (poor)	From 0.09 to the lower industrial minimum	A, B	E, F

At the present time it is considered that the mining of ores from natural uranium sites with very large stocks of uranium is best from the economic viewpoint when there is a content of 0.05-0.07% U_3O_8 and higher. The large-scale handling of the raw material makes it possible to extract uranium when the content in the ore is 0.01-0.03% U_3O_8 (e.g., from the phosphorites of Florida and Morocco, the gold-bearing conglomerates of Witwatersrand). On the basis of data on the uranium content in ores of natural uranium and complex formations [10-14], and on the basis of tests for their processing [1, 8, 13, 14], the ores can be classified according to the scheme in Table 3.

Ores of the first and second sorts are essentially industrial concentrates which can be subjected to immediate chemical processing [13]. Ores of the third, fourth, and fifth sorts are either subjected to preliminary mechanical dressing with observance of the necessary conditions or are sent immediately for hydrometallurgical processing [13]. Ores with a uranium content below the industrial minimum (poor ore containing not less than 0.01-0.02% U_3O_8) can be processed only under exceptionally favorable conditions.

Presence in the Ore of Concomitant Valuable Components

Together with natural uranium formations there are complex formations, the ores of which contain, in addition to uranium, other valuable components. In the evaluation of such deposits the industrial minimums both for uranium and for the accompanying components can be lowered to economically permissible limits [9, 15]. Thus, at the formations of Witwaterstrand, where uranium is extracted as a by-product with gold, ores containing 0.01-0.03% U_3O_8 are processed; the extraction of uranium from Florida phosphorites is done with contents of 0.01-0.02% U_3O_8.

The following uranium ores are distinguished according to the content in them of other components of practical interest: gold-uranium, uranium-molybdenum, uranium-polymetal, uranium-phosphate, uranium-vanadium, etc.

Depending on the form of coexistence of the uranium with other valuable components, ores can be distinguished in which:

1) the uranium and other useful components enter into the composition of natural uranium minerals (carnotite – vanadium, uranium);

2) uranium enters into the composition of uranium-bearing minerals having industrial value for the other components (monazite – rare earths, thorium, uranium; fergusonite – tantalum, niobium, rare earths, uranium, and others);

3) uranium enters into the composition of powdery minerals, the base components of the latter having industrial value (calcium phosphate – phosphor, uranium; uranium-bearing coals, etc.);

Declassified and Approved For Release 2013/02/14 : CIA-RDP10-02196R000100060003-5

Declassified and Approved For Release 2013/02/14 : CIA-RDP10-02196R000100060003-5

TABLE 5

Classification of Industrial Types of Uranium Ore

Ore group	Ore type according to uranium mineralization	Ore type according to composition of the lode											
			carbonate			sulfide				phosphate		
		silicate and aluminosilicate	with low carbonate content	with medium carbonate content	with high carbonate content	with low sulfide content	with medium sulfide content	with high sulfide content	Iron oxide	with low phosphate content	with medium phosphate content	with high phosphate content
Endogenous	Pitchblende	□	□	□	□	□	□	×	□			
	Uraninite	Δ	×			×	×	×	□			
	Brannerite	Δ										
	Ores with uranium-bearing minerals of titanium, zirconium, niobium, tantalum, thorium, and rare-earths	Δ	×									
Exogenous	Pitchblende	×	Δ		×							
	Coffinite											
	Black ores	□	□	Δ	□	□	Δ	×			Δ	×
	Hydroxides	Δ	×									
	Uranophane-kasolite	□	×									
	Otenite-torbernite	Δ	×	×								
	Uranospinite-zeunerite	×	×									
	Carnotite-tyuyamunite	Δ	Δ	□	□							
Mixed	Mixed (pitchblende-black ore, pitchblende-hydroxide, pitchblende-uranophane-kasolite, pitchblende-carnotite-tyuyamunite, etc.)	□	Δ	Δ	Δ	□	Δ		Δ			
With indefinite form of uranium mineralization		Δ	×	×	×					Δ	□	□

Note: In the table, the following notation is adopted: □ – very common; Δ – common; × – not too common.

Declassified and Approved For Release 2013/02/14 : CIA-RDP10-02196R000100060003-5

Declassified and Approved For Release 2013/02/14 : CIA-RDP10-02196R000100060003-5

caustobiolithic				Ore subtypes according to form of uranium mineral deposits										Ore sort				
coals	bitumens	coal and bitumen shales sandstone and other rocks	Mixed	Disseminated (from coarse to very fine grained)	soil-like (powder form)	compact	striated	fibrous	mottled (clustered)	fibrous-disseminated	flaky and nodular	disseminated (emulsion-disperse)	first (very rich)	second (rich)	third (medium)	fourth (mediocre)	fifth (poor)
			□	□		△	□	□	□	□		△	□	□	□	□	□
			×	□				×	×			×			×	×	△
				□												×	△
				□													△
				□								×				×	△
△	×	×	×	△				×	×	×		△			×	△	△
	□	△		□								□			×	□	△
△	△	△	□	□	□		△	△	□	△					△	□	□
				△		×	×	△	△	×		×	×	×	×	×	×
			×	□	×			×	△	×		×			△	□	△
			×	□	×				△	×	△	×			×	△	△
				△					×		×	×				×	×
			△	□			×	×	△			×			×	□	△
△	×	×	△	□	×	×	△	△	△	△	×	△	×	△	△	□	□
□	□	□										□				□	□

Declassified and Approved For Release 2013/02/14 : CIA-RDP10-02196R000100060003-5

Declassified and Approved For Release 2013/02/14 : CIA-RDP10-02196R000100060003-5

TABLE 6

Classification of Industrial Complex Uranium Ores

Form in which uranium found in ore	Ore type according to association of valuable components	Minerals of uranium and other useful components of industrial interest
Uranium and other useful components enter into the composition of natural uranium minerals	Uranium-vanadium	Carnotite, tyuyamunite
	Uranium-rare earth-titanium	Brannerite
Uranium and other useful components enter into the composition of uranium bearing minerals	Uranium-rare earth-thorium	Monazite
	Uranium-thorium	Thorite, uranothorite
	Uranium-zirconium	Cyrtolite, malacon
	Uranium-titanium	Davidite
	Uranium-rare earth-titanium-niobium	Fergusonite, ellsworthite, betafite, polycrase, wiikite, euxenite, etc.
Uranium and other useful components enter into the composition of powdery minerals	Uranium-phosphor	Francolite, kurskite, fluorapatite
	Uranium-carbon	Pitchblende, black uranium ores metallo-organic compounds (?), coals
Uranium and other useful components enter into the composition of different minerals	Gold-uranium	Uranium, pitchblende, native gold
	Uranium-iron	Uraninite, pitchblende, hematite, magnetite
	Uranium-copper	Pitchblende, black uranium ores, chalcopyrite, bornite, chalcosite
	Uranium-molybdenum	Pitchblende, black uranium ores, molybdenite, powellite, wolfenite
	Uranium-copper-molybdenum	Uraninite, pitchblende, chalcopyrite, molybdenite
	Uranium-polymetallic	Pitchblende, black uranium ores, galenite, sphalerite
	Uranium-copper-bismuth	Pitchblende, black uranium ores, bismuthite, native bismuth
	Uranium-copper-cobalt	Pitchblende, uraninite, hydropitchblende, chalcopyrite, cattierite, bornite, chalcosite, native copper, vaesite
	Uranium-nickel-cobalt-silver-bismuth	Pitchblende, hydropitchblende, black uranium ores, diarsenides and sulfoarsenides of nickel, cobalt, silver, bismuthite, native bismuth, silver
	Uranium-nickel-cobalt	Pitchblende, millerite, cobaltite, polydimite, gersdorffite, chloanthite

Note: In the table the following notation is adopted: □ – very common; Δ – common; x – not too common.

Declassified and Approved For Release 2013/02/14 : CIA-RDP10-02196R000100060003-5

Declassified and Approved For Release 2013/02/14 : CIA-RDP10-02196R000100060003-5

Ore types according to composition of the lode															
silicate and aluminosilicate	carbonate			sulfide			Iron oxide	phosphate			caustobiolithic			mixed
	with low carbonate content	with medium carbonate content	with high carbonate content	with low sulfide content	with medium sulfide content	with high sulfide content		with low phosphate content	with medium phosphate content	with high phosphate content	coals	bitumens	coal and bitumen shales, sandstone, limestone, and other rocks	
△ □	□ □	□ ×	□											
□ □ □ □ □	□ □	×												
		□	□		□	□			□	□	□		□	△
□ □ × × △	□	□	□	□ □ × □ □ □	△ □ □ △ △ △	□ □ □ × × ×	□							□ □ △
	×	□		×										

Declassified and Approved For Release 2013/02/14 : CIA-RDP10-02196R000100060003-5

Declassified and Approved For Release 2013/02/14 : CIA-RDP10-02196R000100060003-5

TABLE 4

Classification of Uranium Ores According to Dimensions of the Aggregates and Grains of the Uranium and Uranium-Bearing Minerals*

Characteristic of ores as to aggregate and grain size	Predominant dimensions, mm	Average dimensions, mm	Processing methods
Coarse-grained	25-300	162	Radiometric sorting
Medium-grained	3-25	14	Radiometric sorting and settling
Fine-grained	0.1-3	1.5	Sedimentation, separation in heavy suspensions, concentration on tables, radiometric sorting
Very fine-grained	0.015-0.1	0.057	Flotation (rarely employed), radiometric sorting, hydrometallurgical processing
Emulsion, submicroscopic	0.001-0.015	0.008	Separation into uranium- and non-uranium-bearing products, multistage classification on hydrocyclones or immediate hydrometallurgical processing
Colloid-disperse	< 0.001	–	The same

* The classification in [16] is adopted as the basis.

4) uranium and other valuable components are separately encountered in different minerals (gold-uranium ores, etc.).

In the first three groups, the separation of the useful components in processing is possible only by chemical methods. In the ores of the fourth group, the uranium minerals and minerals of other components can be separated into the individual products by mechanical methods of dressing (before and after hydrometallurgical processing).

Dimensions of the Mineral Aggregates and Textural-Structural Characteristics of Uranium Ores

For the technological processes such factors as the sizes of precipitates of the uranium minerals and their textural-structural properties are of great importance.

The classification of uranium ores according to dimensions of the mineral aggregates is made in Table 4.

Depending on the effect of dressing on the processes, the following textures and structures of uranium ores may be distinguished:

1) Compact, mottled (clustered), fibrous, striated, disseminated, nodular textures; the sizes of the uranium mineral aggregates range from a few millimeters (1.5-3 mm) to several centimeters; such ores are relatively easily dressed by the radiometric or gravitation methods;

2) finely disseminated, fragmented, cement-like, cork-like, reticular, meshed, cockaded, flaky textures; the sizes of the uranium mineral aggregates range from tenths of a millimeter to 1-1.5 mm; such ores are difficult to dress mechanically;

3) soil-like (powder form), thinly disseminated, submicroscopic textures; the grain sizes of the uranium minerals are less than 0.015-0.020 mm; such ores are never subjected to mechanical dressing, since the uranium minerals are very sparsely and relatively uniformly scattered throughout the ore-bearing powders.

Declassified and Approved For Release 2013/02/14 : CIA-RDP10-02196R000100060003-5

Declassified and Approved For Release 2013/02/14 : CIA-RDP10-02196R000100060003-5

Contrast of the Lode

With uniformity of distribution of the uranium as criterion, formations can be distinguished with uniform, nonuniform, very nonuniform, and extremely nonuniform mineralization. Uniform and nonuniform mineralization are characteristic of sedimentary deposits, very uniform and extremely uniform mineralization are characteristic of hydrothermal deposits.

Within the confines of the ore body, uranium minerals form individual impregnations, fibers, clusters, and agglomerations, in connection which the uranium content, both at different points of the ore bodies and in the dislodged ore mass, fluctuates within wide limits. The most abrupt transitions from portions with a high uranium content to nonore-bearing portions are observed in hydrometallic and pegmatite deposits.

The discontinuity and nonuniformity of uranium mineralization, as well as the textural and structural features and nature of uranium mineralization, determine the degree of radiometric contrast of the dislodged ores, this being understood as the excess uranium content in individual lumps over and above the content in the over-all formation. Ores of high, medium, and weak contrast, as well as noncontrast ores, are distinguished [4]. In ores of high and medium contrast the uranium content in separate lumps is ten to a hundred times greater than the average uranium content in the over-all formation. Contrast ores have compact, mottled, densely disseminated, fibrous, striated textures and are characterized by coarse, medium, and fine aggregate dimensions of the uranium minerals (ores of hydrothermal and pegmatite deposits).

Ores with weak contrast are distinguished by a comparatively small surplus (two to five times) in uranium content in the ore lumps in comparison with the mean content of the main formation. They have very finely disseminated ore textures with more uniformly distributed mineral impurities (ores of hydrothermal-metasomatic and metamorphogenetic deposits).

In noncontrast ores, the uranium minerals are dispersed in the ore mass relatively uniformly in the form of emulsion-type and very finely dispersed impregnations (predominantly ores of sedimentary deposits).

SUMMARY

General schemes for the classification of uranium ores, reflecting in combined form the principal factors affecting their technological processing, are shown in Tables 5 and 6. Several types and varieties of ore are broken down according to the nature of uranium mineralization, composition of the lode, textural features, and the presence of other concomitant components. In the classifications given (as opposed to the existing classifications), certain properties of uranium ores and the influence of these properties on technological processes are represented most completely.

The proposed classification provides the opportunity for performing on approximate technological evaluation of ores, for referring them to certain standard types, and to channel the ores more readily into industrial processing.

LITERATURE CITED

1. W. Lennemann, Eng. and Min. J. 155, No. 9 (1954).
2. Thunaes, Can. Mining and Matellurg. Bull. 47, 506, 128 (1954).
3. D. Ya. Surazhskii, Methods of Prospecting Uranium Deposits [in Russian] (Atomizdat, Moscow, 1960).
4. R. Zitting, Mines Mag. No. 3, 53 (1957).
5. R. V. Getseva and K. T. Savel'eva, Handbook on the Determination of Uranium Minerals [in Russian] (Gosgeoltekhizdat, Moscow, 1956).
6. V. G. Melkov and L. Ch. Pukhal'skii, Prospecting Uranium Deposits [in Russian] (Gosgeoltekhizdat, Moscow, 1957).
7. D. Everhardt, Proceedings of the First International Conference on the Peaceful Uses of Atomic Energy, Geneva, 1955 (United Nations, New York, 1956).
8. Yu. L. Chernosvitov, Industrial Requirements for the Quality of Mineral Ore. Uranium, No. 67 [in Russian] (Gosgeoltekhizdat, Moscow, 1959).

Declassified and Approved For Release 2013/02/14 : CIA-RDP10-02196R000100060003-5

Declassified and Approved For Release 2013/02/14 : CIA-RDP10-02196R000100060003-5

9. B. N. Nevskii, Atomnaya énergiya 6, 1, 5 (1959).*
10. V. I. Gerasimovskii, Uranium Sites in Foreign Countries [in Russian] (Izd. AN SSSR, Moscow, 1959).
11. V. S. Domarev, Geology of Uranium Deposits in the Capitalist Nations [in Russian] (Gostekhizdat, Moscow, 1956).
12. M.M. Konstantinov and E. Ya. Kulikova, Uranium Provinces [in Russian] (Atomizdat, Moscow, 1960).
13. G. E. Kaplan, B. N. Laskorin, and B. V. Nevskii, Atomnaya énergiya 6, 2, 113 (1959).*
14. V.N. Kotlyar, E. S. Kabanova, and B. V. Kristal'nyi, On the State of the Uranium Raw Material Base in the Capitalist Countries and Uranium Prospecting Procedure [in Russian] (Izd. AN SSSR, Moscow, 1956).
15. N. S. Zontov, Atomnaya énergiya 6, 6, 613 (1959).*
16. V. A. Glazkovskii, Geological-Mineralogical Bases for the Technological Evaluation of Iron Ore Deposits [in Russian] (Gosgeoltekhizdat, Moscow, 1954).

* Original Russian pagination. See C. B. translation.

Declassified and Approved For Release 2013/02/14 : CIA-RDP10-02196R000100060003-5

Declassified and Approved For Release 2013/02/14 : CIA-RDP10-02196R000100060003-5

THE USE OF FLOTATION IN THE PURIFICATION OF RADIOACTIVE EFFLUENTS

S. A. Voznesenskii, G. A. Sereda, L. I. Baskov,

E. V. Tkachenko, and V. F. Bagretsov

Translated from Atomnaya Énergiya, Vol. 9, No. 3, pp. 208-213, Sept., 1960
Original article submitted March 26, 1969

This paper shows that ferric hydroxide with sorbed radioactive isotopes is floated from aqueous solutions. It is shown that during flotation the radioactive isotopes are hardly desorbed at all. A study is made of the flotability of ferric hydroxide in relation to the alkalinity of the solution, initial concentration of reacting materials, foreign impurities. A suggestion is made as to the chemical character of reaction between the ferric hydroxide and the studied flotation reagent.

The article also discusses some experimental data on the flotation of ferric hydroxide precipitates forming during the purification of radioactive effluents.

Several papers have been published recently dealing with the treatment and removal of radioactive liquid wastes [1, 2]. The strict sanitary requirements regarding effluents when they are discharged into open reservoirs and the complexity of the chemical and radiochemical composition of the effluents require the simultaneous use of different methods for treating these wastes. In the preliminary treatment use is often made of coagulation by ferric or aluminum salts [1, 3]. It is stated in the literature that the hydroxides of these metals are good sorbents for most radioactive isotopes [4, 5]. Furthermore, during coagulation the effluent is freed from suspended particles. However, a large volume of precipitates is obtained (up to 2% of the volume of water treated). To reduce the volumes, further treatment is necessary [1].

The existing methods for reducing the volumes of hydroxide precipitates (dehydration, treatment in centrifuges and vacuum filters, thermal drying [6]) have a number of disadvantages. New methods should therefore be sought.

The present paper gives the results of work on the reduction of hydroxide precipitate volumes by the flotation method. This work is an attempt to improve the method for purifying the radioactive effluents described in the report to the Second International Conference on the Peaceful Use of Atomic Energy (in Geneva) [1].

Method

The precipitates were prepared in distilled or tap water (chemical analysis given in Table 1) in the following way. The suspension of $Fe(OH)_3$ precipitate of the required concentration was prepared in 1 liter of water by coagulating $Fe_2(SO_4)_3$ with a solution of caustic soda; to a fixed volume of the radioactive effluent, additions were then made of a solution of iron containing 100 mg/liter while the medium was made alkaline with caustic soda. The coagulated precipitate was allowed to settle to the required volume. The settling took up to 15 days. To each gram of the obtained precipitate, 1 g of flotation reagent was added. Tens of different flotation reagents were tested, kindly provided by V. G. Plyusnin of the Institute of Chemistry, Urals Branch of the Academy of Sciences. The best results for the flotation of ferric hydroxide were obtained using the Petrov kerosene product [7], petroleum benzenesulfonic acids – the products of oxidation of kerosene distillate by sulfuric anhydride. All subsequent work was carried out using this flotation reagent which had first been neutralized by caustic soda.

Declassified and Approved For Release 2013/02/14 : CIA-RDP10-02196R000100060003-5

Declassified and Approved For Release 2013/02/14 : CIA-RDP10-02196R000100060003-5

TABLE 1

Chemical Analysis of Tap Water

pH	Elements, mg/liter					Oxidizability, mg/liter	Dry precipitate, mg/liter
	Ca^{2+}	Mg^{2+}	SO_4^{2-}	Cl	Co_3^-		
7.1	30.6	13.8	20.6	24.8	12.1	4.9	200

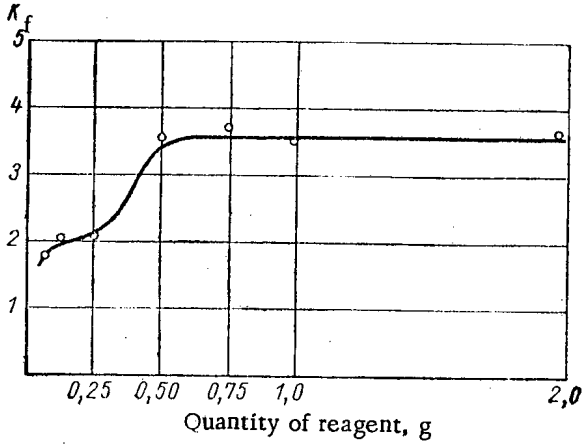

Fig. 1. Effect of quantity of flotation reagent on K_f.

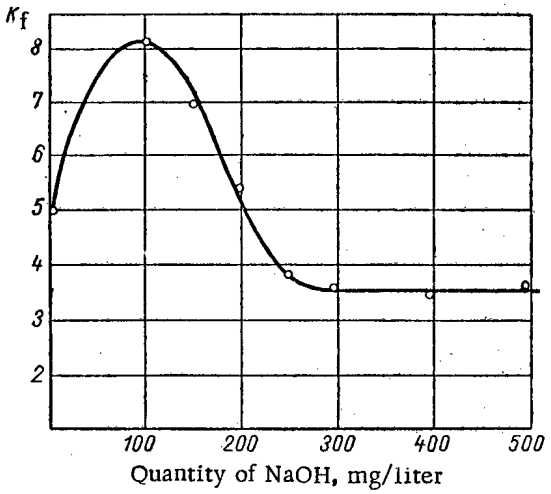

Fig. 2. Effect of quantity of NaOH on K_f.

In experiments on the study of the behavior of radioactive isotopes, the latter were added to the original solution before the addition of ferric salts. The behavior of the following uranium fission fragments was studied: Sr^{90}, Pm^{147}, $Zr^{95} - Nb^{95}$, $Ru^{106} - Rh^{106}$. All preparations were chemically and radiochemically pure and carrier-free. The preparations of Sr^{90}, Pm^{147}, and $Ru^{106} - Rh^{106}$ were solutions of chlorides, $Zr^{95} - Nb^{95}$ were oxalate solutions. The initial specific activity of the precipitate was 0.03-1.0 μC based on 1 g of ferric hydroxide.

From the precipitates of ferric hydroxide prepared in this way, 100 ml samples were taken and flotation was carried out in a laboratory flotation machine of 500 ml capacity, made from plexiglas. The solution was mixed by an impeller with a blade of height 15 mm, diameter 30 mm, angle of inclination 40-45°. The mixing speed varied between 4300 and 5000 rpm.

Preliminary experiments established the optimum mixing speed (4600 rpm) and the time of mixing (2 min) and the time of separation of the floated precipiate from the solution (40-60 min). All experiments were carried out under these conditions. After separating the precipitate, the volumes of this precipitate and the remaining solution were measured. On the basis of data obtained by the flotation method, determinations were made of the coefficient of reduction in the volume of the precipitate – the coefficient of flotation K_f.

The behavior of the radioactive isotopes in the experiments was checked by the ordinary radiometric method using an end-type counter and a B-type apparatus. The relative error of the count was ± 5%; the pH of the solutions was measured by a glass electrode with a P-6 potentiometer, the accuracy of the measurement being 0.1 pH unit. All experiments were carried out at 17-19°C and each experiment was repeated three or four times.

Experimental Data

At the start of the investigation a determination was made of the optimum quantity of flotation reagents per unit weight of the floated ferric hydroxide precipitate. The amount of precipitate in this experiment and in all subsequent experiments was 7 g/liter, and the pH of solution was 8.5. The obtained data are given in Fig. 1, from which it can be seen that the optimum quantity of flotation reagent is 1 g per 1 g of $Fe(OH)_3$. Further addition of it under the selected conditions of the experiment does not lead to an increase in K_f. Therefore, in all later experiments the same ratio of flotation reagent to precipitate was chosen.

Declassified and Approved For Release 2013/02/14 : CIA-RDP10-02196R000100060003-5

Declassified and Approved For Release 2013/02/14 : CIA-RDP10-02196R000100060003-5

TABLE 2

The Effect of Aging Time of Ferric Hydroxide Precipitate on Flotation (speed of mixing 2000 rpm)

Age of precipitate, days	K_f	Flotation time needed, min
Freshly prepared	4	3.0
3	4	3.5
6	4	5.0
9	4	7.0
12	4	8.5
24	4	10.0
540	2	25.0

TABLE 3

Distribution of Activity in Solutions, %

Isotope	Initial solution	Solution after coagulation	Solution after flotation
$Ru^{106} - Rh^{106}$	100	37.60	−1.27
Pm^{147}	100	0.40	−0.03
Sr^{90}	100	6.50	+0.02
$Zr^{95} - Nb^{95}$	100	1.10	+0.01

Note: The minus sign means that during flotation a part of the radioactivity had transferred from the precipitate to the solution; the plus sign indicates the opposite effect.

Discussion of Results

As already stated, at the start of the work, tests were made on a number of substances used as flotation reagents. Those studied in greater detail were kerosene products, subjected to additional treatment. These products were crude kerosene, cracked petroleum asphalt, hydrochlorinated kerosene, hydrochlorinated saponified kerosene, and sulfonated saponified kerosene. It was found that the capacity to float ferric hydroxide precipitates from aqueous solutions is shown by sulfonated saponified kerosene having a sulfo group in its composition. All other materials studied gave unfavorable results.

The capacity of sulfonated kerosene to float ferric hydroxide is due to the fact that during mixing, a chemical reaction probably takes place with the formation of a new compound which floats, in contrast to the "pure" ferric hydroxide. This assumption is confirmed by the data of the following experiments: a ferric hydroxide precipitate was mixed with flotation reagents, and after standing it was washed with twenty times its volume of water. In the case of physical reaction of the precipitate with the flotation reagent, due to Van der Waals' forces, after this washing the flotation reagent is easily removed from the surface of the flotation material and flotation does not occur [9]. In our experiments, after washing with water flotation occurred normally.

Treatment of precipitates which had stood for up to $1\frac{1}{2}$ years showed that they also float, but the time needed for flotation depends on the time of "aging" of the precipitate. It is well known that the "older" the precipitate the less developed is its surface, and it has lower sorption properties. In our case longer mixing was needed for reaction of the flotation reagent with ferric hydroxide. The coefficient of flotation remained the same as for the freshly deposited precipitate, i.e., only the speed of flotation changed. This also indicates the chemical character of reaction between the precipitate and the flotation reagent.

As can be seen from Fig. 2, the minimum volumes of floated precipitate (K_f values are large) are obtained in a neutral medium. The isoelectric point of ferric hydroxide is at pH $\simeq$ 7, i.e., in this region the precipitate is less hydrated; therefore the volume of the floated precipitate is also at a minimum.

Declassified and Approved For Release 2013/02/14 : CIA-RDP10-02196R000100060003-5

Declassified and Approved For Release 2013/02/14 : CIA-RDP10-02196R000100060003-5

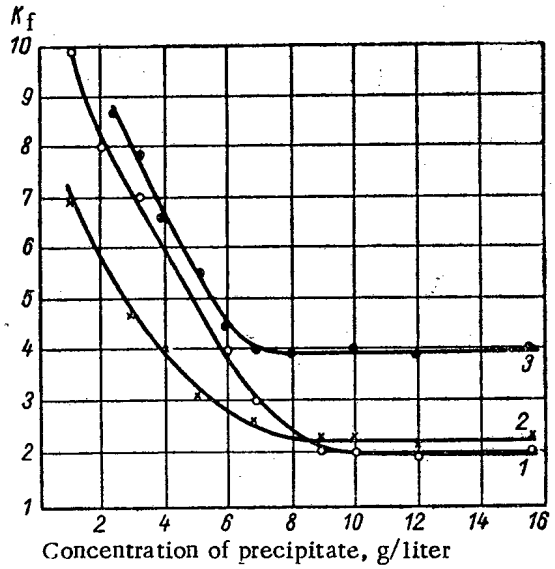

Fig. 3. The dependence of K_f on the concentration of precipitate in the suspension: 1,2) with pneumatic and mechanical mixing, respectively, for the precipitates formed under actual conditions; 3) for precipitates of ferric hydroxide formed in 1 liter of tap water.

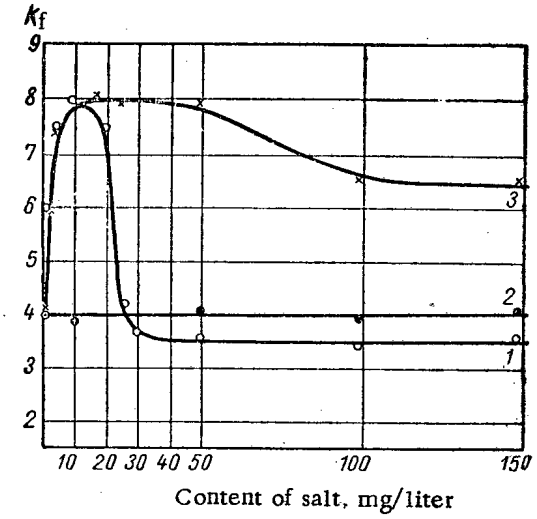

Fig. 4. The effect of foreign impurities of K_f: 1) on the addition of $Ca(NO_3)_2$; 2) on addition of Na_2CO_3; 3) on the addition of a mixture of $Ca(NO_3)_2$ and Na_2CO_3.

It is a well-known fact that the pH of the medium affects the flotation of many minerals. The same might also have been expected in our experiments. As already shown, there are no data in the literature on the flotation of ferric hydroxide, and we do not know the effect of pH of the medium on K_f. Experiments were therefore conducted to establish the effect of pH of the solutions from which the precipitate of ferric hydroxide was obtained. The data of the experiments are given in Fig. 2.

As shown by the curve of Fig. 2, K_f actually changes with change in the quantity of NaOH. The maximum value of K_f (~8.0) is observed in a neutral medium.* With increase in alkalinity to 200 mg/liter (pH of the solution after mixing was ~8.0), the value of K_f drops sharply to 3.8 and later remains almost constant.

For the practical use of the flotation method it is important to know the dependence of K_f on the concentration of ferric hydroxide in the pulp. The data are given in Fig. 3.

Since in the treatment of ferric hydroxide precipitates, "aged" precipitates may be encountered, kept from 1 month to $1\frac{1}{2}$ – 2 years, experiments were carried out on the flotation of such precipitates. Furthermore, this gives additional data which can be used in deciding on the mechanism of flotation. The results of the experiments are given in Table 2.

Radioactive effluents always contain various cations or anions. Those most frequently encountered are Ca^{2+}, Mg^{2+}, CO_3^{2-}, SO_4^{2-}, Cl^-, NO_3^-, etc. It has been observed that the rate of coagulation of $Fe(OH)_3$ precipitates depends on the concentration of certain salts, particularly $CaCO_3$. It is known from the literature [8] that various anions have various effects on the properties of the foam, particularly on its stability. To explain the effect of foreign impurities, experiments were carried out, the data of which are given in Figs. 4 and 5.

The Behavior of Radioactive Isotopes, Sorbed by a Ferric Hydroxide Precipitate, during Flotation

The aim of the present paper, as already mentioned, is to determine the possibility and conditions for flotation of ferric hydroxide precipitates formed during the purification of radioactive effluents. Therefore, after establishing the optimum conditions for flotation of the ferric hydroxide precipitate, experiments were conducted to determine the behavior of various radioactive isotopes which had previously been sorbed on precipitates. The data are given in Table 3.

* On the addition to the solution of 100 mg/liter $Fe_2(SO_4)_3$ and 100 mg/liter NaOH, the pH of the solution after mixing was ~7.0.

Declassified and Approved For Release 2013/02/14 : CIA-RDP10-02196R000100060003-5

Declassified and Approved For Release 2013/02/14 : CIA-RDP10-02196R000100060003-5

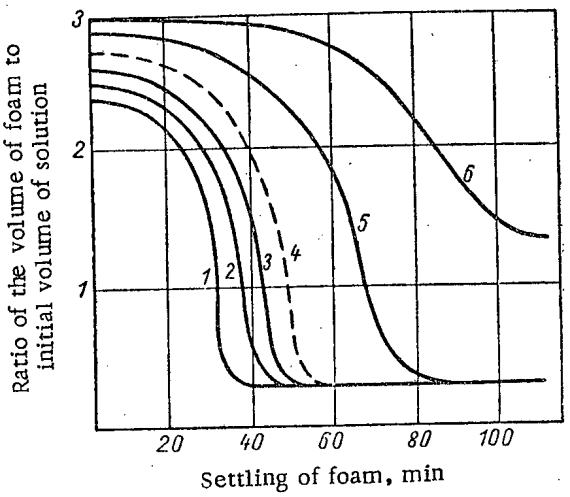

Fig. 5. The effect of various anions on the stability of the foam: 1) addition of $NaNO_3$ or Na_2SO_4; 2) addition of Na_2CO_3 or $Na_2C_2O_4$; 3) addition of $Na_2Cr_2O_7$ or NaAc; 4) precipitate formed under real conditions; 5) addition of Na_3PO_4 or Na_2SiO_3; 6) addition of NaCl.

In the purification of radioactive effluents, the most complete sorption of radioactive microcomponents by ferric hydroxide occurs at pH > 8.0 [1, 4]. Therefore, all further experiments were carried out at a pH of formation of the precipitate greater than 8.0. Naturally, K_f was then less than the maximum value.

It can be seen from the data of Fig. 4 that the lower the concentration of precipitate in the suspension, the higher the value of K_f. This is due to the high moisture content of the hydroxide precipitated from dilute solutions. The moisture content of the precipitates after flotation is roughly the same; therefore K_f changes sharply with change in the concentration of precipitate in the suspension. Starting with a concentration of 8 g/liter, further increase in the quantity of ferric hydroxide does not lead to a reduction in K_f.

It was mentioned above that the addition of certain materials, for example, finely ground chalk or marble, considerably accelerates the precipitation of ferric hydroxide. A precipitate with lower water content is then obtained. The results of the experiments (see Fig. 4) show that the addition of a small amount of calcium nitrate to the suspension increases K_f (curve 1). This increase should be explained by the fact that at this concentration of $Ca(NO_3)_2$, there is formation of $CaCO_3$ precipitate due to the Co_3^{2-} in the solution. The addition of a large amount of calcium nitrate does not lead to an additional separation of calcium carbonate precipitate, and begins to act as a foreign electrolyte. Since in this work we used water containing small amount of hardness salts and a large quantity of CO_3^{2-} ions, the addition of soda did not affect K_f (curve 2). It is probable that when working with hard waters containing small amount of CO_3^{2-} ions, the effect of soda and calcium nitrate will be the reverse.

The addition of Ca^{2+} and CO_3^{2-} ions of a definite concentration (in our experiments 10-50 mg per 100 mg of $Fe(OH)_3$) also leads to an increase in K_f.

Figure 5 gives data showing the effect of various anions on the stability of the foam. These data agree with results obtained by other workers [8, 10, 11]. The anions, having the capacity to foam solutions, stabilize the foam. Among the anions which we studied, these properties are shown by Cl^-, PO_4^{3-}, and SiO_3^{2-}. Special mention should be made of the effect of Cl^-, since it stabilizes the foam to a large extent. In the effluents, it is therefore very undesirable to have large concentrations of Cl^- and to use ferric chloride for coagulation. During flotation, anions such as NO_3^-, SO_4^{2-} reduce the stability of the foam (after flotation the volume of foam is sharply reduced). A similar effect on the foam stability is shown by the anions CO_3^{2-}, $C_2O_4^{2-}$, $Cr_2O_7^{2-}$, and Ac^-, although their effect is not as strong as NO_3^- and SO_4^{2-}. The presence of these anions in effluents in quantities of up to 2 g per 100 mg $Fe(OH)_3$ does not change K_f. Furthermore, the presence of these anions accelerates the reduction in volume of the gloated deposit, and consequently increases the output of the apparatus.

The experiments carried out on the flotation of ferric hydroxide precipitates on which various radioactive elements had previously been sorbed (see Table 2) showed that during flotation there is no noticeable desorption of radioactive elements. This indicates the very good reaction of radioactive elements with ferric hydroxide and the formation, as shown by a number of workers [5, 6], of chemical compounds or solid solutions.

The results of the present work indicate that colloidal precipitates can be floated as well as crystalline oxidized materials. For this purpose it is essential to select the correct material as the flotation reagent. It might also be expected that the flotation capacity would be shown by other metal hydroxides (for example aluminum) and also certain salts. In conclusion, it should be mentioned that the flotation of ferric hydroxide precipitates obtained during the purification of radioactive effluents can become a promising method for reducing the volume of precipitates.

Declassified and Approved For Release 2013/02/14 : CIA-RDP10-02196R000100060003-5

Declassified and Approved For Release 2013/02/14 : CIA-RDP10-02196R000100060003-5

LITERATURE CITED

1. S. A. Voznesenskii et al., Proceedings on the Peaceful Uses of Atomic Energy, Second International Conference, Geneva, 1958; The Chemistry of Radioelements and Radiation Transformation [in Russian] (Atomizdat, Moscow, 1959) p. 189;
2. R. Burns and M. Stedwell, Nucl. Eng. Sci. Conf. 3, 57-58, 11 (1957).
3. A. Wolman and A. Ghorman, J. Inst. Water Eng. 7, 4, 319 (1957).
4. V. V. Pushkarev, ZhNKh 1, 1, 170 (1956).
5. S. A. Vosnesenskii, V. V. Pushkarev, and V. F. Bagretsov, ZhNKh 3, 1, 235 (1958).
6. E. Horner and G. Sifrin, Eng. News Rec. 151, 6, 37 (1953).
7. Petrov Kerosene Product , GOST 463-453.
8. E. A. Filatova, Trudy Khar'kov. politekhn. inst. No. 8 (1956).
9. O. S. Bagdanov, Flotation (Problems in the Theory and Practice) [in Russian] (Metallurgizdat, Moscow, 1945).
10. W. Lockett, J. and Proc. Inst. Sewage Purific. No. 3, 225 (1956).
11. T. Nash, J. Appl. Chem. 7, 7, 392 (1957).

Declassified and Approved For Release 2013/02/14 : CIA-RDP10-02196R000100060003-5

Declassified and Approved For Release 2013/02/14 : CIA-RDP10-02196R000100060003-5

LETTERS TO THE EDITOR

THE γ-RAY SPECTRUM OF THE TVR REACTOR

N. A. Burgov, G. V. Danilyan, I. Ya. Korol'kov,

and F. Shterba

Translated from Atomnaya Énergiya, Vol. 9, No. 3, pp. 214-215, Sept., 1960
Original article submitted February 24, 1960

Using an "elotron" type magnetic γ spectrometer [1], measurements were made of the spectrum of γ rays leaving the radial channel of a TVR reactor [2]. Figure 1 shows the geometry of the experiment. In the active zone 1 of the reactor, there is a special "pocket" to harden the neutron spectrum. Because of the pocket the spectrum of the reactor should contain the almost nonattenuated γ radiation of uranium 1a. The apparatus spectrum less the background of random coincidences, measured with a 1.25% resolution (for $E_\gamma \geq 2$ Mev) is given in Fig. 2. Figure 3 shows this spectrum with allowance for the efficiency of the instrument and the absorption of γ quanta in the neutron filter, reduced to the same ranges of $\Delta H\ \rho$. The relative intensity of the γ lines is plotted along the ordinate axis. For the unresolved part of the spectrum, $\nu(E_\gamma)$ determines the relative number of γ quanta of given energy per unit range of energy.

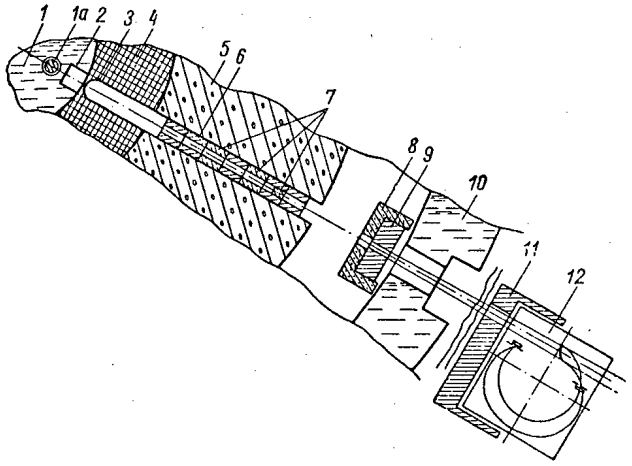

Fig. 1. Geometry of experiment. 1) active zone; 1a) uranium rod; 2) "pocket" and housing of reactor (aluminum); 3) stainless steel pipe; 4) graphite reflector; 5) concrete shield; 6) lead collimator; 7) neutron collimator and B_4C filter; 8) neutron shield; 9) lead collimator; 10) water shield; 11) lead shield; 12) γ spectrometer.

The results for the processing of the spectrum and the identification of the separate lines are given in the table. The first column gives the designation of the line used in Fig. 2, the second column gives the values of energy for the γ line (the numbers in brackets indicate the error in the last figures). The third column gives the relative intensity of the γ lines. The values of energy and intensity of the γ lines, which were not determined sufficiently reliably, are given in brackets. The error in determining the relative intensity of a resolved line is about 10%.

The separate lines are identified from the data of [3] for the constructional elements of the reactor, with an allowance for the microscopic cross section and the absolute yield of γ quanta per capture. The last column gives the elements radiating the given line and the designation of the line used in [3]. In those cases where several elements may make a contribution to the γ line, they are shown in the order of reducing contribution. Forty of the 45 γ lines within the limits of error of measurement can be ascribed to constructional elements of the reactor. The contribution from iron to the intensity of the γ line 33 cannot exceed 20%. The authors of [4] observed a relatively intense γ line with a close energy in the spectrum of aluminum, which was not confirmed in [5]. According to the data of [6], the γ line with an energy 4.062 ± 0.010 Mev and absolute intensity 7% exists in the spectrum of γ rays of neutron capture in U^{238}; this is not fully resolved and the authors indicate the presence of a γ line with a somewhat lower energy.

Declassified and Approved For Release 2013/02/14 : CIA-RDP10-02196R000100060003-5

Declassified and Approved For Release 2013/02/14 : CIA-RDP10-02196R000100060003-5

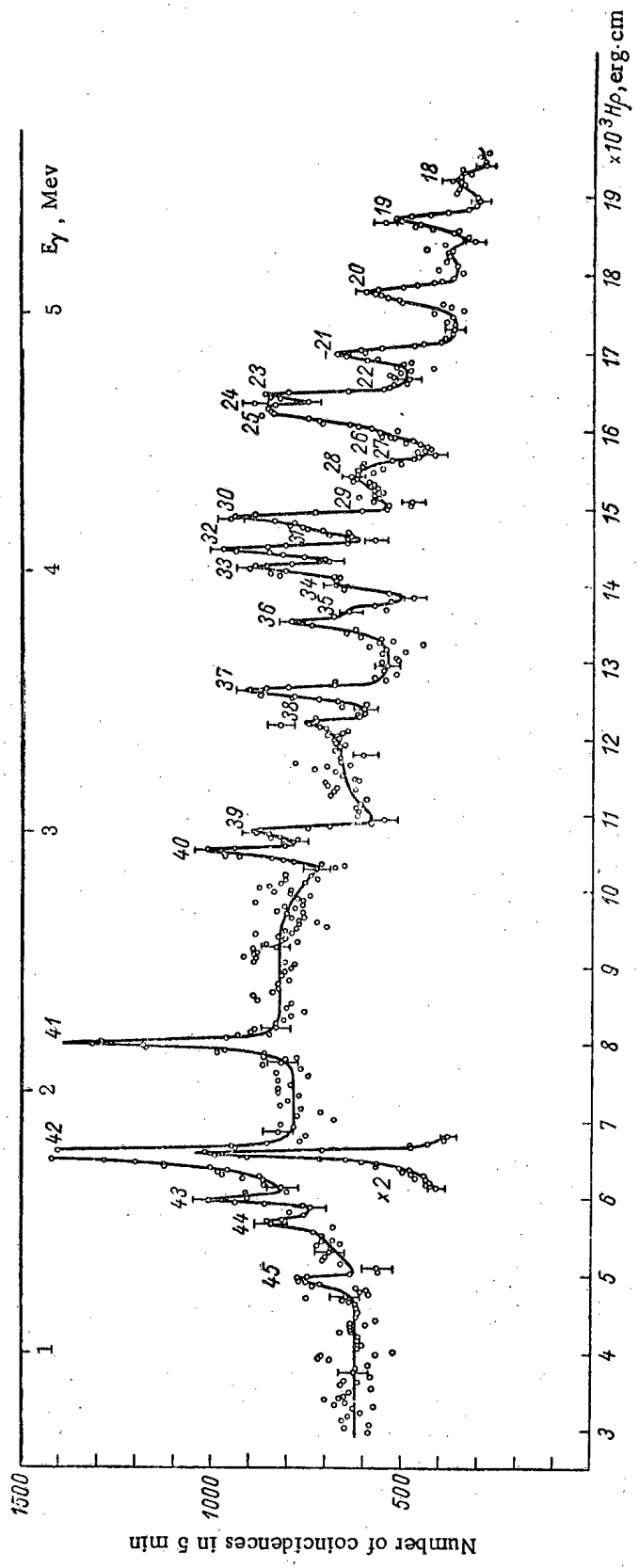

Fig. 2. (See caption on facing page.)

Declassified and Approved For Release 2013/02/14 : CIA-RDP10-02196R000100060003-5

Declassified and Approved For Release 2013/02/14 : CIA-RDP10-02196R000100060003-5

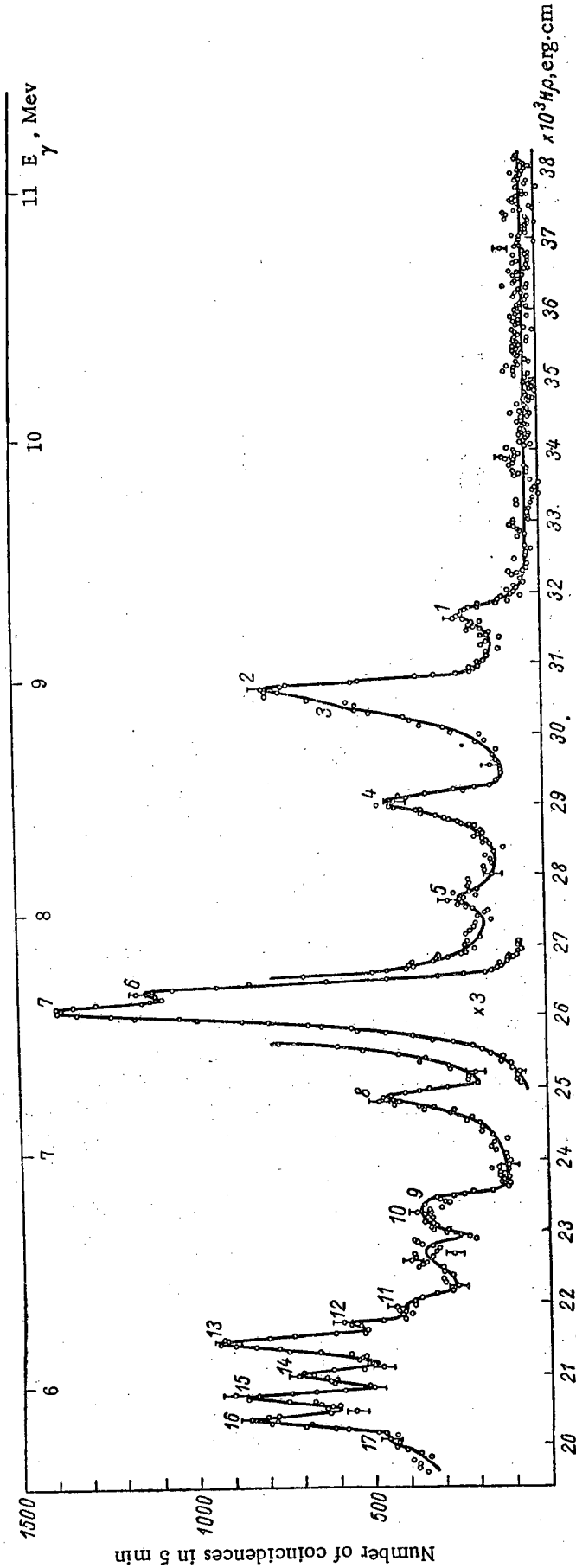

Fig. 2. Apparatus spectrum of γ-rays from the TVR reactor.

Declassified and Approved For Release 2013/02/14 : CIA-RDP10-02196R000100060003-5

Declassified and Approved For Release 2013/02/14 : CIA-RDP10-02196R000100060003-5

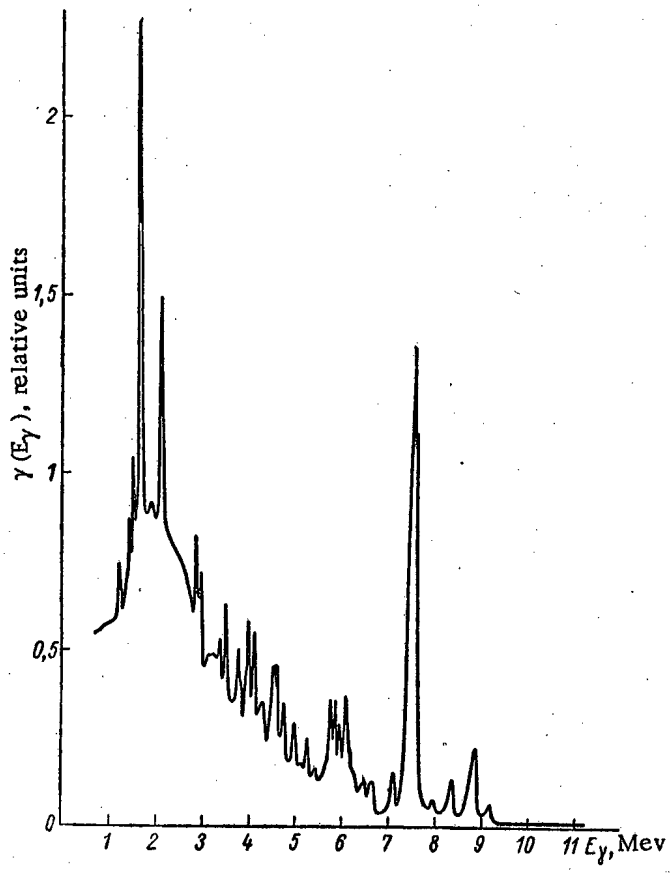

Fig. 3. Corrected apparatus spectrum of γ rays of the TVR reactor.

Consequently, γ lines with energies of 4050 and 3987 Mev can be ascribed to U^{239}. The evaluation of absolute intensity does not contradict this assumption.

The bond energy of the last neutron in U^{239}, determined on the basis of a study of the (d, p) reaction [7] is 4.63 ± 0.15 Mev, which agrees very well with the value of energy for the γ-line 25, equal to 4.640 ± 0.015 Mev. The evaluation of the absolute intensity on the assumption that the radiator is U^{239} gives a value of 1% per capture. This does not contradict the data of [6] in which this line was not observed. As can be seen from Fig. 3, a large part of the γ-radiation spectrum of the reactor is not resolved and is apparently caused by γ rays of neutron capture in U^{235} and U^{238} and γ rays of fission.

The integral intensities of the unresolved spectrum per unit of energy range (1 Mev) are as follows:

E_γ, Mev	$S_\gamma (E_\gamma) dE_\gamma$, relative units
1-2	530
2-3	512
3-4	252
4-5	149
5-6	82
6-7	35
7-8	16
8-9	10
9-10	8
10-11	7

Declassified and Approved For Release 2013/02/14 : CIA-RDP10-02196R000100060003-5

Declassified and Approved For Release 2013/02/14 : CIA-RDP10-02196R000100060003-5

Measured Spectrum of γ Rays of the TVR Reactor

Spectrum of reactor			Identification	Spectrum of reactor			Identification
No.	E_γ, Mev	I_{rel}		No.	E_γ, Mev	I_{rel}	
1	9,334(5)	1,0	Fe, 1	24	4,670(15)	(4)	Al, 10
2	9,012(3)	4,7	Ni, 1	25	4,640(15)	(3)	—
3	8,919(15)	(1,2)	Cr, 2; Fe, 2	26	(4,57)	(1)	—
4	8,533(3)	2,5	Cr, 3; Ni, 2	27	(4,46)	(3)	Al, 11
5	8,119(30)	(1)	Cr, 4; Ni, 3	28	(4,40)	(3)	Fe, 12
6	7,733(2)	28,0	Al, 1	29	4,325(15)	(2)	—
7	7,649(3)	22,6	Fe, 4	30	4,250(10)	(8)	Al, 12
8	7,275(5)	2,9	Fe, 5	31	4,202(15)	(3)	Fe, 13; Ni, 16
9	6,832(3)	1,9	Ni, 8	32	4,123(15)	(8)	Al, 13
10	6,760(30)	(1)	Al, 2	33	4,050(15)	(7)	U^{238} [4]; Fe, 14; Al(?)
11	6,404(30)	(1,7)	Fe, 6; Cr, 8	34	3,987(15)	(3)	U^{238} [4]
12	6,314(20)	(2)	Al, 3	35	3,887(14)	(5)	Al, 14
13	6,236(10)	5,4	D(n, γ)T	36	3,839(14)	(5)	Fe, 15; Al, 15 (?)
14	6,095(15)	3,6	Al, 4; Cr, 9; Ni, 11	37	3,573(7)	6,5	Al, 16; Fe, 17
15	5,997(15)	4,9	Fe, 7; Cr, 10; Ni, 12	38	3,447(17)	(4)	Al, 17; Fe, 18
16	5,904(15)	4,7	Fe, 8; Al, 5	39	3,029(6)	7,3	Al, 19; Cr, 17; Ni, 20
17	5,796(30)	(0,9)	Ni, 13	40	2,953(10)	8,3	Al, 20
18	5,557(20)	(0,9)	Cr, 11; Fe, 9	41	2,205(3)	17	H(n, γ)D
19	5,404(6)	2,8	Al, 6; Cr, 12	42	1,778(2)	43	$Al^{28} \xrightarrow{\beta} Si^{28}$
20	5,123(6)	3,4	Al, 7	43	1,594(10)	(10)	Fe, 27(?)
21	4,868(6)	4,1	Al, 8; Cr, 14	44	1,508(20)	(4)	Fe, 28(?)
22	4,788(30)	(1)	Fe, 11; Cr, 15	45	1,297(13)	(7)	Fe, 29(?)
23	4,716(10)	6	Al, 9				

Comparison of the obtained results with the data of [8] probably indicates the softening of the unresolved spectrum of γ rays as they pass through the graphite reflector of the IRT reactor, due to the repeated Compton scattering.

In conclusion the authors would like to thank the operating personnel of the TVR reactor.

LITERATURE CITED

1. B. Dzhelepov, N. Zhukovskii, and Yu. Khol'pov, Izv. AN SSSR, ser. fiz. 18, 5 (1954).
2. A. I. Alikhanov et al., Proceedings of the First International Conference on the Peaceful Uses of Atomic Energy, Geneva, 1955 (United Nations, New York, 1956); V. V. Goncharov, S. A. Gavrilov, and G. N. Karavaev, Proceedings of the Second International Conference on the Peaceful Uses of Atomic Energy, Geneva, 1958 (United Nations, New York, 1960).
3. L. V. Groshev et al., X-Ray Spectra for the Radiation Capture of Thermal Neutrons [in Russian] (Atomizdat, Moscow, 1958).
4. B. Kinsey, G. Bartholomew, and W. Walker, Phys. Rev. 83, 519 (1951).
5. L. V. Groshev et al., Atomnaya énergiya 3, 9, 187 (1957).*
6. P. Campion, J. Knowles, and G. Bartholomew, Can. J. Phys. 37, 377 (1959).
7. J. Harvey, Phys. Rev. 81, 353 (1951).
8. L. V. Groshev and A. M. Demidov, Atomnaya énergiya 7, 3, 257 (1959).*

* Original Russian pagination. See C. B. translation.

Declassified and Approved For Release 2013/02/14 : CIA-RDP10-02196R000100060003-5

Declassified and Approved For Release 2013/02/14 : CIA-RDP10-02196R000100060003-5

FINDING THE SPACE-ENERGY DISTRIBUTION OF NEUTRONS FROM A PLANE SOURCE IN AN INFINITE MEDIUM

A. R. Ptitsyn

Translated from Atomnaya Énergiya, Vol. 9, No. 3, pp. 216-217, Sept., 1960
Original article submitted March 17, 1960

In [1] a method was developed for finding the density $\psi(x, u)$ and flux $\varphi(x, u)$ of neutrons from the spatial moments

$$\psi_n(u) = \int_{-\infty}^{\infty} x^n \psi(x, u)\, dx \quad \text{and} \quad \varphi_n(u) = \int_{-\infty}^{\infty} x^n \varphi(x, u)\, dx$$

of the functions $\psi(x, u)$ and $\varphi(x, u)$. It was shown that if the problem is symmetric relative to the plane of the source, then

$$\begin{aligned} \psi(x, u) &= \beta e^{-\beta|x|} \sum_n a_n(u)\, U_n(\beta|x|); \\ \varphi(x, u) &= \gamma(\gamma x)\, e^{-\gamma|x|} \sum_n b_n(u)\, V_n(\gamma|x|), \end{aligned} \tag{1}$$

where

$$a_n = \sum_{\nu=0}^{n} \xi_{n\nu} \psi_{2\nu} \beta^{2\nu}, \quad \xi_{n\nu} = \frac{1}{2} \frac{(-1)^\nu}{(2\nu)!} C_\nu^n;$$

$$b_n = \sum_{\nu=0}^{n} \eta_{n\nu} \varphi_{2\nu+1} \gamma^{2\nu+1}, \quad \eta_{n\nu} = \frac{1}{2} \frac{(-1)^\nu}{(2\nu+1)!} C_{\nu+1}^{n+1}; \tag{2}$$

$U_n(x)$ and $V_n(x)$ are polynomials defined by the equations

$$U_n(x) = \frac{(-1)^n}{2^n n!} \left[\frac{\partial}{\partial x} - 1\right]^{2n} \sum_{j=0}^{n} \frac{(n+j)!}{j!\,(n-j)!\,2^j} x^{n-j}; \tag{3}$$

$$V_n(x) = \frac{1}{2(n+1)} \left[\frac{\partial}{\partial x} - 1\right]^2 U_n(x)$$

and the conjugate polynomials

$$U_n^+(x) = \sum_{\nu=0}^{n} \xi_{n\nu} x^{2\nu}; \quad V_n^+(x) = \sum_{\nu=0}^{n} \eta_{n\nu} x^{2\nu+1} \tag{4}$$

Declassified and Approved For Release 2013/02/14 : CIA-RDP10-02196R000100060003-5

Declassified and Approved For Release 2013/02/14 : CIA-RDP10-02196R000100060003-5

so that

$$\int_{-\infty}^{\infty} e^{-|x|} U_n(x)\, U_{n'}^{*}(x)\, dx = \delta_{nn'};$$
$$\int_{-\infty}^{\infty} x e^{-|x|} V_n(x)\, V_{n'}^{*}(x)\, dx = \delta_{nn'}. \tag{5}$$

Since, in practice, a finite number of moments only can be found, it is necessary to be restricted by an approximation, where the series in Eq. (1) contains a finite number of terms. In this case it is not possible to ensure a specified accuracy (at a given distance x_0) for all values of the energy variable u, if we use parameters β and γ that do not depend on u. One possible approach to finding $\beta(u)$ and $\gamma(u)$ is proposed in the present communication.

Since $\psi(x, u)$ is an even and $\varphi(x, u)$ an odd function of x, for the function $\psi(x)$ only even moments will have nonzero values, while for $\varphi(x)$ only odd.

Let us assume that N + 1 even moments of the function $\psi(x, u)$ are known. Then approximating the (N + 1)th function $\psi(x, u)$ by the (N + 1)th term of the series (1) will yield

$$\psi^{(N+1)}(x, u) = \beta e^{-\beta|x|} \sum_{n=0}^{N} a_n(u)\, U_n(\beta\,|\,x\,|). \tag{6}$$

From the definition of spatial moment, N + 1 of the even moments of the function $\psi^{(N+1)}(x, u)$ for any value of β will coincide with the corresponding moments of the desired function $\psi(x, u)$.

We now require that the function of the Nth approximation

$$\psi^{(N)}(x, u) = \beta e^{-\beta|x|} \sum_{n=0}^{N-1} a_n(u)\, U_n(\beta\,|\,x\,|) \tag{7}$$

give the proper value for the (N + 1)th (even) moment; i.e.,

$$\psi_{2N}^{(N)}(\beta) = \psi_{2n}(u), \tag{8}$$

from which follows an equation for determining $\beta(u)$. We want to write it in explicit form. Multiplying Eq. (7) by $(\beta x)^{2N} = \sum_{p=0}^{n} q_{Np} U_p^{+}(\beta x)$, integrating it over all space, taking due account of Eq. (5), and equating $\psi_{2N}^{(N)}$ according to Eq. (8) to the exact value of $\psi_{2N}(u)$, we obtain

$$\beta^{2N}\psi_{2N} = \int_{-\infty}^{\infty} e^{-\beta|x|}\Big(\sum_{n=0}^{N-1} a_n U_n(\beta\,|\,x\,|)\Big)\Big(\sum_{p=0}^{N} q_{Np} U_p^{+}(\beta x)\Big) = \sum_{n=0}^{N-1} a_n q_{Nn}.$$

Substituting here the values of the coefficients a_n from (2), we find an Nth degree equation for $\beta^2(u)$:

$$\psi_{2N}(u)\,(\beta^2)^N \sum_{\nu=0}^{N-1} A_\nu(u)\,(\beta^2)^\nu, \tag{9}$$

where

$$A_\nu(u) = \psi_{2N}(u) \sum_{n=\nu}^{n-1}$$

Declassified and Approved For Release 2013/02/14 : CIA-RDP10-02196R000100060003-5

Declassified and Approved For Release 2013/02/14 : CIA-RDP10-02196R000100060003-5

Values of the Neutron Spatial Distribution Function

x	$-\lg \varphi(x)$	
	from Eq.(13)	from [2]
0	1,10	1,05
1	1,08	1,06
2	1,10	1,09
4	1,21	1,24
5	1,31	1,34
10	2,11	2,10
15	3,03	3,07
20	4,32	4,25

Of the N roots of this equation, we select the required real positive root β_0^2. The root $\beta_0(u)$ is then substituted into the solution (6):

$$\psi^{(N+1)}(x,\ u)=\beta_0(u)\,e^{-\beta_0(u)|x|}\sum_{n=0}^{N}a_n(u)\,U_n[\beta_0(u)|x|]. \tag{10}$$

For $\gamma^2(u)$, which determines the neutron flux $\varphi(x, u)$, as in Eq. (9), we obtain an Nth degree equation:

$$\varphi_{2N+1}(u)(\gamma^2)^N=\sum_{\nu=0}^{N-1}B_\nu(u)(\gamma^2)^\nu,$$

where

$$B_\nu(u)=\varphi_{2\nu+1}(u)\sum_{n=\nu}^{N-1}\varrho_{Nn}\eta_{N\nu},$$

and ρ_{Nn} are coefficients of the expansion of x^{2N+1} into the polynomials $V_n^+(x)$:

$$x^{2N+1}=\sum_{n=0}^{N}\varrho_{Nn}V_n^+(x).$$

In particular, when four (N + 1 = 4) spatial moments of the neutron density $\psi(x, u)$ are known, Eq. (9) takes on the form

$$\psi_6(u)(\beta^2)^3-45\psi_4(u)(\beta^2)^2+540\psi_2(u)\beta^2-720\psi_0(u)=0. \tag{12}$$

As an example of the application of the method described, we determine the density distribution of neutrons in hydrogen from four moments, assuming the range to be constant (λ = 1), and compare the solution obtained

$$\psi(x,\ u)=\beta_0(u)\,e^{-\beta_0(u)|x|}\sum_{n=0}^{3}a_n(u)\,U_n[\beta_0(u)\ |x|] \tag{13}$$

with the exact solution of Wick [2], which was calculated for a value of the energy variable u = 10.

Let us take the values of the moments from [3] for u = 0 and u = 10:

Declassified and Approved For Release 2013/02/14 : CIA-RDP10-02196R000100060003-5

Declassified and Approved For Release 2013/02/14 : CIA-RDP10-02196R000100060003-5

$$\psi_0(0)=1,\ \psi_2(0)=2!,\ \psi_4(0)=4!,\ \psi_6(0)=6!,\ \psi_0(10)=1,\ \frac{1}{2!}\psi_2(10)=10{,}667,$$

$$\frac{1}{4!}\psi_4(10)=65{,}578,\ \frac{1}{6!}\psi_6(10)=278{,}44. \tag{14}$$

Then if u = 0, we have $\beta_0(0) = 1$, $a_0(0) = \frac{1}{2}$, $a_1 = a_2 = a_3 = 0$, $\psi(x,0) = \frac{1}{2}e^{-|x|}$. It is easily seen that this is the exact solution of the kinetic equation. If u = 10, then for $\beta_0(10)$ and $a_n(10)$, we obtain from Eqs. (2) and (12) $\beta_0(10) = 0.351$, $a_0 = 0.5$, $a_1 = -0.158$, $a_2 = -0.318$, $a_3 = -0.241$. Substituting these values into Eq. (13), we find $\psi(x,10)$. A comparison of the results obtained with the solution of Wick is made in the table.

It is seen that four moments give an approximation of $\psi(x,u)$ up to 20 times the mean free path.

LITERATURE CITED

1. L. Spencer and U. Fano, J. Res. Nat. Bur. Standards 46, 446 (1951).
2. G. Wick, Phys. Rev. 75, 738 (1949).
3. A. R. Ptitsyn, Collection: Neutron Physics [in Russian] (Atomizdat, Moscow, 1960) (in press).

Declassified and Approved For Release 2013/02/14 : CIA-RDP10-02196R000100060003-5

Declassified and Approved For Release 2013/02/14 : CIA-RDP10-02196R000100060003-5

A SIMPLE MULTICHANNEL PULSE-HEIGHT ANALYZER

V. F. Mikhailov

Translated from Atomnaya Énergiya, Vol. 9, No. 3, pp. 217-219, Sept., 1960
Original article submitted May 28, 1960

The great possibilities arising in connection with the use of pulse-height analyzers in experiments involving the study of the radiation spectra of radioactive substances are frequently not taken advantage of, owing to the complexity of constructing analyzers in laboratory conditions. However, for the solution of many problems whose scope is limited to the study of samples of weak activity, the analyzer circuit can be considerably simplified and made very stable.

Below, we shall discuss a circuit which, when connected to a recording potentiometer, gives good results.

Figure 1 shows the diagram of a circuit which shapes pulses of amplitude proportional to the amplitude of an input pulse of given duration equal to the time interval between two operations of the printing device. It is convenient to use with the analyzer a potentiometer of the ÉPP-09 type with a pen carriage and millivoltmeter scale.

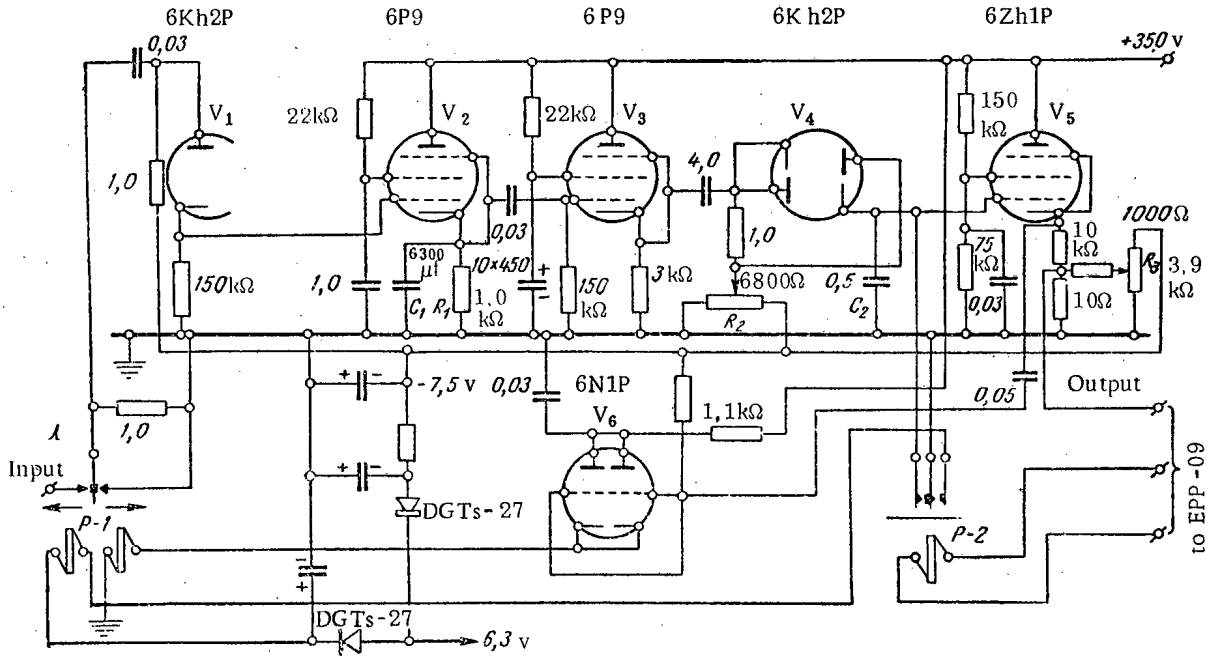

Fig. 1. Schematic diagram of the pulse-shaping circuit.

A short pulse from the output of the amplifier is clipped by the diode discriminator V_1 and fed to the control grid of the first cathode follower V_2. At the output of this cathode follower, a pulse is formed proportional in amplitude to the initial pulse, but with a longer trailing edge depending on the time constant R_1C_1. The

Declassified and Approved For Release 2013/02/14 : CIA-RDP10-02196R000100060003-5

Declassified and Approved For Release 2013/02/14 : CIA-RDP10-02196R000100060003-5

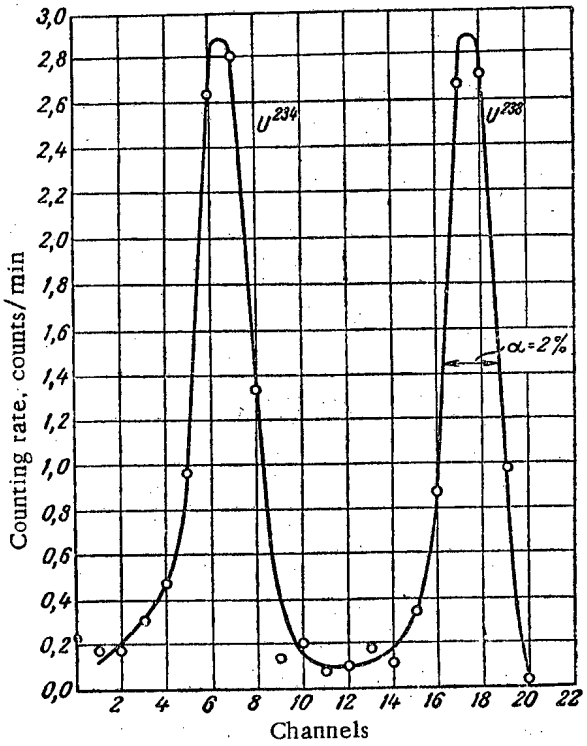

Fig. 2. Energy distribution curve for pulses from α particles from uranium isotopes.

second cathode follower V_3 charges the "memory" condenser C_2 through a 6Kh2P diode (V_4) to the height of the pulse. The circuit output is obtained from the 6Zh1P cathode follower, whose control grid draws practically no current. Owing to this arrangement, the charge on the condenser C_2 does not change, at least not during the time necessary for the operation of the potentiometer printing mechanism (up to 12 sec).

From the cathode of V_5 the pulse causes the tube V_6 to conduct and actuates the polarized blocking relay, which grounds the input circuit. During the operation of the printing device, relay P-2, connected in parallel with the solenoid of the printer, discharges the "memory" condenser and throws the armature of relay P-1 back to its initial position.

The potentiometer R_2 provides a negative bias for the diode V_4 in order to prevent the charging of the memory condenser as a result of the ac background from the filament current of the tube.

Potentiometer R_3 is used as the zero adjustment of the potentiometer pen carriage. The paper record chart can be divided into channels, as required. The deflection of the pen carriage to the right is proportional to the input pulse height.

The circuit has a linear amplitude characteristic up to 100 volts at the input. The spread of a standard pulse does not exceed 2 mm. The analyzer circuit is very stable for lengthy measurements; the zero line remains practically in one place over several days. The difficulty in deciphering (visual reading of the points for the channels) is compensated by the stable operation of the equipment and the clarity of the obtained data. Figure 2 shows the channel (amplitude) distribution constructed by deciphering the record of pulses from α particles of uranium isotopes (U^{234} and U^{238}) obtained from a pulse ionization chamber.

The author expresses his sincere gratitude to E. M. Kolesnikov for aid in constructing the circuit.

Declassified and Approved For Release 2013/02/14 : CIA-RDP10-02196R000100060003-5

Declassified and Approved For Release 2013/02/14 : CIA-RDP10-02196R000100060003-5

INVESTIGATION OF THE SYSTEMS Al_2O_3–Sm_2O_3 AND Al_2O_3–Gd_2O_3

S. G. Tresvyatskii, V. I. Kushakovskii, and V. S. Belevantsev

Translated from Atomnaya Énergiya, Vol. 9, No. 3, pp. 219-220, Sept., 1960
Original article submitted March 24, 1960

The systems Al_2O_3–Sm_2O_3 and Al_2O_3–Gd_2O_3 have already been studied in preliminary fashion. For example, in [1, 2] it was shown that in these systems the compounds $SmAlO_3$ and $GdAlO_3$, which have the perovskite structure, are formed. In [3] the probable fusibility diagrams of the indicated systems are given, the melting temperatures of the compounds formed in them are determined, experimental values are cited for the solidus and liquidus temperatures in the interval 1700-1820°C. However, the solidus and liquidus temperature curves in the interval 1820-2300°C are constructed provisorily in [3] and are plotted on broken-line diagrams, while the melting temperature of the eutectic between Gd_2O_3 and $GdAlO_3$ and its composition are not even preliminarily evaluated.

The authors experimentally determined the solidus and liquidus temperatures in the systems Al_2O_3 – Sm_2O_3 and Al_2O_3–Gd_2O_3 in the temperature interval 1700-2350°C by means of high-temperature thermal analysis, following the procedure of [4, 5]. Calibrated tungsten–molybdenum thermocouples were used: heating and cooling curves were recorded with an electronic potentiometer. This made it possible to construct the state diagrams of these systems with a higher degree of accuracy and reliability than in [3].

For the initial materials we chose Sm_2O_3 and Gd_2O_3, containing more than 99.5% by weight of the base component (the main impurities were other rare earth oxides), and Al_2O_3 of ChDA quality.

Chemical analysis showed that after thermoanalysis, the Al_2O_3 in the alloys was less than in the corresponding charge compositions of the mixtures. This difference increased with increasing Al_2O_3 in the charge compositions, but never exceeded 2-3 molecular percent in the region rich in Al_2O_3. In this connection, when determining the solidus and liquidus temperatures no corrections were made for the evaporation of Al_2O_3 (because of their insignificance).

It was established by thermal analysis that the eutectic from the Al_2O_3 side in the system Al_2O_3–Sm_2O_3 (Fig. 1) is melted at a temperature of 1770 ± 20°C and the system Al_2O_3–Gd_2O_3 (Fig. 2) at 1760 ± 20°C. The eutectic from the side of the rare earth oxide in the system Al_2O_3–Sm_2O_3 has a melting point of 1860 ± 20°C and in the system Al_2O_3–Gd_2O_3 of 1930 ± 20°C. The compounds $SmAlO_3$ and $GdAlO_3$ are melted without decomposing at practically the same temperature, equal to 2060 ± 20°C.

Investigations in reflected light of the microstructure of the alloys after thermoanalysis showed that in alloys containing 0 – 20 mol. % of the rare earth oxide, the Al_2O_3 is initially crystallized, for 25 – 70 mol. % the compounds $SmAlO_3$ or $GdAlO_3$, correspondingly, and for 75 – 100 mol. % Sm_2O_3 or Gd_2O_3.

On the basis of the studies of microstructure of the alloys, it may be assumed that their eutectics lie between compositions containing 20 and 25 mol. % rare earth oxide (low-melting eutectic), 70 and 75 mol. % (high-melting eutectic).

Declassified and Approved For Release 2013/02/14 : CIA-RDP10-02196R000100060003-5

Declassified and Approved For Release 2013/02/14 : CIA-RDP10-02196R000100060003-5

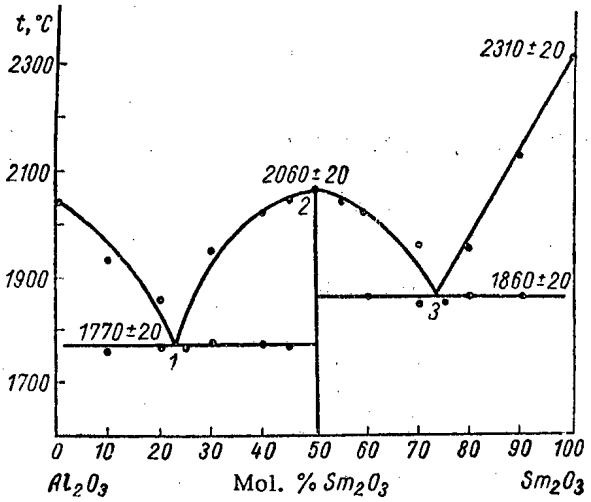

Fig. 1. Solidus and liquidus of the system Al_2O_3 – Sm_2O_3.

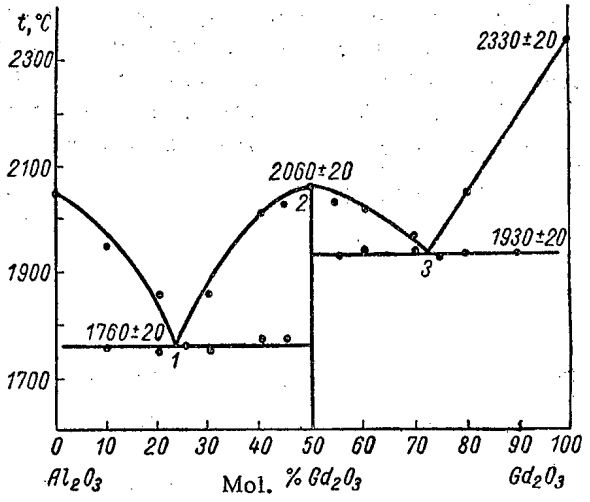

Fig. 2. Solidus and liquidus of the system Al_2O_3–Gd_2O_3.

Invariant Points in the Systems Al_2O_3–Sm_2O_3 and Al_2O_3–Gd_2O_3 at Temperatures of 1700°C and Above

Points in Figs. 1 and 2	Phase	Reaction	Data of [3]			Data of present paper		
			temperature, °C	composition, mol.%		temperature, °C	composition, mol.%	
				Al_2O_3	R_2O_3		Al_2O_3	R_2O_3
		System Al_2O_3—Sm_2O_3						
1	Al_2O_3+$SmAlO_3$	Eutectic	1720±20	80	20	1770±20	77	23
2	$SmAlO_3$	Incongruent melting	1920±20	50	50	2060±20	50	50
3	Sm_2O_3+$SmAlO_3$	Eutectic	1860±40	73	27	1860±20	73	27
		System Al_2O_3—Gd_2O_3						
1	Al_2O_3+$GdAlO_3$	Eutectic	1740±20	80	20	1760±20	77	23
2	$GdAlO_3$	Incongruent melting	1980±40	50	50	2060±20	50	50
3	Gd_2O_3+$GdAlO_3$	Eutectic	no data	no data	no data	1930±20	73	27

The investigations of microstructure of specimens quenched from temperatures of 1700-1950°C revealed that in specimens containing more than 1 mol. % of the rare earth oxide, as in the specimens containing less than 99 mol. % of the rare earth oxide, two phases are present. This indicates that in the systems Al_2O_3 – Sm_2O_3 and Al_2O_3–Gd_2O_3, the oxides are not noticeably soluble in the solid state.

In the table are cited the invariant points in the systems Al_2O_3–Sm_2O_3 and Al_2O_3–Gd_2O_3, and these are compared with the data of [3]. From the table it follows that our data at the points 1, 2, and 3 in the system Al_2O_3–Sm_2O_3 coincide with the data of [3] regarding composition, but there is a discrepancy in the melting points for the points 1 and 2. The values we determined for the temperatures at these points are higher by 50 and 140°C, respectively. In the system Al_2O_3–Gd_2O_3, a discrepancy is observed in the melting point for point 2. The values we found are approximately 80°C higher in comparison with the data given in [3]. For point 3 of this system, no data is given in [3] on either the composition or temperature. Our data for point 1 of the system Al_2O_3–Gd_2O_3 is in satisfactory agreement with the data of [3] both in composition and in temperature.

Declassified and Approved For Release 2013/02/14 : CIA-RDP10-02196R000100060003-5

Declassified and Approved For Release 2013/02/14 : CIA-RDP10-02196R000100060003-5

LITERATURE CITED

1. M. Keith and R. Roy, Amer. Mineralogist 39, 1, 1 (1954).
2. C. Curtis and J. Johnson, J. Amer. Ceram. Soc. 40, 1, 15 (1957).
3. F. Aldred and A. White, Trans. Brit. Ceram. Soc. 58, 4, 199 (1959).
4. P. P. Budnikov and S. G. Tresvyatskii, Ogneupory, No. 4, 167 (1955).
5. S. G. Tresvyatskii, V. I. Kushakovskii, and V. S. Belevantsev, Ogneupory. No. 4, 180 (1960).

Declassified and Approved For Release 2013/02/14 : CIA-RDP10-02196R000100060003-5

Declassified and Approved For Release 2013/02/14 : CIA-RDP10-02196R000100060003-5

NEWS OF SCIENCE AND TECHNOLOGY

ALL-UNION CONFERENCE ON THE ASSIMILATION OF RADIOACTIVE TRACER TECHNIQUES AND NUCLEAR RADIATION APPLICATIONS IN THE NATIONAL ECONOMY OF THE USSR

The All-Union Conference on the Assimilation of Radioactive Tracer Techniques and Nuclear Radiation Applications in the National Economy of the USSR met in Riga, April 12 to 16, 1960, under the auspices of the State Science and Technical Committee of the Council of Ministers of the USSR. The State Committee of the Council of Ministers of the USSR on uses of atomic energy, the Academies of Sciences of the various republics of the USSR, the State Committee of the Council of Ministers of the USSR on Automation and Machine Design, and the Council of Ministers of the Latvian SSR were co-sponsors.

The Conference was inaugurated by J. V. Peive, Chairman of the Council of Ministers of the Latvian SSR.

Over 700 delegates were in attendance, these including representatives of the Council of Ministers of the USSR and of the councils of ministers of the sister republics, chairman of state planning board, state committees, Council of the National Economy, of factories and enterprises throughout the nation, and of science research institutes.

One-hundred and sixty-seven reports and communications were read. Panels were formed at the Conference on prospecting and mining of minerals, metallurgy, mining and ore processing, construction and structural materials industry, light industry, machine design, radiation chemistry, chemical processing and petroleum processing industries, agriculture, food industry, medicine, and instrumentation based on the use of radioactive sources.

Two plenary sessions were held, at which reports were presented on the status and perspectives of the assimilation of radioactive techniques in the national economy (P. S. Savitskii, State Committee on Uses of Atomic Energy attached to the Council of Ministers of the USSR), on experience accumulated in the adaptation of radioactive tracer techniques in enterprises of the Latvian council of the national economy (G. I. Gaile, Latvian council of the national economy), on the economics of radioactive isotope applications in industry (G. F. Mikheev, Institute of Economics of the USSR Academy of Sciences), on the perspectives of the use of instruments using radioactive sources for automating manufacturing processes in various branches of industry (V. S. Sokolov, State Committee of the USSR Council of Ministers on Automation and Machine Design), on the perspectives of industrial applications of radiation chemistry in the USSR and outside (V. L. Karplov, L. Ya. Karpov Physical Chemistry Research Institute), on the status of and measures for enhancing safe working conditions where ionizing radiations are being handled (P. I. Moiseitsev, Health Ministry of the USSR), on new industrial monitoring and measuring instrumentation for work with radioactive isotopes (S. V. Mamikonyan, V. S. Zhirnov, State Committee of the Council of Ministers of the USSR on Uses of Atomic Energy), and an informative report on the present order of delivery and shipping of isotopes and on shielding techniques (I. I. Kolomytov, All-Union "Isotop" office).

The Riga Conference was the first large-scale gathering offering an exchange of experience on the assimilation of tracer and nuclear radiation techniques in the national economy. This also determined the composition of the participants of the Conference, the proceedings of which were contributed to predominantly by representatives from factories, mills, and councils of national economy units. Reports by workers from research institutes and in-plant laboratories on work leading to and resulting in the assimilation of such techniques in industry were also heard.

Declassified and Approved For Release 2013/02/14 : CIA-RDP10-02196R000100060003-5

Declassified and Approved For Release 2013/02/14 : CIA-RDP10-02196R000100060003-5

In the course of the Conference, the participants took advantage of the opportunity to become acquainted with radioactive tracer applications in the industries of Riga.

Concrete measures for further expansion of the utilization of radioisotopes and nuclear radiations in industry were spelled out in the resolution adopted at the Conference. In particular, attention was focused on the improvement of coordination of research work and on work geared toward assimilation of radioisotopes and radiations in the national economy, on the intensification of scientific research work geared toward development of high productive means of quality control and process control, expansion of the training of engineering and technician cadres for research and engineering-drafting work on industrial uses of isotopes and radiations, as well as on the operation of the related equipment.

Below, grouped under the proper headings, we survey the problems taken up in the various panel sessions.

The proceedings of the Conference will be published during 1960.

USES OF RADIOACTIVE ISOTOPES AND NUCLEAR RADIATIONS IN PROSPECTING AND DEVELOPMENT OF MINERAL RESOURCES

F. A. Alekseev

The Conference completed a program of intense and useful work and exchange of experience on the assimilation of new and efficient techniques into mineral prospecting and exploration practice. The Conference also heard extensive information submitted by representatives of research institutes, on new developments in this area of work.

The reports delivered presented evidence that, as a result of the development of nuclear physics, atomic industry, and measurement techniques, new geophysical methods in prospecting, exploration, and development of mineral resources, based on the use of radioactive isotopes and nuclear radiations, have come to the fore and have been firmly put into practice. The economic benefits resulting from the use of radioactive logging techniques during 1959, at petroleum and coal fields alone, amounted to about 600 million rubles.

In the exploration of oil and gas fields, gamma logging and neutron-gamma logging methods are being used to map rock strata and correlate borehole cross sections. The advantages of these techniques reside, as is the case for other radiometric techniques when compared to electrical methods, in the possibility of studying steel-cased boreholes.

Techniques of neutron-gamma logging, neutron-neutron logging, and induced activity have been successfully employed, under favorable conditions, in mapping the position of the oil-water contact surface in the process of developing petroleum fields. In addition, the possibility of employing the method of induced activity to monitor the flow of formation water was demonstrated.

Reports by representatives of the Tatar Council of the National Economy and of the Volga-Ural branch of the All-Union Science Research Institute of Geophysics showed that neutron techniques are excellent tools for monitoring the development of the nation's largest oil deposit, the Romashki field. Neutron techniques were applied to the study of 229 oil wells in 1959.

The distribution of casing cement outside the casing string, following completion of oil wells, is being monitored by gamma logging and gamma-gamma logging techniques.

Radioactive isotopes are being used in the exploration of petroleum and gas fields to determine the break points of casing tubes, sites of water infiltration into cased holes, locating thief zones where drilling mud seeps out of the well, monitoring the hydraulicking of oil beds. Most of these tasks resist solution by virtually all other geophysical techniques, while the remainder are handled more readily, more precisely, more reliably, and more economically by radiometry techniques.

Declassified and Approved For Release 2013/02/14 : CIA-RDP10-02196R000100060003-5

Declassified and Approved For Release 2013/02/14 : CIA-RDP10-02196R000100060003-5

The depth of coal seams, their thickness, and their structure may be determined by combined gamma-gamma logging and electrical logging in coal fields.

Coals of all stages of coal metamorphosis existing under varying geological conditions can be reliably mapped by including gamma-gamma logging techniques in the repertory of logging research tools used to investigate coal fields. The sharply increasing efficiency of logging techniques has made it possible to formulate rules for the use of logging data in calculating coal-in-place, and affords the possibility of greatly increasing economic returns and quality of exploration work.

Gamma-gamma logging yields completely reliable results in tracing boron-bearing zones in borehole cross sections, resulting in a sharp cut in the time required for sampling rock cuttings. Anomalies due to presence of water are eliminated by this technique, which provides a tentative estimate of the content of boron anhydride, within limits of 0.1-10.0%.

Photoneutron logging is being employed with success in the exploration of beryllium deposits. Mapping of ore zones in borehole sampling, with estimates of the quantitative beryllium content to within 0.01% accuracy, has become possible.

A highly interesting communication on the use of photoneutron logging for calculating beryllium reserves must be noted.

Equipment for determining the content of boron and beryllium in samples has been developed and is in use, facilitating the processing of logging data and the reduction of the volume of chemical analyses required.

A method of selective gamma-gamma logging to delineate ore zones of relatively heavy elements (Fe, Pb, W, Hg, etc.) to an accuracy of 0.2% has been tested and is in use. Use of this technique yields well-defined anomalies for all conditional lead contents. Excellent agreement between selective gamma-gamma logging data and results of sampling has been found for siderite ores.

Positive results were obtained in the adoption and assimilation on a production basis of neutron logging and activation logging techniques applied to bauxite, manganese, and copper deposits.

The labeled-atom technique is being used in oil fields. In particular, an application has been found for tritium as a monitor of water flow in oil seams, and in determining the hydrodynamic relations obtaining between discrete oil strata.

At the Karabulak-Achikulak oil field, tritium has been successfully used to establish the hydrodynamic relationship of two thick oil deposits lacking any direct communication, and the application was of great value in finding out the best way of developing the entire oil reservoir.

An interesting report was made on methods and equipment for determining natural tritium. The high sensitivity of natural tritium measurements made it possible to use this method for a broad range of applications going beyond the solution of hydrogeological and hydrological tasks to the study of various geophysical media (motions of atmospheric air masses, of water masses in oceans, etc.).

Opportunities for isotope and nuclear radiation applications are nowhere near exhausted by the techniques known at present. For instance, highly promising results were obtained in 1959 by testing out pulsed neutron techniques and borehole neutron generators. The use of neutron generators inside the borehole increased the depth at which radiometry of the boreholes can be successfully pursued, thus assuring reliable monitoring of the migration of water-oil and gas-fluid interfaces while the oil fields are being developed, including here the process of removing salt from edgewater, and significantly widens the range of applications of neutron logging methods in the exploration and development of mineral deposits.

An appreciable increase in the efficiency of radioactive logging used in studying the composition of rocks and ore by elements is achieved, as has been demonstrated by some investigations, by gamma-ray spectrometry. A new (x-ray) method has been developed for high-speed ultimate analysis of materials.

A high-efficiency neutron measuring equipment (the "Neitron" facility) has been designed for high-speed ultimate analysis of boron, lithium, cadmium, and several other elements.

However, the report noted the fact that positive experience amassed in the assimilation of radiation and tracer techniques in mineral prospecting practice has not been accompanied by anywhere near adequate

Declassified and Approved For Release 2013/02/14 : CIA-RDP10-02196R000100060003-5

Declassified and Approved For Release 2013/02/14 : CIA-RDP10-02196R000100060003-5

exploitation of the possibilities inherent in radiometric techniques. The radiometric methods employed in oil and gas fields have resulted in the successful solution of only a limited range of problems. Methods for sure determination of porosity and petroleum saturation are yet to be worked out. In the exploration of ore deposits and nonore minerals, methods of proved efficiency have yet to be integrated into standard practice.

In some coal fields where electrical logging methods are not sufficiently efficient, gamma-gamma logging techniques have not been included in the logging research program as yet. Work on analysis of the economic efficiency of over-all geophysical research following the adoption of radiometric techniques is lagging.

The integration of the radiometric methods, whose efficiency has already been demonstrated, into prospecting, exploration, and development practice, and the full exploitation of the possibilities opened up by these techniques constitute an unpostponable task of enormous significance for the entire national economy.

USES OF RADIOACTIVE ISOTOPES AND NUGLEAR RADIATIONS IN METALLURGY

P. L. Gruzin and Yu. F. Babikova

Research and practical investigations in metallurgy where tracer and radiation applications are important were begun during 1948-1949 in the USSR. The following general trends took shape: use of radioactive and stable isotopes as tracers (labeled atoms), use of high-level radiation sources and of radioactive isotopes in process monitoring and control.

Under actual production conditions, radioactive isotopes found their first application historically in the Novaya Tula Metallurgical Plant and in the Kuznetsk Metallurgical Combine. At the present time, radioactive isotopes are in use in many enterprises.

One of the principal tasks in the use of isotopes in pig iron production is the working out of new ways of increasing the output of blast furnaces, and the solution of problems related to the automating of separate units. Work is being pursued on radiometric methods for monitoring the flow of burden materials and monitoring hot spots in the refractory lining of blast furnaces, on tracer techniques for monitoring coke density, agglomerate, and level of furnace charge. The use of radioactive isotopes to determine the optimum conditions for desulfurization of pig iron by magnesium metal and by lime and clay slags has yielded positive results. Tracers are also being used to solve some problems related to the study of the performance of blast-furnace tuyeres.

Experimental radiometric equipment for monitoring charge level in a blast furnace has been installed at the Dzerzhinskii Plant. Test results showed the feasibility of utilizing this equipment in other metallurgical plants. Similar equipment is being developed to determine the amount of ore dust removed from blast furnaces. A proposal has been made to employ a servo technique to set up a continuous measurement and control loop.

The Central Ferrous Metallurgy Research Institute and the Dzerzhinskii Plant have collaborated in elaborating and testing a procedure for control of burden materials. Existing methods of burden control are not capable of facilitating rapid determinations of the size of individual lumps of burden materials directly prior to their being charged into the furnace. The radiometric method of burden control makes it possible to continuously monitor changes in density of the materials charged. Similar work is being approached at the Kuznetsk Metallurgical Combine and in other plants.

The output of blast furnaces is to a considerable extent determined by the prior processing of iron ore stock. An important link in the preparatory process is control over the beneficiation of the iron ores and over sintering of agglomerate. Experience in the use of radioactive isotopes during the pretreatment of iron ore stock has also proved them efficient. A radiometer intended for determinations of agglomerate density has been designed at the Kuznetsk Metallurgical Combine. Tests of this device in an agglomerate mill have shown that it serves well for monitoring the ore sintering process which yields the agglomerate.

Declassified and Approved For Release 2013/02/14 : CIA-RDP10-02196R000100060003-5

Declassified and Approved For Release 2013/02/14 : CIA-RDP10-02196R000100060003-5

Wear on furnace liners and mixers is being monitored at several factories by radioactive inserts and radiometric probes, by means of which the state of the lining is being closely monitored even with the furnace in operation. The Kuznetsk Metallurgical Combine, the Dzerzhinskii Plant, the "Azovstal' " Plant, the Makeev Metallurgical Plant, and other enterprises are currently employing radiometric techniques to monitor wear on the refractory brickwork of blast furnaces.

According to preliminary data supplied by the Dzerzhinskii Plant and the Institute of Economics of the USSR Academy of Sciences, use of results on blast furnace investigations involving isotope tracers has made it possible to cut fuel costs and increase pig iron melts by about 80 thousand tons, corresponding to 2.5 millions of rubles saved annually, in money terms. Tentative calculations indicate that the adoption of radiometric techniques for monitoring sintering of agglomerate at the Kuznetsk Metallurgical Combine may yield annual savings of about 2 million rubles. These investigations also contributed to the improvement of the design of various blast furnace components and subassemblies. This applies in the first instance to the shafts and hearths of blast furnaces (plants in the Kuznetsk Metallurgical Combine, the Manitogorsk Metallurgical Combine, the Il'ich and Dzerzhinskii Plants). The economical efficiency which may be tapped by use of isotopes in blast furnace production is difficult to estimate, since other research on improving the process is pursued simultaneously. Interesting data are available from the Dzerzhinskii Plant, from which we learn that the use of isotope tracers in conjunction with other research resulted in a 2.5-3% increase in pig iron output, reduction of 3-3.5% in fuel costs, and a 5-8% increase in blast furnace life.

Radioactive isotope tracers are being used to good advantage in many applications in the steelmaking industry, at present, to improve steelmaking technology.

At the Magnitogorsk Metallurgical Combine, tracer studies are being made of the slag-forming process, the result being an optimization of the charging sequence for charging open-hearth furnaces. Similar work has been conducted at the "Azovstal' " Plant and at the Stalino Metallurgical Plant.

The isotope dilution technique has been used at the "Azovstal'," Stalino, and Zaporozhstal' Plants to determine the rate of melting of scrap and the weight of molten steel in open-hearth furnaces during the melt. At the Kuznetsk Metallurgical Combine, isotopes were used to determine the hydrodynamic characteristics of the smelting bath, leading to new approaches in shortening the time of the melt, i.e., increasing by the same token the output of steel in existing open-hearths by tens of thousands of tons without incurring additional expense. At the Il'ich Plant, use of isotopes made possible a reduction of the dwell time of metal in casting molds, an improvement which is directly linked to increased output in open-hearth workshops.

A study of the nature of nonmetallic inclusions by means of radioactive tracers was carried out at the Kuznetsk and Magnitogorsk Metallurgical Combines, at the Serov Combine, at the Stalino Chelyabinsk, "Serp i molt," "Dneprospetsstal'," "Elektrostal' " Plants, and in Institutes.

Radiometric techniques for monitoring weak on the refractory lining of open-hearth furnaces have been developed at the Kuznetsk Metallurgical Combine, the Makeev Metallurgical Plant, and the "Azovstal'" Plant, with a consequent reduction of 30-40 min in the time required for overhaul of open-hearth furnaces.

There is a great interest in the work carried out at the Kuznetsk Metallurgical Combine and the Stalino Metallurgical Plant investigating the process of metal flow during rolling. These data are needed to arrive at a rational calibration of rolling rods.

Radioactive isotopes of iron and lead are being used to work out a new technology in tinplating. The results of this research are being used in the practical work of the Novaya Moskva and "Zaporozhstal' " Plants.

Science research institutes and metallurgical plants have elaborated a variety of radiometric instruments with applications in metallurgy for the monitoring of variables and process control.

Laboratories of the Central Research Institute for Ferrous Metallurgy have produced instrumentation for measuring the liquid-metal level in the crystallizers of continuous casting machines. Level gages are being used at present in several factories. Cupola charging was automated at the Khartsyz tubing factory by employing radiometric level gages. The May First Mill at Kalinin is employing liquid-metal level controllers in crystallizers, controlling the speed at which ingots are drawn. A similar control system was incorporated in a facility of semicontinuous casting of cast-iron tubes at the Sinar tubing factory, and is being assembled at the Moghilev Metallurgical Plant. The use of a liquid-metal level controller in the crystallizer of a continuous steelcasting machine opens the way for completely automating the teeming process.

Declassified and Approved For Release 2013/02/14 : CIA-RDP10-02196R000100060003-5

Declassified and Approved For Release 2013/02/14 : CIA-RDP10-02196R000100060003-5

A level gage has been developed at the Stalino Metallurgical Plant to determine the amount of dust trapped in the dust catchers of blast furnaces. At the Makeev Metallurgical Plant, a radiometric annunciator device has been put in use, monitoring the critical water level in the high-pressure scrubber, which has an important bearing on the performance of blast furnaces where increased gas pressure is developed at the furnace mouth.

In many plants, applications for radiometric rolling thickness gages have been found. Several types of thickness gages (with useful ranges from 0.003 to 10 mm) have been developed. The use of thickness gates to monitor rolled-sheet thickness during cold-rolling results in improved quality control, reduction of waste scarp, stepping up of rolling speed, and considerable savings in metal. Over-all savings in expenditures achieved by the use of such thickness gages are quite appreciable. Tentative data relating to one 12-high rolling mill at the Leningrad Steelrolling Plant report yearly savings of about 700 thousand rubles just by using the lower tolerance in rolling. According to data from the Zaporoshstal' Plant, the use of thickness gages halved the amount of scrap resulting from a simultaneous tightening of the tolerances on rolled metal. Use of a thickness gage for hot rolled sheet of up to 45 mm thickness may mean considerable economy. A thickness gage for hot rolled metal is now being put into production line service at the Izhor Factory.

In nonferrous metallurgy, radioactive isotopes are being used in working out new methods of quality control and in studying the mechanics and kinetics of processes. At the South Ural Nickel Combine, a radiometric level gage capable of monitoring the charge in a shaft furnace has been put into service, as well as 122 other radiometric level gages designed to automate charging of hoppers in a crushing and sintering mill. The alumina processing shop of the Volkhov Aluminum Mill is employing radioactive density gages to automate the process of loading and unloading filter-thickeners in the leaching department. At the Dneprovsk Titanium and Magnesium Mill, the pulp density in the titanium tetrachloride spraying cycle may be effectively measured by means of radioactive isotope density gages. These devices have made it possible to effect contact-free control of laborious processes, to continuously monitor and to maintain at set points various process variables, and to assure safe working conditions for servicing personnel.

The use of radioactive isotope tracers has made it possible to develop and improve the technology of several nonferrous and rare-earth metals of high purity. High-purity zinc production technology at the "Ukrtsink" Plant and high-purity tin technology at the Novosibirsk Tin Factory have been brought up to standard. Suggestions have been advanced for improving copper electrorefining technology and minimizing the carry over of noble metals, improving electrowinning of zinc with high current efficiency and the required purification of various zinc-electrolyte solutions, separation of rhenium and molybdenum for many metallurgical products. The interaction between metal and electrolyte in aluminum electrolysis has been subjected to tracer research techniques, by means of which the causes of lowered current efficiency in magnesium electrolysis (namely, anodic dissolution of the cast-iron bath tank lining) was also resolved. Tracer methods combined with activation analysis resulted in an improvement of existing techniques and the working out of new techniques for determining tiny trace impurities (of zinc, lead, antimony, tin, arsenic, phosphorus, germanium, thallium, indium, cadmium, gallium, selenium, tellurium, nickel, cobalt, iron, silver, etc.) in pure metals.

The net result of much research conducted with the aid of radioactive tracers is the accumulation of abundant material providing a firm basis for correct assessment of nonferrous metallurgy technological processes, for monitoring variables associated with these processes, and for finding the way to practical improvements in the processes.

Applications of radioactive isotopes and nuclear radiations in metallurgy are providing the national economy with great economic benefits, and are providing the prerequisites for improvements in labor and productivity conditions. Further assimilation of isotope tracer techniques and nuclear radiations by industry will require an expansion and deepening of research geared to elaborating new techniques and principles in radiometric sensing and control of technological processes.

This detailed discussion of the fundamental results of the adaptation of isotopes to metallurgical production will contribute to the further expansion of research in this field.

Declassified and Approved For Release 2013/02/14 : CIA-RDP10-02196R000100060003-5

Declassified and Approved For Release 2013/02/14 : CIA-RDP10-02196R000100060003-5

USES OF RADIOACTIVE ISOTOPES IN THE MINING AND ORE PROCESSING INDUSTRY

M. L. Gol'din

Research conducted in recent years in this field, in the USSR, may be broken down into instrumentation research and development, and assimilation of the instrumentation into practice. This work was discussed in the panel on the mining and ore processing industry.

The basic trends apparent in instrumentation research and development were pushed by the industry, which felt the need for level sensors, pulp density gages and coal ash meters, devices for measuring burden moisture and concentrate moisture. The success of automatic process control ventures depended on the development of such devices. The specific features of the mining and ore processing industry required contactless sensors making use of radioactive tracers and nuclear radiations.

A report by I. I. Savitskii, E. G. Litichevskii, and M. L. Gol'din touched on process control and automation problems in mills of the South Ore Processing Combine at Krivoi Rog; the solutions of these problems retain their generality for crushing and grading mills, beneficiation facilities, and sintering plants used in ferrous metallurgy.

A gamma-ray relay put into service by the Kharkov Plant, the KIP relay, provides reliable control over the work handling capacity of loading buggies, slipping of conveyor belting, and the presence of ore on conveyor belts. Much work was carried out on automatic loading of a parabolic-shape hopper of 40,000 tons ore volume, which provided uniform feed of raw material to all bins it serviced, and automatic control of the unloading trolley. Worth noting is the fact that an attempt to resolve this problem with the aid of contact sensors, capacitive pickups, and variable inductors failed because of abrasion effects and the high breaking strength imposed by the ore falling from a 12 meter height into the bins.

K. F. Fadeev presented data on a trial run of gamma-ray relay devices at enterprises under the jurisdiction of the Chelyabinsk Council of the National Economy. These devices were used to monitor the presence of coal on conveyor belts, to expedite automation of dumpcar loading and unloading, for counting and recording the number of cars unloaded, to automate loading of jaw crushers, and other processes.

A research program has been completed at the "Yuzhuralnikel' " Combine, in collaboration with workers of the "Tsvetmetavtomatika" (KB TsMA) nonferrous metallurgy drafting department. In a report delivered by V. V. Sevost'yanov, I. M. Likhterov, and others, the operating principles and design features of multiposition level gages were outlined. Because of the corrosive nature of the atmosphere, the environmental conditions affecting instruments used in nonferrous metallurgy processing plants are worse than in ferrous metallurgy. KB TsMA instruments of the gamma-ray relay type exhibit such high stability that the activity of the radiation sources could be safely lowered with no concomitant penalty in accuracy.

Problems related to the performance reliability of electronic relay units under field conditions prevailing in ore processing mills were dealt with in a report submitted by Ya. M. Ber, Kh. É. Gunne, V. A. Yanushkovskii, and A. V. Chashchinov. The report cited operational experience gained with such an instrument, based on work carried out at the Cherepovets metallurgical plant with KIP devices fabricated at the Tallinn Pilot Plant, and designed to sense the level of metallurgical ore charge in hoppers. This report also provided data on a gamma-ray relay sensor working into a magnetic amplifier. This device is suited for a broad variety of process-control applications in mine pits, since it is designed to be explosion-proof. The undisputed reliability of the circuitry and its long service life are offset to some extent by the limitation of a slow response (~ 3 sec).

A report submitted by V. G. Segalin shed light on some over-all results of research conducted by the Mining Institute of the USSR Academy of Sciences. The paper discussed cases of monitoring the presence of the protective layer in the receiving bin of a ventilation shaft, control of stoppage in chutes and cars, counting of loading cars and number of dumpcar lifts, automatic control of ventilation doors, etc. Much work, and interesting work at that, has been pursued on automatic control of coal combines, with the aid of radiation detectors capable of recording backscattered radiation whose intensity varies depending on the presence of gangue or coal.

Declassified and Approved For Release 2013/02/14 : CIA-RDP10-02196R000100060003-5

Declassified and Approved For Release 2013/02/14 : CIA-RDP10-02196R000100060003-5

The adaptation of pulp density gages to production at the Mizurskii Beneficiation Mill was discussed in a paper by E. Ya. Ovcharenko, V. I. Kotik, and others. One interesting feature of pulp density measurement is, aside from corrosive attack by the environment, the high specific weight of the solid component, the intrinsic radioactivity of the pulp, and the large diameter (150 mm) of the pulp pipelines. Research work initiated in 1957 has been successfully completed, and there are at present several instruments which have passed protracted industrial field tests for precision and reliability in measurements. It was explained that when the solid constituent of the pulp contains elements of high atomic number, the only suitable gamma-ray source is Co^{60}. The effect of using Cs^{137} would be the fluctuations in the mineralogical make-up of the ore would cause the radiation flux to vary by several percent, which is inadmissible. A phosphor was picked as the radiation detector because of the large diameter of the pulp pipelines, and the compensation method of measurements was resorted to in order to minimize instrumental error deriving from instability of photomultiplier and electronic circuitry gain. Two gamma emitters each of 80 mg-equ Ra activity execute oscillatory motions. Each emitter is housed in a lead enclosure with openings. The phosphor is therefore illuminated alternately by the basic radiation flux traversing the pulp, and by the standard flux passing through the compensation wedge. Tests of the device have shown that their accuracy is 1.5% with a speed of response of 1 sec.

A second report on pulp density measurement was presented by A. K. Val'ter, I. N. Plaksin, and M. L. Gol'din. The report contained a description of the design of a density gage and run-in tests of the device at the Yuzhnyi Ore Processing Combine, the tests being spaced over the last three years. The device is designed to be enclosed in a leaktight housing. The radiation detectors employed are ionization chambers with a multi-layered lead-coated electrode surface. The chambers are not connected differentially, but by a bridge circuit, so that they have a voltage of the same sign (+). This last fact greatly simplifies the electronic circuitry and acts to minimize instrumental errors. Measurement of the ionization currents in both chambers are performed by an electrometer circuit with the aid of a vibration transducer, operating at an industrial-use frequency and alternately connecting the collecting electrodes to the control grid of a 2Ê2P tube. The radiation flux is compensated by a wedge, and telemetering by ferrodynamic sensors. In this circuit, measurement of ionization current is performed by a single electronic network with an ac amplifier. Tests under industrial field conditions have shown that, at the 50 mg-equ Ra activity of a Cs^{137} source, and maximum density 2.1 g/cm^3 of iron ore pulp, the accuracy of the measurements is 0.6%. The device being mass-produced by the KIP Kharkov Plant therefore falls in the 1.5% precision category. The time required for the indicating pointer to run the entire length of the scale is 45 sec.

The report also presented some data on experiments specially designed to choose the optimum sampling point for further monitoring of the pulp variables (in two-helix classifiers).

A. Z. Kulishenko shed light on research pursued in the field of radioactive sensor applications, where the tracer devices send command signals to the actuating and control elements. Two fundamental variables of the flotation process in the flotation cells of coal dressing plants, namely loading and rate of flow, were brought under control and incorporated in an automatic control loop by means of these devices. Industrial piloting tests of the process control loop worked out for the Yasinovka Mill in the Donbas region showed that the load on flotation machines may be increased under such conditions concomitant with simplification of the flotation process flow scheme, reducing operating costs in reprocessing of coal sludge, and cutting down on the number of operating personnel required. Kulishenko also told of a device for measuring ash content in coal.

Of the various communications delivered, we might mention one by I. G. Zubilin on determination of bulk weight of a coal charge. This report cited the testing procedure, effect of moisture and granulometric make-up of the coal on the accuracy of the measurements.

One thread running through all the papers was the special attention reserved for problems of safety conditions and economical efficiency of radioactive techniques in process control, monitoring, and automation.

An analysis of the reports submitted disclosed that a variety of gamma-ray relay devices and pulp density gages have been developed and are currently in use in the mining and ore processing industry.

Assimilation of instrumentation and control loops based on the use of isotope tracers and radiations on an industry-wide scale will require taking some organizational steps, the most prominent being the creation of a network of central laboratories under the various councils of the national economy, backed up by special training of the needed engineering and technical cadres in the institutes.

Declassified and Approved For Release 2013/02/14 : CIA-RDP10-02196R000100060003-5

Declassified and Approved For Release 2013/02/14 : CIA-RDP10-02196R000100060003-5

THE USE OF RADIOACTIVE ISOTOPES AND NUCLEAR RADIATIONS IN CONSTRUCTION WORK

A. I. Yakovlev

Increasingly numerous applications have been found in recent years for radioactive isotopes in the construction industry and the building materials industry, for research, quality control, and process control.

The RIU type radioactive level gages and gamma-relay devices of the URAP type are being used for automatic monitoring and control of filling of hoppers, and the RIU-1 radioactive level gage has been applied to monitoring the filling of ore hoppers and bins in asbestos processing mills.

Automatic monitoring and control of the density of two-phase slurries (pulp, grout, sludge, etc.) is carried out by using PZhR-2 radioactive density gages, overflow gages of the "Sliv" type, and gamma-ray soil-density gages (the "gamma-gruntomer"). In particular, the density of dredged pulp is monitored by gamma-ray soil-density gages capable of determining the content of earth in the pulp to 2% accuracy. Gamma-ray soil-density gages may also prove useful in achieving automatic control of dredge performance and dredging operations. The dredges employed in the construction of the hydroelectric stations at Kakhovka, Gorky, and Stalingrad, and the V. I. Lenin Volga hydroelectric station were equipped with gamma-ray soil-density gages.

The radioactive density gage PZhR-2 has been used to effect continuous monitoring of the consistency of cement grout while cementing the foundations of hydraulic engineering installations. The same instrument has been used to measure the concentration of asbestos-cement slurry at asbestos processing plants. Radioactive density gages are being used to monitor the performance of cyclones (at processing plants) and to monitor the process of asphalt oxidation.

Radioactive noncontacting weight measurement devices (BIV) are being utilized in the production of insulating structural materials.

Gamma-ray flaw detection techniques are being brought to bear in monitoring the quality of weldment seams in the piping of electric power stations, gas mains, gas and oil pipelines, reservoir mains, and other metal products. Gamma-ray flaw detection is being applied to the quality control of weld seams in reinforced concrete work on hydroelectric power plant sites, making it possible to detect internal defects in the welding of reinforcement rods 30 mm in diameter and larger. The use of this technique in the construction of the Stalingrad hydroelectric works resulted in savings of 200,000 rubles. Gamma-ray nondestructive testing is also being employed in the quality control of prefabricated concrete members and centrifuge-spun reinforced-concrete supports for electric high-tension transmission lines.

Techniques based on measurement of the intensity of absorbed or scattered gamma radiation or neutron radiation as it intereacts with matter are being used in construction applications to measure various characteristics of building materials and to monitor process variables.

Gamma-ray techniques have been found useful in determinations of the density of earth foundations, earth-dams, embankments, and other structures.

Determinations of the density of subsurface earth were carried out in one instance either by gamma-ray scanning of a volume of earth from two parallel borehole cuttings (with a Co^{60} or Cs^{137} gamma source lowered into one hole and a radiation detector lowered into the other) or by driving a radiometric fork instrument into the ground, one prong with a gamma source attached, the other prong with a radiation detector attached. The accuracy achieved in measuring the weight of the earth by volume was within ± 2%, and the time required for a single run of measurements was 2 to 3 min. Density determinations were conducted on surface layers of the earth to a depth of one-half meter, by means of the radiometric forked probe. The use of jigs of special design in drilling test boreholes affords the possibility of determining the density of soil to a depth of 1.5 meter by gamma-ray penetration.

In another case, the density of earth was found by measuring the intensity of scattered gamma radiation (gamma-gamma logging). The gamma source and detector used in this instance were placed one above the

Declassified and Approved For Release 2013/02/14 : CIA-RDP10-02196R000100060003-5

Declassified and Approved For Release 2013/02/14 : CIA-RDP10-02196R000100060003-5

other in a probe, but separated by a lead screen to shield the detector from the direct radiation emanating from the source. Five percent accuracy was achieved in measurements of soil density, and this degree of accuracy was open to improvement by employing differential (spectrometric) radiation indicators. Determination of soil density by gamma-gamma logging can be performed either at surface layers or at deep-hole levels.

Under laboratory conditions, the density of soil samples may be determined by irradiating probes without disturbing their structure. Under field conditions, the moisture present in surface layers of soil samples can be ascertained by running a gamma exposure of the ground layer having a constant degree of soil compaction.

Neutron-gamma logs and neutron-neutron logs are being run at various borehole depths to determine the moisture tension of ground samples. The neutron logging techniques open the way to pinpointing the hydrogen content of the soils contained in borehole cutting cross sections, and the amount of moisture present by volume can be ascertained simultaneously.

Techniques based on recording the intensity of gamma absorption as gammas are passed through the specimen are useful in moisture determinations of concrete, gravel, sand, and other building materials. The error incurred by such methods, e.g., moisture determinations of high-porosity concretes of 900-1100 kg/m^3 weight by volume, is held within 2% of the moisture by weight of the specimen.

Gamma-ray inspection is being put into use in many production applications involving determinations of volumetric weight, moisture content, and homogeneity of concrete and reinforced-concrete components, and monitoring of unit processes in the preparation and pouring of concrete mixes. The degree of compaction of a freshly poured concrete mix may be determined with the aid of a radioactive density gage, providing a means of monitoring the performance of vibrators used to tamp down the mix. Keeping track of the density of a batch of concrete takes on particular importance when special concretes, e.g., heavy concretes used in the construction of biological shielding for nuclear reactors and rigid concrete placed in high-head waterworks structures, are being used. Use of a radioactive density gage makes it possible to obtain precise data on the composition of a concrete mix during its preparation, and to monitor the homogeneity of batches of concrete as they are released from the point of manufacture. During transportation and placing of the concrete, density gages are useful in detecting uneven layering of the mix, and in solving other engineering problems.

Radioactive logging techniques are being employed in building work for engineering and geological research on footings and foundations, in exploratory drilling operations (detection of water sources), and in quality control in the consolidation of foundations.

Radioactive indicators are being used to determine the weight by volume of particle board. Samples of particle board were impregnated to saturation with transformer oil for this purpose, with a radioactive tracer (P^{32}) added. By measuring the intensity of radiation from the specimens, their porosity was determined, and the weight by volume of the particle board could be found by carrying out the indicated calculations. A comparison of results obtained by this approach to the stereometric method for determining weight by volume of particle board showed excellent agreement between the sets of data.

Radioactive isotopes are being used in many applications in still another field, in research on structural materials and technological processes. Studies on the determination of the specific surface area of disperse-phase materials (cement, sand, etc.) are being conducted by adsorbing radioactive tracer indicators from solution. The isotopes used as tracers include W^{185}, Sr^{89}, Ca^{45}, Cs^{137}, and Co^{60}. Adsorption isotherms obtained as a result show that rapid and accurate determinations of the specific surface area presented by cements and sands are possible by this method. The radioactive tracer method is being put to use in research on cement hydration processes. The investigation of the kinetics and mechanism of the hydration process affecting minerals present in cement clinker is expedited by introducing the radioisotope Ca^{45} into the cement mortar. By varying the activity of the mortar, the interaction between water and the clinker minerals, into whose crystal lattices the isotope has been introduced, is brought under study. Research on changes in the structure and strength of cement brick subjected to alternating cycles of freezing and thawing in a water-saturated state has been carried out by determining the amount of adsorption of Sr^{89}-labeled cement mortar. Measurements of mortar activity are relied upon to determine the quantity of Sr^{89} adsorbed, and to get an idea of the amount of change in void ratio and increase in strength of the test sample at the same time.

Investigations probing the properties of asphalt materials from several directions have been conducted by means of Ca^{45} employed as a radioactive tracer. This method was used to study the processes of water flow

Declassified and Approved For Release 2013/02/14 : CIA-RDP10-02196R000100060003-5

Declassified and Approved For Release 2013/02/14 : CIA-RDP10-02196R000100060003-5

through an asphalt film into stone and rock materials, as a function of the properties of the constituents of asphalt concrete. The method was also applied to a study of the nature of water infiltration into the bulk phase of asphalt concrete, and the effect of surface-active additives on the properties of the asphalt concrete, to tests of water permeability and water-resisting properties of the asphalt coating on prefab sandwiched slabs.

Radioactive tracer isotopes have been employed in investigations of diffusion processes accompanying the interaction between refractories and foundry dust, slag, metal, etc. These investigations have been conducted to probe the performance conditions and ways of improving the fabrication of refractories. Fe^{59} and Ca^{45} are among the more frequently used isotopes, introduced into the constituents of the refractories. Contamination of steels by nonmetallic inclusions has been studied by the same method.

The study of sulfate corrosion of concrete by means of the S^{35} tracer isotope revealed the nature of the penetration of the sulfate ion into cement brick as a function of various factors. The investigations resulted in data on the effect of exposure of cement brick specimens to an aggressive environment, the effect of the cement-water ratio, of the content of hydraulic admixtures and the fineness to which the cement is ground, on the penetration and distribution of the sulfate ion into the bulk of the material. The same method was used to study the effect of various aggressive media on cement brick.

Variations in the intensity of reflected gamma radiation were used in a study of the change in wall thickness of steel pipes, as a result of corrosion wear and cavitation processes. A radioactive wall-thickness gage is used in research along these lines.

The radioactive tracer method is in wide use in construction work, as a tool for investigating the processes by which various materials, slurries, and fluids flow through matrix materials. A study of the rate of advance of such material in a rotary furnace and in the coarse-grinding and fine-grinding chambers of a ball mill during the process of firing and grinding of cement clinker was expedited by adding radioactive Fe^{59} to the original materials. In the construction of the Stalingrad hydroelectric power plant, the radioactive isotope Cr^{51} was used as a tracer to follow the flow of cement in cement chutes where the cement was impelled pneumatically. The study of the rate of travel of a concrete mass down steel piping was made with Co^{60} tracer. The isotope was introduced, in the form of a piece of wire (activity 0.6-0.15 microcurie), into a hole drilled into the crushed rubble, and left embedded therein. The rate of flow of the concrete mass is determined by the speed at which the tagged pieces of crushed rock introduced into the concrete can be traced in their motion through the cement piping. The same method was used, but with Br^{82} tracer, to determine the speed of water flow through the diversion waterways of one of the hydroelectric plants. For this purpose, the isotope was introduced into the water admitted into the conduit, and the speed of water flow through the conduit was measured by the time at which activity was detected at various test sections along the flowpath.

A study of the flow processes of pulp dredged by suction dredges involved the use of radioactive tracers in the dredged spoil. In pilot tests, the effect of the consistency and specific flowrate of the pulp on the integral density of the spoil dredged up was successfully investigated by using Ta^{182} as labeling isotope. Exceedingly laborious investigations were telescoped into a brief research program with the aid of this technique.

Tracer techniques have also been called upon in recent years to aid in the study of filtration processes and flow dynamics of ground water. The isotopes used as tracers in these studies are H^3, P^{32}, Co^{60}, Rb^{86}, Zr^{95}, I^{131}, and Cs^{134}. Laboratory-scale tests have demonstrated that the radioactive tracer technique is in no way inferior to the calorimetric method when used to study filtration problems, and in some cases proves to be more efficient. Flow processes involving the displacement of fluids in a porous medium are also studied to advantage by the tracer technique, under laboratory conditions. The different types of fluids used in the investigations were labeled with isotopes having different energies (I^{131} and Rb^{86}), so that the process of intermixing between two fluids could be studied by means of two-channel radiometric equipment. Under field conditions, the tracer technique has been applied to the study of seepage of water through cofferdams, of the performance of water drainage networks, throughput of deep-well pumps, and direction of flow of ground water, etc.

Gamma-ray detection techniques are used to study the flow of suspended detritus in a water channel, and to determine the amount of material in suspension. The study of the concentration of debris in a water channel is carried out by measuring the intensity of the scattered gamma radiation. The amount of debris suspended in water samples is determined by transmission of gammas through the samples in laboratory analyses.

Declassified and Approved For Release 2013/02/14 : CIA-RDP10-02196R000100060003-5

Declassified and Approved For Release 2013/02/14 : CIA-RDP10-02196R000100060003-5

THE USE OF RADIOACTIVE ISOTOPES IN LIGHT INDUSTRY

A. N. Slatinskii

Methods of automatic control, process control, and quality control based on the use of radioactive isotopes and nuclear radiations are being employed at present in various branches of light industry. The session of the panel on light industry was devoted to a discussion of these problems.

It is common knowledge that an increase in the productivity of labor and machinery, as well as efficient and economic consumption of raw and semifinished materials, in some light industry lines depend significantly on rapid and continuous weight determinations of the material during the manufacturing process. This applies to such commodities as paper, cardboard, plastics, fabric coatings, etc.

The Central Research Institute for the Cotton Industry (TsNIKhBI) developed a BIV noncontacting weight checker in 1955. The device operates on the principle of measuring the absorption of beta radiation passing through the material, with the aid of two ionization chambers included in a balanced circuit. The working transducer and the compensation transducer comprising the device consist of radioactive sources and ionization chambers. A movable metal blind coupled to the weight-indicating scale of the device is placed between the radioactive source and the ionization chamber of the compensation transducer. The ionization currents in the chambers are opposed, and the differential current is fed to the input of an electrometer amplifier. The amplifier output current is fed to an indicating device graduated in units of deviation of the weight of the sample material from set-point value, in g/m^2. The measuring circuit of the device, made in console enclosure design, is mounted on a special bogie by means of which it can be moved across the material flowing by during the weighing procedure.

The BIV line of weighers are a success in many light-industry plants. On the leatherette production line at the Nogin linoleum and leatherette manufacturing works in Kuntsevo, BIV instruments are being used to determine the amount of coloring applied to fabric, and have been incorporated into the fabric-treating equipment for that purpose.

The introduction of BIV devices did away with the need for stopping the machinery to take samples, cutting off specimens of material, weighing by an inspector, or converting the results of an analysis to square meters of finished material.

According to calculations reported by the planning department of the factory, the use of BIV devices on the production line has paid off in annual savings of about 100 thousand rubles.

Trial use of BIV instruments on a cardboard-making machine used to produce light roofing products (tar paper, asphalt roofing, Ruberoid roof sheeting, parchment products) at the "Kartontol' " Factory in Leningrad also demonstrated the high efficiency and feasibility of the instruments.

One of the fundamental criteria in judging the quality of goods manufactured is the uniformity of weight and thickness in a sheet of cardboard, and its capacity for impregnation by asphalt, which in turn is a determining factor in the service life of the material.

The BIV devices used at the "Kartontol' " monitor the thickness and weight of the continuously moving line of cardboard sheet. The result of equipping all the plant machinery with these weight checkers has been a reduction in the laboratory staff, elimination of inspectors, an increase in quality, higher labor productivity, all of which adds up to about 250 thousand rubles a year in savings.

Putting BIV weighers on the production line at the Krasnogorodskaya papermaking machine shop of the Leningrad District Council of the National Economy has been a successful venture; year-round performance demonstrates high efficiency.

The use of BIVs in various branches of industrial production not only does away with any need to set up a continuous monitoring scheme for the goods passing down the production line, but also opens up broad perspectives for automated process control, since data on the weight or thickness of the material are converted to electrical signals which can be employed in any associated control loop. Work on this line is already in progress. The BIV devices are being mass-produced at the KIP Plant in Tallinn.

Declassified and Approved For Release 2013/02/14 : CIA-RDP10-02196R000100060003-5

Declassified and Approved For Release 2013/02/14 : CIA-RDP10-02196R000100060003-5

The TsNIKhBI laboratories have developed an instrument for checking the unevenness of fabric on a fiber-beating machine. When the weight of the uneven areas of fabric deviate sensibly from the technologically set values, the instrument emits light signals. The measuring device in this instrument assembly consists of sources of radioactive emission, two ionization chambers, and an automatic electronic potentiometer measuring the difference in the currents of the two ion chambers, by the compensation method. The measurement is carried out over the entire width of the fabric, and the transducer is placed between the calender rollers of the fiber beater.

The All-Union Scientific Research Institute for the Printing Trades has developed a BTP-1 device, a beta gage for measuring the thickness of metal plating. This instrument operates on the principle of measuring the back-scattered beta radiation, and is designed to determine the thickness of platings applied to flat objects used in the printing trades.

The BRP-1 consists of a removable measuring head with a mount and an electric measuring unit. The measuring head is made in cylindrical form, with an annular radiation source placed in the lower face. The radiation flux reflected from the measured object is recorded by a differential ion chamber.

At the Zhdanov First Master Printing House of the Moscow (municipal) Council of the National Economy, the BRP-1 was used to monitor the thickness of chrome plating on the bimetallic forms of an offset press, and aided in normalizing the processes of chrome-plating and etching of bimetallic forms, not to mention reduction of scrap. Savings in the manufacture of plates and forms alone amounted to about 8 thousand rubles yearly for a plant with a single chrome-plating bath.

The BTP-1 was also been put into production use at the "Krasnyi proletarii" printing house to provide selective control of the process of nickel-plating type-metal stereotypes.

The Central Scientific Research Institute for the Footwear and Leather Industry has developed radioactive thickness gages for raw and processed leather. These thickness gages make it possible to measure the average thickness of skins over the 2 to 5.5 mm range without having to cut off a specimen. The instruments are based on the principle of measuring the attenuation of beta emission from a Ce^{144} source by the material. A similar thickness gage may be successfully applied to sorting and grading of furs as they enter the processing plant.

A device capable of determining the density of the hair covering of fur skins, a radiometric densimeter, has been designed by the Scientific Research Institute for the Fur Industry. Testing of the device at fur processing plants demonstrated the high degree of precision in measurements of the density of the hair covering of fur skins, as compared to existing methods.

The Tallinn KIP factory, in collaboration with the Academy of Sciences of the Latvian SSR, has developed a radioactive thickness meter known as URIT-1. The performance of this instrument is based on the phenomenon of attenuation of the recorded radiation as it passes through the material being measured. Measurement of the radiation is effected by means of a differential ion chamber. A null-indicating compensation method of measurement is used in the device. The meter employs an automatic self-tuning circuit.

Besides measuring instruments and circuits, devices and circuitry based on relay engineering are finding many and varied applications in light industry.

A radioactive level gage, RRU, designed at the Research Institute for the Cotton Industry to monitor and control the level of cloth in the steam chambers of textile-finishing equipment, is being used in the textile industry. Conventional methods are inadequate where the prevailing conditions are a steam environment, high moisture in the surrounding area, and high ambient temperature, where measurement of the cloth level inside the machinery is required.

The RRU device is a stationary type installation, which includes two radioactive gamma-ray sensors, two radiation detectors in the form of STS-8 type self-quenching halogen detectors, an amplifier unit, a relay automatic control unit, and a signal-light panel. A Cs^{137} preparation is employed as a radiation source.

At present, the RRU device is in service in several textile plants in the Moscow, Kalinin, and Ivanovo regions. Limited lots of the device are being manufactured by the "Tekstil'pribor" Plant attached to the Central Research Institute for the Cotton Industry.

Declassified and Approved For Release 2013/02/14 : CIA-RDP10-02196R000100060003-5

Declassified and Approved For Release 2013/02/14 : CIA-RDP10-02196R000100060003-5

Relay-based automatic control techniques have proved to be a highly efficient means of monitoring and process control at the Dzintars perfumery and cosmetics works in Riga.

Selective sampling was the approach previously used to monitor overfilling and underfilling of tubes and vials on the production line. This means that large batches of rubes had to be weighed and the rejects sorted out by hand. Automatic tube-filling heads now include a radioactive RK-4 empty container checker. This device consists of a standard BI-1 beta source, an RD-6 radioactive transducer, a URAP-ZD electronic relay unit, and a BSK-1 counter and switcher assembly. The tube fill level is checked by passing betas through a cross section near the crimped edge as the tubes pass down the line.

When a defective item reaches the control point, the transducer senses intense radiation, and the electronic relay circuit actuates a relay which in turn energizes the electromagnet controlling a reject mechanism, which ejects the defective tube into the discard box.

An automatic tube shearing machine continuously processes aluminum rubing stock. One of the operations included in this cycle involves feeding a disk-shaped cutting tool to a steel die, into which the tubing stock is inserted, to thread a screw track. Should the delivery of tubing stock be interrupted for any reason whatever, the die surfaces would be left exposed and the cutters would be damaged on coming into contact with them. Radioactive limit switches consisting of radioactive sources of beta rays (Tl^{204} sources), a radioactive transducer RD-6, and a URAP-ZD electronic relay circuit were installed to prevent such an accident. Whenever interruptions occur in the supply of tubing stock in the feed chute of the automatic shears, the electronic relay URAP-ZD breaks the circuit of the magnetic starter controlling the electric power for the automatic shears. The efficiency of this radioactive stop device, in economic terms, has meant savings of about 150 thousand rubles annually as a result of using them on two automatic tube-shearing machines.

The Dzintars factory is also using a radioactive pressure regulator consisting of a manometer with a beta source mounted on the indicating pointer, and RD-6 radioactive transducers on the scale. Ports are cut out on the scale facing the transducers, to allow passage of radiation. The transducers are included in the circuit of a two-channel electronic relay unit (URAP-2A) coupled to the magnetic starter of an electric motor. The economic advantage gained thereby amounts to about 46 thousand rubles annually.

A radioactive on-off level controller is being used with great success at the Dzintars Factory (on a turntable automatic pouring machine), as well as RD-6 radioactive transducers (for metering liquid constituents of eau de cologne).

The Central Scientific Research Institute for the Silk Industry is engaged in research on the application of radioactive isotopes to the neutralization, by ionization, of static electricity in the air. The electricity is a by-product of artificial fiber processing.

The sources used for this purpose are Pu^{239} and Pm^{147}. The use of a Pu^{239} source to neutralize electrostatic charges on acetate fiber, at the "Krasnaya Roza" Combine, has clearly demonstrated the efficiency of this measure.

The use of a Pm^{147} beta-emitting source to remove electrostatic charges from acetate and viscose fibers on the warper machines of the "Krasnaya Roza" textile combine, and on the spinning frames of the Naro-Fominsk spinning and weaving mill brought in appreciable technological dividends.

In the weaving department of the Moscow Textile Institute, original work has been done on a study of clothmaking during the weaving process, with the aid of radioactive isotopes as research tools. This work led to the conclusion that normalized optimum parameters related to loom set-up (tension of warp and weft threads, left-off and take-up, etc.) could be arrived at, thus aiding in maximizing loom output, improving fabric design by reducing over-all weight, and improving the distribtion of threads in the weave repeat.

Some interesting research work is being conducted with the aid of radioactive isotopes in the lumber industry. For example, we may cite experimental investigations in some aspects of gamma-ray nondestructive testing of wood species at the Rostov Civil Engineering Institute and at the Scientific Research Institute for Machine Design Technology of the Rostov Council of the National Economy. The Moscow Forestry Institute is studying a modification of wood brought about by grafting monomers and subsequent irradiation, as well as the effect of gamma bombardment on several physical and mechanical properties of wood.

Declassified and Approved For Release 2013/02/14 : CIA-RDP10-02196R000100060003-5

Declassified and Approved For Release 2013/02/14 : CIA-RDP10-02196R000100060003-5

Increasingly more versatile use is being made of radioactive techniques in the various branches of light industry, and these techniques are becoming reliable allies of technologists and research workers.

THE USE OF RADIOACTIVE ISOTOPES AND NUCLEAR RADIATIONS IN MACHINE DESIGN

S. V. Rumyantsev

Radioisotopes and nuclear radiations are being used in industry for automatic process control and monitoring, for quality control of industrial commodities, in metallurgical and metal-physics research, in the foundry industry, in welding, etc.

Automation of the leading branches of machine design depends on the scientific and engineering level of development of the means available for instituting active control, among which process control instruments using radioactive isotopes and nuclear radiations occupy a prominent and often the decisive place. At the present time, many organizations in our country are engaged in scientific research programs aimed at the development of new radioactive process control techniques.

The most frequent applications for radioactive isotopes in machine design involve nondestructive testing of weld seams, castings, angle tolerances in machinery, whole assemblies, and defects in the performance of existing machinery. Special laboratories have been outfitted for this purpose in most large machine building factories.

The photographic-film method of gamma-ray nondestructive testing has been thoroughly incorporated into the productive process in many factories. Imposing savings have been achieved in industrial economy by assimilating radioactive techniques. For example, at the S. M. Kirov hoisting and hauling equipment factory in Leningrad, the economic advantage accruing from the use of gamma-ray nondestructive testing amounts to 65 thousand rubles annually. Savings at the Taganrog "Krasnyi kotel'shchik" (Red Boilermaker) factory were 260 thousand rubles, at the Dnepropetrovsk metallurgical equipment manufacturing works, 686 thousand rubles, and so forth.

Nine types of sources with different degrees of hardness of gamma rays have been produced for gamma radiography: the most frequently used sources are Co^{60}, Ir^{192}, Cs^{137}, Eu^{142}, Se^{75}, Tm^{170}.

The gap currently existing between the output of radioactive sources and the corresponding facilities (with respect to energy and radiating power) for irradiating manufactured goods is a conspicuous one. The lag is felt particularly in lightweight, small-sized, and portable gamma facilities specialized for various branches of industry and construction work.

The photographic-film method of gamma radiography currently in use has relatively high sensitivity and objectivity in its results, but is operated at a low rate of productivity, which restricts the possibility of successfully integrating it into process control procedures. Methods bearing promises of higher productivity are radiographic tests using image converters, television techniques, ionization techniques, and xerography. However, all of these methods are still in the laboratory stage.

The following questions of procedure and methodology were probed to expedite the use of radioactive isotopes in metal working, metallurgy, casting production, and welding engineering: methods involving the introduction of radioisotopes into liquid metal, into electrode coatings, and into electrode bodies; methods of qualitative and quantitative study of the distribution and redistribution of elements in metals and alloys by autoradiography; a method of analysis of metal and slag samples in terms of the simultaneous content of isotopes in these two phases; a method for determining diffusion constants in metals and alloys at high heating rates by means of isotopes.

Declassified and Approved For Release 2013/02/14 : CIA-RDP10-02196R000100060003-5

Declassified and Approved For Release 2013/02/14 : CIA-RDP10-02196R000100060003-5

The isotopes of greatest interest for metal working and metallurgical researches are the following, suitable for use in experimental work: C^{14}, P^{32}, Si^{31}, S^{35}, Cr^{51}, Ni^{59}, Mo^{99}, Ca^{45}, Ce^{141}, Ce^{144}, W^{185}, as well as the tritium isotope of hydrogen.

As a result of work carried out on the study of the distribution of elements in cast structural steels, and the diffusion of elements during homogenization, the distribution of the principal elements in the macrostructures and microstructures of steel as steel crystallizes was found. The effect of heat-treatment conditions on the ultimate distribution of elements in steel was studied. Optimum heat-treatment conditions for castings manufactured for special purposes were arrived at.

Research on the mechanism responsible for the formation of a structure leading to intercrystalline fracture in steel and to a sharp deterioration in its strength characteristics, in cast or reheated steel, was conducted with the aid of radioactive isotopes; these studies provided the basis for a method warning of any such serious defect arising under production conditions, as a consequence of processing molten steel with special additives. The effect of these additives is to simplify the heat-treatment conditions for high-strength alloy steel.

In order to elaborate an efficient technological process of steelmaking with the use of tungsten extracted from tungsten-containing discard, the conditions governing separate oxidation of tungsten and phosphorus in the main furnace were studied. The possibility of using tungsten recovered from such sources was demonstrated in principle.

The technique of using radioisotopes to study the formation of impurities in castings is a highly promising one. This technique provides a possibility of finding out the reasons for the formation of impurities, of evolving methods for sharply reducing impurities and effecting a significant increase in the output of serviceable castings. The processes observed to take place during modification of cast iron have been studied with the aid of radioactive isotopes of calcium, cerium, and sulfur as tracers. The effect of cerium, zirconium, vanadium, and titanium additives on the distribution of sulfur and the composition of sulfides in chrome-molybdenum-nickel steel were studied. This has made it possible to shed light on the nature of sulfur compounds forming in response to melt conditions, to the chemical composition of steel, and other factors. The effect of separate components on the plastic and elastic properties of steel, particularly on the nature of temper embrittlemenet, has also been studied by those means, and the conditions relating to the formation of the most desirable sulfur compounds were found.

The processes of crystallization and distribution of impurities in the ingot have been studied with the aid of radioactive isotopes C^{14}, Si^{31}, and S^{35}, in working out a technology of continuous steel casting at new industrial plants in the Perm and Gorky Councils of the National Economy. The research has resulted in an optimized crystallizer design.

Extremely interesting results were obtained in radiographic examination of the distribution of hydrogen in alloys with the aid of tritium, a radioactive isotope of hydrogen.

At the Metallurgy Institute of the USSR Academy of Sciences, work has been carried out to establish the relationship between microscale inhomogeneities in alloy and the cooling rate of light alloys in casting, the extent of deformation in pressworking, heating conditions in homogenization. Ca^{45} and Fe^{59} radioactive tracer indicators were used to develop new refractory alloys.

One of the principal tasks encountered in welding is that of establishing the extent of participation of the base metal, electrode wire and flux in the alloying of a seam by different elements and saturation of the seam by harmful contaminants. By introducing the elements to be tested into the base metal, wire, or electrode coating, the amount of a particular element entering the weld seam from any given source was studied. It was found that 9 to 14% of the sulfur found in a seam in hand welding comes from the sulfur contained in the electrode covering. The base metal accounts for from 15 to 35% of the sulfur in the seam, and the electrode rod accounts for from 51 to 72%. These relationships are severely altered by changes in current during welding.

The mechanism of hydrogen diffusion in austenitic seams was studied radiographically, and the reasons for resoftening of the weld zone.

The radioactive tracer technique also opens up new possibilities for improving welding technology. The reasons for the formation of hot cracks in austenitic weldments were established with the aid of the radioisotopes mentioned above. The reasons for local fracture in the weld seams of high-pressure steam lines made from

Declassified and Approved For Release 2013/02/14 : CIA-RDP10-02196R000100060003-5

Declassified and Approved For Release 2013/02/14 : CIA-RDP10-02196R000100060003-5

ÉI-257 steel were studied. It was found that one of the reasons for the appearance of cracks in a weld is the sharp enrichment of the interface zone between the oriented metal and the base metal by various elements.

An increase in the resistance to wear of machine parts and tool parts is one of the basic tasks to be met in machine design. The performance and technological servicing of mechanisms and machinery was optimized by means of isotope techniques, with minimization of time and means, and isotopes also made it possible to hit upon the most wear-resistant pairs of materials, to evaluate the design decided upon, the quality of lubrication and fuel, etc.

Scientific research institutes have developed several techniques of bench-stand and production tests for wear on parts of internal-combustion engines, gear transmission boxes, the wear-resistant properties of different greases and lubricants, the wear on cutting tools.

The experience accumulated in incorporating techniques for keeping track of wear on parts into regular procedure has demonstrated the effectiveness of radioactive isotopes in that task, at the Vladimir and Altai tractor factories. At the Vladimir factory, for example, the wear suffered by parts in the cylinder and piston section in the case of a new air-cooled engine being run-in under winter conditions was reduced to one fourth (on the outer cylinder surface). The total service lifetime of the cylinder and piston section of the engine was increased by about 50%. Performance tests at the factory's field station showed that 5 hours are adequate to find out all the necessary data to establish the tempo of wear concerned.

Radioactive isotopes were a help in investigating fouling of piston rings at the Khar'kov tractor works, and were used to arrive at rational oil changing schedules. The new and lengthened oil changing schedules, already put into practice, had the result of not only increasing savings in means and diesel oil, but also of lengthening engine lifetime by minimizing wear on parts.

As a result of investigations of the mechanism responsible for the effects and properties of oil additives, carried out by the All-Union Scientific Research Institute for Oil and Gas Refining and Artificial Fuels Production, the new additive VNIINP-360 for greases used in locomotive diesel engines has been developed and is already in mass production. Laboratory investigations carried out by the Central Research Institute of the Ministry of Roads, Highways, and Communications have contributed to the improvement of the wear-resistant properties of axle greases.

A procedure developed for high-speed testing of motor oils has enabled the All-Union Mechanization Institute to present recommendations on the service life of crankcase oil in the engines of DT-54 tractors. The annual savings resulting from observance of these recommendations amount to 25 thousand tons of diesel oil and 32.5 million rubles in the Russian Soviet Federated Socialist Republic alone.

Applications for radioisotopes in metal cutting operations include obtaining data on the cutting properties of tool materials, determining the workability of structural materials and rational cutting conditions, the proper choice of cooling and lubricant fluids, the elaboration and correction of rules for cutting conditions, the compilation of initial data needed in the designing of metal-cutting lathes, etc.

The use of radioactive isotopes makes possible a rapid measurement procedure of the amount of products of wear on tool material, without interrupting the cutting operation. Compared to micrometer techniques, the radioactive technique means shorter inspection time, less waste in metals and other material means, by a factor greater than 50, and with it increased accuracy, stability, and reliability in the results of measurements of wear products. Easy conversion of linear data on instrument wear to recording data on wear products in terms of weight or volume measurements can be had by means of isotope techniques.

The main trend in the use of radioisotopes in machine design, the area in which economic advantage comes out most clearly, is that of gamma radiography of castings and weldments.

The lengthy experience acquired in the use of gamma radiography techniques at industrial enterprises enabled the Moscow Bauman Institute of Advanced Technical Training and the Economics Institute of the USSR Academy of Sciences to carry out a study program of work at almost 100 machinery manufacturing plants, and to produce figures on the economic gains accruing from the institution of those techniques. Gamma radiography paid off economically in the reduction of defective manufactured items and improvement of product quality, detection of flaws in good time to correct them, process control in welding and casting operations, and the substitution of gamma radiography for other more expensive quality control techniques. Gamma radiography has reduced weld seam defects by three to eight times on the average, according to an analysis of reports and complaints.

Declassified and Approved For Release 2013/02/14 : CIA-RDP10-02196R000100060003-5

Declassified and Approved For Release 2013/02/14 : CIA-RDP10-02196R000100060003-5

Seven thousand rubles were saved in one year at the Dnepropetrovsk metallurgical equipment factory simply by the detection of flaws in good time and the reduction of scrap which would have resulted from those flaws; by eliminating the costs associated with reprocessing of defective items, and the 150 thousand rubles saved annually at both the "Russkii dizel' " diesel engine works and the "Krasnyi kotel'shchik" boiler works. Expenditures on quality control of castings and weldments in steel of 30-40 mm thickness were reduced by 15-20% by instituting x-ray and gamma-ray flaw detection methods. An average of 50 thousand radiographic plates means savings of about 100 thousand rubles at each enterprise. Total economic impact brought about by the instituting of gamma radiography at enterprises all over the nation may be evaluated, in the light of 1958-1959 data, at 200-250 million rubles annually.

More and more applications for radioactive isotopes are cropping up in various types of instruments used for process control.

The results of the use of radioactive isotopes to monitor the thickness of rolled strip and the thickness of lead plating on tin have been successful automatic process monitoring, reduction in costs of raw materials and semifinished materials, reduction of scrap, increased productivity, and an increase in net output without altering the productive capacity of the enterprise concerned.

The economic advantage resulting from the integration of radiation type controllers regulating the thickness of lead plating on tin into production practices could, in terms of the amount of lead economized (718 rubles per ton of tin plate used), in terms of laboratory personnel freed for other tasks, reduction in the amount of subsidiary materials consumed, etc., amount to 80-90 million rubles annually, should the entire machinery and metalworking industry be completely equipped with these control devices.

Replacement of contacting control instruments by noncontacting devices (i.e., radioactive devices) brought about a reduction of three to four times in scrap and a 10% increase in the productivity of rolling mills (an analysis of the performance of over 10 steel rolling plants). The economies resulting from adoption of a single isotope-based controller for thickness of rolled sheet amounted to approximately 500-550 thousand rubles annually.

The use of a beta relay device as an interlock device on automatic transfer machines at the Riga electrical machinery factory brought about savings of 15 thousand rubles in instrumentation on a single machine, while savings in labor costs came to 1.2 million rubles a year.

In each case where a new device or new control technique is to be considered for adaptation to production procedures, the engineering and economic justification of the feasibility of isotope devices and techniques as against conventional means must be clearly established.

RADIOACTIVE ISOTOPES AND NUCLEAR RADIATIONS IN THE SERVICE OF AGRICULTURE

V. M. Zezulinskii

The use of radioactive isotopes in agriculture began with the study of the interaction of plants, soils, and fertilizers to develop a rational approach to fertilization procedures.

The achievements of the isotope techniques include finding the best topography for fertilizer applications, and periods for introducing phosphorus-containing mineral fertilizers to supply plants with the elements of mineral nutrients in all stages of vegetation. The effect of various constituents of organic and mineral mixtures on phosphorus uptake of plants was also found through these techniques.

Radioactive phosphorus played the deciding role in justifying spray dressing of plants as an agricultural practice. It was proved by tracer methods that phosphorus sprayed on cotton plant leaves was assimilated by the plant in short order, and was absorbed in large quantities at such growing points as young leaves and fruit primordia. Spray dressing of the cotton plant during its ripening stage contributes to higher yield and better-quality fibers. The spray application technique for feeding plants has come into its own as an agronomical practice in Uzbekistan, Tadzhikistan, and other cotton-planting regions of the USSR.

Declassified and Approved For Release 2013/02/14 : CIA-RDP10-02196R000100060003-5

Declassified and Approved For Release 2013/02/14 : CIA-RDP10-02196R000100060003-5

Radioactive labels not only aided in correctly accounting for the high efficiency attained in the use of granulated fertilizer, but also in determining the optimized grain size for the various types of fertilizers, crops, and soils. On the basis of data compiled from field work, a proposal was advanced to change the standards of the granulated superphosphates manufactured by the chemical processing industry. A. V. Sokolov employed a radioactive tracer in developing a procedure for directly determining the extent to which phosphorus fertilizers are utilized by plants, and as a result showed that despite the generally prevailing assumption to the contrary, no rapid binding of the applied phosphates occurs in the soil, so that systematic fertilization with phosphate manures over a many-year period results in an excess of phosphates, in an "overphosphatization" of the soil. Additional phosphate manuring of soils beyond their point of saturation with respect to phosphates will not pay off in bigger harvests.

The widespread use of Sokolov's tracer techniques in the practical work of experimental agronomical stations to determine the reserves of assimilated phosphates and the utilization factor of phosphate fertilizers may provide state farms (sovkhozes) and collective farms (kolkhozes) with the necessary justification for sowing crops on soils where greatest economic benefit should be expected from systematic manuring.

According to data cited by B. A. Neynylov, the use of Sokolov's approach in the Vladivostok region made it possible to improve the phosphate fertilizing procedures on the fields of a local rice-growing sovkhoz, and to bring in an increased crop topping one million rubles worth of rice from a tilled area of 1400 hectares.

However, the data obtained by scientists are not being given sufficient publicity and have been accessible to the interested practical workers in agricultural production only to a limited extent.

Another area of promising practical interest where the isotope technique might be of service in justifying the use of particular agronomical methods capable of yielding increased production with no exorbitant expense is the maximum mobilization of the plastic substances in the green parts of plants to developing a crop by spraying plants with chemicals. According to data furnished by the Institute of Potato Farming, preharvest spraying of potato plant leaves with a solution of copper sulfate pays off in a crop increase reaching 50 centners per hectare (for a crop usually totaling 200 centners per hectare).*

It is commonly known that prompt defoliation of cotton plant leaves prior to machine harvesting requires the use of chemicals and defoliants. The use of radiophosphorus at the Central Asia Cotton Farming Institute revealed which defoliant causes the greatest outflow of nutrients from the shed leaves into the cotton bolls. In particular, in the case of natural slow drying of the leaf, 25% of the phosphorus applied to the leaf migrates to the glumes and bolls of the plant, compared to 19% when calcium cyanide is used as defoliant, and only 3-6% when magnesium chlorate is used. It is to be assumed that the proper choice of defoliating chemical should yield large economic returns in the shortest time.

Another trend has been shaping up in this field in recent years: the use of tagged atoms in the practical selection and breeding of crop plants. Radiophosphorus has been used to develop a procedure for the early diagnosis of frost-resistance in winter wheat strains by effecting relative changes in the rate of phosphorus uptake by wheat shoots. A certain correlation has been established between the frost-resistance of a given variety and the rate of P^{32} uptake. The method of differential uptake of radiophosphorus has proved suitable for determining early ripening in the cotton plant, as well as in cucumbers, during the stage when the first true leaves come out.

A question which has long been in the fore, namely the possibility of making practical use of gamma irradiation of seeds of farming crops prior to sowing them, in order to increase crop yield, was brought up again during the conference.

Various research agronomists had arrived at contradictory results, but the existence of such a stimulating effect was not repudiated, on the whole. A. M. Kuzin and his associates proposed a method for farming practice in which gamma irradiation of seeds of agricultural crops took place prior to sowing the seeds, beginning with vegetable crops (carrots, radishes, tomatoes, and cabbages), and using doses from 300 r to 3000 r, which will raise the yield of these crops by 15-30%. According to calculations made by the Economics Institute of the USSR Academy of Sciences, irradiation of 25% of the seeds sown (for the crops mentioned) will mean an additional 200 million rubles worth of annual crop yield.

* Centner = 100 kg, hectare = 2471 acres (Translator's note).

Declassified and Approved For Release 2013/02/14 : CIA-RDP10-02196R000100060003-5

Declassified and Approved For Release 2013/02/14 : CIA-RDP10-02196R000100060003-5

Another important trend in the use of radiations in agriculture is the use of ionizing radiations to accelerate hereditary changes in farming plants, with the idea of encouraging new and useful properties. A panel on this topic heard material submitted on the successful raising a radiation mutants of winter wheat (the wheat – couch grass hybrid No. 186) of agricultural and economical interest. This particular mutant exhibits the advantage of short firm chaff, large ears, resistance to smut and to powdery mildew.

To cope with crop pests, chemical pesticides are being used in many instances. Until recently, a method with sufficient sensitivity to enable agronomists to estimate trace quantities of toxic substances remaining in foodstuffs after plants and animals have been treated with toxic chemicals has been sorely lacking. Work with the C^{14} isotope has now proven that even tiny traces of highly toxic substances cannot be neglected with impunity. Specimens have been detected in milk over 4.5 months after their application to the food source. After gaining access to the animal's organism via milk, the toxic chemicals are deposited for a protracted period, primarily in fatty tissues, but also in brain tissue, spinal tissue, and in the brain marrow.

A report was made at the panel on a tracer technique elaborated to trace the effectiveness of processing farming crops with toxic chemicals, by finding the ratio of sample radioactivity (radioactivity in the leaves of stalks and peduncles) to the activity of a unit volume of the sprayed solution. Testing of this technique under field conditions demonstrated its applicability for arriving at the optimum technical and economical parameters describing the performance of various types of spraying equipment.

Work carried on at the Tomilin hatcheries by their experts in collaboration with the Institute of Genetics of the USSR Academy of Sciences demonstrated the possibility of using minute doses of gamma radiation (0.001-2.0 r) during the incubation period for chicks to stimulate the growth of chick embryos (resulting in a 3.5% increase in chicks raised) and improving the egg production of pullets (by 12%) irradiated during embryogenesis. This increase in the viability of chicks and egg-laying capacities of hens may yield enormous economic returns in practice.

In the area of land reclamation and mechanization of agriculture, attention should be given to reports on a study of the migration of labeled ground water through the soil; these papers contributed to justifying the need for a new and less expensive method of drainage operations on heavy clay loams. The method envisages sparse drainage work combined with surface agricultural-land improvement measures, and the returns anticipated are about 2 million rubles annually in savings. A report was presented on research and development work on radiometric devices capable of shortening the time required for carrying out various observations or measurements by as much as ten times. In particular, a gamma-ray turbidimeter was designed to determine the concentration of debris in suspension or dragged to the bottom of flowing streams. By comparison to the conventionally employed techniques, this device is capable of measurements lasting 2-5 min rather than the usual 5-12 hrs. Also worthy of mention is the designing of a neutron moisture meter which is capable of carrying out absolute measurements of soil moisture, in grams water per cubic centimeter, in a matter of minutes. Gamma-ray humidity gages for soil humidity measurements and a gamma-ray device for determining water resources present in a snow cover were also designed on the same principle of absorption and scattering of gammas. These instruments are beginning to make their way into routine work in scientific and experimental institutions. About 60 such gamma-ray humidity gages will be in use in 1960. The devices enumerated will increase labor productivity, and widespread use of such instrumentation in production will be rewarded by yearly economies totaling not less than 2-3.5 million rubles.

Yu. N. Artem'ev and R. A. Srapenyants have evolved a simple and precise method for determining the time to fouling of piston rings while the parts are in service on a tractor engine. The procedure has proved feasible for rapid laboratory-on-wheels evaluations of the performance qualities of various brands of diesel oils, and was also used to advantage in optimizing the time for changing oil in tractor crankcases. On the basis of field and laboratory tests, it has been established empirically that service life and reliability in performance may be had, in the case of the DT-54 tractor diesel, by changing the crankcase oil not once every 120 to 180 hr as stipulated in the standard operators' rules up to now, but once every 360 hr of engine operation.

Isotope methods have been used to study the features of the flow of grain kernels through the shakers in grading machines, leading to optimized conditions for separating seeds with respect to specific weight in a dry medium by means of a flow of air and oscillatory motions of the shakers. The data obtained facilitate the design of machinery for grading seeds strictly in terms of specific weight. Planting of sorted seeds means, as commonly known, a crop yield increased by 20-25%.

Declassified and Approved For Release 2013/02/14 : CIA-RDP10-02196R000100060003-5

Declassified and Approved For Release 2013/02/14 : CIA-RDP10-02196R000100060003-5

According to incomplete and scanty calculations, using the tracer and radiations data to good advantage in agricultural applications will be rewarded by annual savings of the order of 450 million rubles.

RADIOACTIVE ISOTOPES AND NUCLEAR RADIATIONS IN THE FOOD PROCESSING INDUSTRY

V. I. Rogachev

The main trends evident in applications of radioactive isotopes and nuclear radiations in the food processing industry are the following:

1) the use of high-level ionizing radiations for processing foodstuffs to increase storage life, cope with insect pests, alter the properties of the raw material being processed, etc.;

2) the use of radioactive isotopes (labeled atoms) in analyzing technological processes and equipment to develop new designs and techniques;

3) the use of radioactive isotopes in automatic process control and monitoring devices.

The use of high-level ionizing radiations, a problem of great complexity in the food industry, is related to the solution of problems not solely of a technological character (choice of required dosage and means of irradiation, development of techniques for preirradiation processing of the products, and deciding on the best conditions for storage of irradiated items, etc.), but also questions relating to the nontoxicity and palatability of irradiated foods.

At the present date, a large fund of data has been accumulated on the absence of induced radioactivity in foodstuffs subjected to radiation up to a level of 5-12 Mev, as well as the absence of toxic and carcinogenic factors. At the same time, it has been ascertained that certain food factors of importance to the human organism (ascorbic acid, thiamine, tocopherol) are degraded by irradiation treatment. These factors, it may be noted in passing, suffer the same fate in heat-processing of foods. Another consequence which cannot be ignored is the appearance of taste and smell effects in some treated foods which are not characteristic of nonirradiated foods of the same type.

The intensity of these changes, due to complex oxidation and reduction processes, depends on the chemical composition of the foods and on the size of the irradiation dose received. For example, when meat is exposed to a dose of 1.5-2 million rads, a specific and peculiar odor results; this odor disappears upon cooking. When the dose is reduced to 500 thousand rads, the odor is not given off. On the other hand, the effect of stepping up the dose to 4-5 megarads is a sharp change in the organoleptic properties and chemical composition (degradation of vitamins, oxidative processes, etc.).

When foods of plant origin are radiation-processed, no strange tastes or odors result as a rule, but some softening of tissues are observed (this softening effect is much less intense than that resulting from heating).

The use of various pretreatment techniques (vacuum treatment, quick-freezing, acceptor additives, etc.) may diminish the intensity of those changes which are by-products of radiation.

When foods are irradiated, the changes owing to enzymes, which are completely inactivated only when the radiation dosage is 10-15 megarads, must be taken into account. When the enzyme system present in food products is a very active one, additional measures must be taken to inactivate the enzymes (mild heating, proper storage temperature, use of enzyme inhibitors, etc.).

One aim to be pursued in radiation processing of foods is, therefore, minimization of the radiation dosage, not only from the engineering costs standpoint, but also with a view to improving the quality of the resultant products. The lower the radiation dosage, the better the probability of the process being adopted in commercial

Declassified and Approved For Release 2013/02/14 : CIA-RDP10-02196R000100060003-5

Declassified and Approved For Release 2013/02/14 : CIA-RDP10-02196R000100060003-5

practice. From these considerations, we may infer that the following fields of ionizing radiation applications stand closest to fruition from a practical industry standpoint; control of potato sprouting, ridding foodstuffs of insect infestation, and lengthening the storage lifetime of readily spoilable foods.

As has been shown by research conducted at the Institute of Biochemistry of the USSR Academy of Sciences, the sprouting of potatoes as the tubers emerge from the dormant state is related to the synthesis of nucleic acids at the growing points. This synthesis is drastically slowed down by irradiation. For example, potato tubers irradiated with a dose of 10 thousand roentgens do not sprout for a 14 month period in storage underground with no artificial cooling. Calculations indicate that irradiation of the potatoes at 5-10 thousand rad doses in combination with other methods should have the effect of lengthening potato storage life to a year and a half.

The Ministry of Health of the USSR has announced a decision to license the release of potatoes irradiated with doses up to 10,000 r as edible material. A pilot tuber-irradiating plant will be set up in the near future; a Co^{60} source will total activity of 50 thousand gram equivalents of Ra will be used at the pilot plant. A total output of 20-25 thousand tons of processed potatoes over the potato season is expected.

According to data released by the Institute of Economics of the USSR Academy of Sciences, the savings projected from the use of radiation-processed potatoes will total 15 million rubles.

Numerous experiments have proven that irradiation at 10-50 kilorad doses will assure genetic sterilization of insect pests and at the same time prevent spoilage of grain, groats, dried vegetables and fruit, and food concentrated during storage. Experiments performed by the Nutrition Institute of the USSR Academy of Medical Sciences have demonstrated that grain irradiated with a dose of 30,000 r differs in no way with respect to nutritive qualities from nonirradiated grain.

Preparatory experimentation on a scale approximating production conditions will be required before radiation sterilization and eradication of food pests will achieve full status. The groundwork is being laid by the All-Union Grain Research Institute, which started work with a special-design high-level cobalt gamma facility (100,000 gram-equivalents of RA) in 1960.

Among the reasons for spoilage of food, microorganisms occupy a prominent place, being capable of greatly altering the chemical composition and properties of foods through their metabolic activities.

Ionizing radiations inhibit multiplication of spoilage microorganisms and suppress their other vital functions either entirely or partially, depending on the applied dosage. A detailed study of the effect of ionizing radiations on the physiological, morphological, and miscellaneous properties of microorganisms has been completed at the Institute of Microbiology of the USSR Academy of Sciences. The size of the dose required to kill microorganisms is a function of the species, strain, external conditions, and other factors. Doses of 1.5-2 megarads are required to inactivate the large number of bacteria present in foodstuffs. There are however more stable and viable microorganisms which require doses up to 5 megarads to bring about their complete destruction. Such high dosages cause fargoing changes in the chemical composition and taste properties of many foods, especially dairy products.

Cells of the same strain of spoilage microorganisms have been found experimentally to differ in radiotolerance. Only a small percentage of cells of a particular strain exhibit radioresistance well above average. Most of the microorganisms perish at comparatively low doses (50-500 kilorads) which are not harmful to the foods being processed. If radiation doses lethal to over 90% of the microbial cells present are used, the storage life can be lengthened three to eight times, as has been demonstrated by studies at the Central Research Institute for the Vegetable Canning and Drying Industry, without harmfully affecting the nutritive properties of the foods.

One rather complicated problem is the use of irradiation to completely sterilize food products. The most promising approaches appear to be combined methods for dealing with microorganisms (mild heating, treatment with antibiotics, etc.).

A study tackling all sides of this problem related to radiation processing of food products is being undertaken in the USSR in line with the erection of two experimental irradiation facilities. One of them is designed to use a radioactive source charged with Co^{60}, total activity 220 thousand gram-equivalents of Ra, dose rate to 2500 r/sec. The other installation is a 5 million electron-volt linear accelerator capable of producing radiation with a dose rate to 100,000 r/sec.

Declassified and Approved For Release 2013/02/14 : CIA-RDP10-02196R000100060003-5

Declassified and Approved For Release 2013/02/14 : CIA-RDP10-02196R000100060003-5

At the All-Union Research Institute for the Brewing Industry, a program of research involving the use of tracer compounds is underway, to investigate yeast metabolism under alcoholic fermentation conditions. One result of the research was the successful telescoping of the secondary fermentation stage into the primary fermentation stage; the stage associated with oxidation-reduction transformations was accelerated by using fermentation-promoting preparations. CO_2 under a pressure of 3-5 excessive atm. was used to saturate the atmosphere; rapid filtration through separators was used for clarification. A new technological process based on a tracer-compound study of fermentation and secondary fermentation processes led to a shortening of fermentation time from eight to two days. The new technological advance has been incorporated into industrial practices.

Investigations of other processes important in alcoholic fermentation have been conducted by the Central Research Institute for the Alcohol Industry. A study of the nutritive value of various media for microorganisms showed that normal yeast activity is sustained by keeping a content of dry material ranging from 15° (according to a saccharometer reading) to higher values in the grain mash. Mashes of this composition also require a certain amount of nitrogen, phosphorus, and vitamins. When such mashes are resorted to, there is no longer any need to add green malt to reduce the rate at which cereals are used up.

At the Moscow Technological Institute of the Meat and Dairy Institute, a study was conducted on the structure of cream butter produced in various ways (churning or continuous flow), using a test solution of Ca^{45}-labeled calcium chloride. In addition, the process by which table salt diffuses into a cheese mass was studied, as well as calcium adsorption on casein during rennet curdling, and the dependence of adsorption of calcium on the acidity of the milk. On the basis of a study of the cheese melting process (salts with labeled atoms were used for the melt), it was found that the interaction between salt anions and cheese protein involves adsorption.

The All-Union Research Institute for the Meat Industry has carried out a research program using tracer atoms to probe into the characteristics of the meat salting process, and to find out what degradative changes take place in meat processes as smoked sausage is being prepared. The findings were that the method of salting the meat simultaneously with immersion of the sausages into the brine slurry enjoys certain advantages over dry salting followed by exposure to air, since no degradation of proteins ensues in the first instance, and the effective components of the smoking medium consequently penetrate more readily into the bulk of the sausage. This speeds up the process of producing high-quality smoked sausage.

Tracer atom research of importance to fisheries was sponsored by the All-Union Research Institute of the Fishing Industry and Oceanography. The investigations showed that an excess content of calcium ions and a low content of magnesium ions in fish is accompanied by lowered metabolism and stunted growth. An increase in the concentration of magnesium salts contributes to the growth of the fish. The data obtained support a recommendation to fisheries to introduce magnesium salts into carp fisheries of above-average water hardness, to bring the magnesium/calcium ratio to 1:4. The important role of cobalt in fish metabolism was laid bare, and it was recommended to add 0.7-0.8 mg ordinary cobalt per 1 kg of weight per day of feed administered to pond-grown fish. This addition to the feed mix improves fish growth and enhances the viability of the stock. Fish fry raised on this diet produced a yield six times greater, under patently unfavorable wintering conditions, than a test stock grown on cobalt-free feed.

Experiments performed by the All-Union Research Institute of Pond and Inland Fisheries showed that addition to trace dosages of cobalt to the daily feed ration administered to commercial carp increases the mean weight per fish by 14% and results in a 25-27% in the over-all fish crop. Assuming that no more than half the pond fisheries in the USSR were to use cobalt feed additives, the added returns would total 75 million rubles by 1965.

Some tracer research was conducted at the All-Union Grain Research Institute to solve problems of interest to the flour-milling and feed-mix industries. The practice of adding vitamins to flour, and vitamins, antibiotics and various metal salts to cattle feed mix has been gaining constant ground during the past few years. Since the amount of these additives remains within thousandths of a percent of the amount of end-product, the uniformity of the distribution of these additives into the bulk substrate depends heavily on the mixer design. An assessment of the degree of homogeneity achieved by the mixing is possible, however, only by using radioactive isotope tracers. Experiments were carried out on five mixing equipments, two types of which were recommended for industrial use as a result of the tests, and flour mills and feed-mix plants will be outfitted with this machinery in the immediate future. Optimized mixing parameters and conditions were also brought to light.

Declassified and Approved For Release 2013/02/14 : CIA-RDP10-02196R000100060003-5

Declassified and Approved For Release 2013/02/14 : CIA-RDP10-02196R000100060003-5

Research soon to be undertaken will deal with absorption and distribution of water in wheat grains, under various sets of temperature and humidity conditions. The solution of this problem is of enormous importance in improving procedures for preparing grain prior to milling.

Radioactive tracers were used in an investigation of some of the parameters of grain flow in grading machines (at the Moscow Institute of Mechanization and Electrification of Agriculture) and in an upright groats husker and polisher (All-Union Grain Research Institute).

The use of control and measuring devices based on radioisotopes. One of the main difficulties encountered in attempts to automate operations at mills and feed-mix plants is the absence of any reliable means for remote monitoring of the filling level of hoppers and silos. The level gages currently in use (membrane, pressure gages, variable-capacitance gages) work only in direct contact with the material, a disadvantage that entails contamination of the sensing instrument, spurious readings, and rapid deterioration of the instruments. Furthermore, most level gages now in use give readings of the level positions only in place on the walls of bins or silos.

These drawbacks highlight the feasibility of using gamma-ray level gages in flour and cereal plants; the gamma devices are available in four-control-position design (two control points at the bottom of the bin, two at the top), and the instrument operating time need not exceed 5 sec. Moreover, the radiation source and radiation detector must be as small as possible to as possible to allow easy positioning inside the silo towers, and the devices must,consequently, have a low operating threshold. Considering the enormous size of silo installations and the heavy dust load on the air in rooms adjacent to silo chambers, it is imperative to have an operating electronic-relay unit placed at a distance of 150 meters from the primary sensors.

The All-Union Grain Research Institute has developed a special four-channel gamma level gage, the GU-2, meeting the above requirements. The radiation source is implanted in the wall of the silo, the radiation being calculated to fall simultaneously on four sensors, so that the required number of radiation sources may be reduced by four times.

The laboratories of this institute have developed a method of noncontacting measurement of the clearance between working wollers, in terms of the intensity of radiation passing through the clearance, replacing the method of finding the clearance between rollers by passing lead plates between them and measuring their thickness. The experiments have shown that the instrument readings are a linear function of the clearance. When a beta source (Sr^{90}) is used, it is possible to determine the clearances to 0.05 mm within microns.

Mass-produced RPRU-4 devices are being used to monitor alcohol level in large vats (400-100 gallons) of the brandy and alcohol bottling departments of alcohol and vodka distilleries. The determination of level need be carried out at only two points (first tentatively, second for control action) in the top half of the vat.

This approach may be supplemented by a constantly operating go-no go control for batch determination of alcohol level in tank cars, providing a fairly accurate indication of the amount of alcohol present. ARIU-9 device may be used in this case, with a tube containing a radioactive float suspended inside the tank car.

At the Saratov Grease and Fats Works, a UR-6 device has been enlisted to monitor and control product level in autoclaves during hydrogenation of fatty materials. At the Krasnodar Grease and Fats Works, a UR-4 level gage is being used to monitor and control the level of the fatty material in a still used for vacuum distillation of glycerine.

In the sugar industry gamma-ray relay units may be used to determine the level to which bins are loaded with sugar beets. Since the bin loading process is accompanied by intense vibration and impact effects, contacting level gages of the conventional type become easily damaged, so that noncontacting devices are obviously a necessity.

Among other possible applications for gamma relays, we may note their use (this refers to the RPS-11 in particular) as counters on a production line. In some cases, automatic testing of the functioning of bottle-filling procedures is feasible by using the RBP-1. For monitoring and process control in the preparation of multicomponent mixtures, the RSDA-1 automatic installations now available may be used in many instances, since they can be set to meter liquid flow to a specified level with an accuracy within ± 1.5-2 mm.

Radioactive density gages (working to ± 0.5%) may be used in the brewery industry to determine the density of the wort pumped into the fermentation room, and also to give density readings of filtered beer.

Declassified and Approved For Release 2013/02/14 : CIA-RDP10-02196R000100060003-5

Declassified and Approved For Release 2013/02/14 : CIA-RDP10-02196R000100060003-5

The Institute of Physics of the Academy of Sciences of the Latvian SSR has developed an on-off density controller to monitor and control the preparation of various liquid mixtures. The controller is based on a conventional area flow meter whose position is sensed by a noncontacting radioactive relay unit. This density monitor was used in the process control loop of a single-tower vacuum-distillation plant for concentrating glycerine sweet water. The use of a radioactive level gage and temperature controller developed by specialists at the Riga Fats and Oils Combine and the Institute of Physics of the Academy of Sciences of the Latvian SSR is being contemplated as a possible component in the same process control loop. Closing this control loop will step up the productivity of the entire distillation plant by 40%, reduce steam costs by 3%, cut electric power and water by 23%, and lower glycerine losses by 0.01%. The total yearly savings for a single vacuum distillation plant amount to 64 thousand rubles.

The All-Union Research Industry for the Dairy Industry made good use of a PZhR-2 device on an experimental automated vacuum-distillation plant to close an automatic monitoring and control loop for handling dry materials in the production of sweetened condensed milk. Temperature fluctuations of ± 2% do not cause any appreciable error in dry-material readings.

An interesting application of gamma-ray relays in the confectionery industry is an automated loop for the manufacture of waffle mix worked out by specialists of the 17 of June Confectionery Plant in Riga, in collaboration with research workers of the Institute of Physics of the Academy of Sciences of the Latvian SSR. The principal component in the process loop is a radioactive automatic mixing and metering RSDA-2 device.

Summarizing, we may safely state that the food processing industry offers a wide range of applications for radioactive isotopes and nuclear radiations. Furthermore, clarity is still lacking in several instances as to the feasibility and economic advantage in using these devices. Feasibility is to be judged in terms of 1) completing complex research on the irradiation of foods at high-level radiation facilities; 2) expanding the area of labeled-atom research, where it is incumbent upon the research institutes of special branches of the food industry to develop the required equipment and labeled organic compounds (proteins, fats, vitamins, etc.) to be incorporated into test foods; 3) developing automatic process control loops using devices based on radioactive isotopes. New isotope devices meeting precision specifications and other requirements of the food industry are also needed to monitor various technological processes. The preparation of experimental devices and short-run production facilities will require an expanded production program for these specialties.

THE USE OF RADIOACTIVE ISOTOPES AND NUCLEAR RADIATIONS IN MEDICINE

F. M. Lyass

The Riga Conference was a sharp contrast to all previous meetings on the problem of radioactive isotope applications in medicine because of its emphasis on practical applications for radioactive isotopes and nuclear radiations in medical clinical practice.

The report at the Conference is that great opportunities are open in our country for significantly expanding the areas of application of radioactive isotopes in medical practice in the years to come, and for providing public health institutions with the latest means in medical radiological techniques.

Radiological physicists have an important place awaiting them in the further development of medical radiology. Because of the rapid pace of development of complex radiological equipment, health physicists will have to be everyday consultants to physicians specializing in radiological therapy, both in the development of radiotherapy treatment and in the unending search and clinical use of new methods of radio diagnostics. The fruitfulness of such joint work was demonstrated in the reports "Autogammaradiography and Automatic Scanning in Isotope Determinations of Spinal Tumor Localization" (O. G. Arakelov, N. A. Gabelova, F. M. Lyass,

Declassified and Approved For Release 2013/02/14 : CIA-RDP10-02196R000100060003-5

Declassified and Approved For Release 2013/02/14 : CIA-RDP10-02196R000100060003-5

E. G. Martusov) and "Multichannel Radiography and Its Clinical Applications" (G. M. Frank, N. A. Gabelova, F. M. Lyass, G. A. Malov). Instruments designed and built at the Institute of Biophysics of the USSR Academy of Sciences: a gamma-sensitive isotope scanner and an eight-channel radiography equipment – smoothed the way for utilizing radioisotopes in clinical practice to determine spinal-chord tumor localization and to probe intricate processes in hemodynamics. The reporters noted that radiotracer methods in diagnostics has a new range of applications opened up to them by the development of specialized equipment, and that the high sensitivity of isotope instruments will mean a possibility of lowering the amount of radioactive preparations introduced into the organism.

V. A. Belyakov, V. A. Volkov, É. G. Gulyaeva, K. D. Kalantarov, I. I. Shvyrkova submitted a report entitled "On the Development of a Dosimeter Device for Recording Beta Activity within Body Cavities, in Early Local Cancer Diagnosis." A scintillation detector which they designed records beta radiation and determines any focus of increased activity in response to ingestion of traces of P^{32} by the patient, and is useful in clinical diagnosis of cancer of the uterine cervix.

D. L. Rozin demonstrated the possibility of using radiophosphorus in diagnosis of metastases of cancer of the mammary glands into bone tissue. Working on a large group of patients, he traced bremsstrahlung above the tumor sites, since the tumor takes up P^{32} in greater quantities than does unaffected tissue.

Among the reports dealing with diagnostic isotope applications, we cite "An Autoradiographic Method in Hematological Studies," submitted by G. I. Kozinets, N. M. Fertukova, M. G. Shitikova. This method can be used to determine the period of growth of cells of the spinal chord, or the adaptability of transfused blood cells, a valuable diagnostic test in some blood disorders.

N. G. Nikulin reported on results of using I^{131} to determine thyroid function in arteriosclerosis as in various phases of rheumatism.

A report by V. A. Petrov and M. M. Palladieva on the use of isodose templates and special charts in clinical dosimetry was heard by the participants with great interest. The method he proposed, determining doses in depth by overlaying the template on schematic charts of anatomical cross sections of the human body, enable the physician to take proper account of the amount of energy exerted both on the irradiated organ and on the surrounding healthy tissue.

Radiotherapy problems were discussed in some papers. A. V. Kozlova devoted her report to a radiosurgical technique for treating malignant neoplasms in which radioactive preparations are inserted into the incision during the operation. The advantage of this therapeutic technique is that irradiation can be limited to a certain volume of tissues in the required dosage and for optimized exposure times. The results cited by the reporter on therapy of patients with malignant neoplasms show great promise in the clinical application of this method both in early and late stages of the disease.

Experience in the therapy of malignant tumors by radiocobalt treatment, at the Gertzen State Oncology Institute, and by radiocesium, radioiodine, and radiogold, was detailed by M. A. Volkova. The material accumulated at the Gertzen Institute showed the advantages of telegammatherapy over conventional x-ray therapy in treating malignancies of the lungs, digestive tract, female urogenital region, etc. Experience in treatment of cancer of the digestive tract (180 patients predominantly in the third stage of the illness) by multiport and rotating-beam irradiation therapy combined with applications introduced within the digestive tract (40 cases) convinced Z. F. Lopatnikova to recommend this approach for practical therapeutic use.

A paper by E. I. Ivanitska, "The Role of Radiation Therapy Following Removal of Cancer of the Uterine Cervix, and in the Treatment of Post-Operative Relapses," dealt with clinical applications of various techniques in radiotherapy and oncology. Covering the same topic were the papers "Experience in Treatment of Metastases of Melanoma by Artificial Radioactive Isotopes," by L. L. Likhovetska, "Experience in the Treatment of Widespread Forms of Thyroid Malignant Tumors with Radioiodine," by L. I. Lushina, "Therapy of Thyroid Cancer Metastases with Radioiodine," by V. K. Modestov, "The Methods and Clinical Observations in Treatment of Inoperable Brain Tumors with Granular Radioactive Gold" by A. A. Volkov. The investigations showed that despite the definite results scored, treatment of malignant neoplasm cases remains one of the major unsolved problems. The widespread use of combined methods of treatment, particularly during the early stages of the disorder, has significantly increased the percentage of long-term recoveries in many forms of malignant neoplasms.

Declassified and Approved For Release 2013/02/14 : CIA-RDP10-02196R000100060003-5

Declassified and Approved For Release 2013/02/14 : CIA-RDP10-02196R000100060003-5

The use of radioisotopes in dermatology was discussed in reports submitted by A. V. Braitsev, A. S. Bezzabotnov, P. M. Zalkan, T. I. Naruzhnyi, B. M. Lebedev, L. L Sych, and E. A. Ievleva, "The Therapeutic Value of Radioactive Isotopes in the Treatment of Some Dermatoses," and A. Ya. Prokopchuk, "Experience in the Use of Radiophosphorus, Radiostrontium, Radiothallium, Radioindium, Radioarsenic, and Radiocesium Isotopes in the Dermatological Clinic."

In connection with the therapeutic applications of radiophosphorus in Opthalmological Practice (E. D. Dubovyi, S. F. Kal'fa), the effectiveness of utilizing the applicator technique in treating serious inflammatory malfunctions of the cornea and sclera were shown.

In a paper by L. M. Rozanova and S. E. Tukachinskii, "Some General Results of the Use of Radioactive Phosphorus in the Treatment of Essential Polycythemia," a method for treating essential polycythemia consisting of massive phlebotomies and implants of radiophosphorus was outlined; this method provides a way of establishing the long-term therapeutic effect resulting from introduction of 6-7 microcuries of P^{32}, delaying the development of chronic myelosis, and eliminating the hazard of serious complications (leukemia, aplastic anemia).

A report delivered by G. P. Nazarishvili, L. G. Parsiya, G. Sh. Zedgenidze entitled "Experience in the Use of Radioactive Isotopes in Clinical Medicine" confirmed the fact that the most effective therapy technique for leukemias and polycythemia is a combination of x-ray therapy and radiophosphorus implants. The reports also recounted their experience in using radioisotopes to treat and diagnose other ailments.

The assimilation of new clinical techniques embodying the use of radioactive isotopes depends to a substantial extent on the job of supplying radiological departments of public health institutions with the necessary tools and accessories. M. F. Vyrzhikovskaya and G. M. Krivchenkov told of experimental surgical equipment and accessories being designed and fabricated at the Scientific Research Institute for Experimental Surgical Equipment and Tools, for work in radiological clinics. The participants were presented with a set for using radioactive needles, a set for inserting radioactive grains into hollow elastic fibers, a propulsion pistol for implanting radioactive grains in tissue, and a set of shielded injection syringes for injecting solutions of radioactive isotopes.

A report by A. Ya. Berlovskii, "Mechanization of Radiological Operations in the Clinic," was devoted to an attempt to rationalize the process of preparing radioactive applicators without extracting them from the system of shielded devices, an approach which allows for a pronounced reduction in the irradiation level to which servicing personnel are observed.

The question of preparatory measures for the organization and equipping of the departmental dosimetric service of the USSR Ministry of Public Health was dealt with by V. A. Petrov in his report. A structuring of the departmental dosimetry service based on a center with first- and second-echelon dosimetry stations was proposed.

A team of research workers at the Leningrad Institute of Radiation Hygiene (A. V. Gorin, V. A. Grossman, A. V. Dranchinskii, B. V. Ekimov, B. N. Raevskii, L. R. Romanov, É. P. Storozhenko, Yu. P. Fedorov, G. M. Shavrin, V. P. Shamov) presented a description of a mobile radiometric express-analysis laboratory using transistorized equipment mounted on a UAZ-450A rolling laboratory truck.

M. M. Mikhailov and B. M. Abakumov, in a paper entitled "Dosimeters for Ionizing Radiation Based on DC Semiconductor Transducers" reported the design of semiconductor transducers built to replace the defective batteries now used in the DK-3 and DK-0.2 dosimeters.

In a survey paper, G. A. Zadgenidze and E. P. Vorob'eva pointed out, in a statement adopted by the panel, that radioactive techniques constitute a powerful tool for treatment of cases, that modern methods of radiation therapy make it possible to give effective relief to patients with malignant neoplastic conditions. However, in both diagnosis and therapy, the use of radioactive isotopes is largely restricted to the large leading health institutions in our country, and has not yet made its way into massive use in ordinary hospitals. Insufficiencies are evident in the development and fabrication of modern radiological equipment. The participants at the Conference proposed that the Ministry of Public Health of the USSR make a careful and thorough study of the proceedings of the Conference, with a view toward elaborating concrete measures for further development of work in the field of medical radiology.

Declassified and Approved For Release 2013/02/14 : CIA-RDP10-02196R000100060003-5

Declassified and Approved For Release 2013/02/14 : CIA-RDP10-02196R000100060003-5

ALPHA, BETA, AND GAMMA SOURCES IN PROCESS CONTROL

E. E. Kulish

The appearance on the scene of artificial radioactive isotopes and radiation detectors offering a wide range of characteristics has paved the way for the development of new process control methods and instruments serving different branches of industry.

The varieties of nucleonic instrumentation now in use and undergoing development in the process industries include noncontacting radioactive thickness gages, density gages, tank level gages, radiographic machines, and many other devices contributing to the solution of a broad range of technological and research problems.

Many of the devices are in assembly line production: the Kaluga pyrometric instruments plant is putting out the RIU-1 level indicator, the UR-6A and UR-7 level gages, the PZhR-2 density gage, the MIR-3A pressure gage, and many others; the Tallinn KIP factory manufactures the ITU-495, ITU-496, and GT-150 thickness gages, the BIV weight measuring cell, the P-4 wall thickness gage, RSP-11 product item counters, etc.; the Kharkov KIP Plant manufactures electronic relays; the Moscow "Mosrentgen" high-voltage equipment plant produces gamma facilities for radiographic flaw detection, etc.

Hand in hand with the development of instruments, there is a continual advance in the development and improvement of manufacturing technology of various radioactive isotope sources for the above instruments and similar devices.

Because of the great variety in possible applications of radioactive sources and the widely differing on-stream environments, special attention is given in the design stage to elimination of safety hazards and any possible contamination of surrounding objects and dwellings.

It has also been necessary to take into account stringent industrial specifications. These include the possibility of the source being used in air and fluid environments at temperatures ranging from several tens of degrees below zero to 200-300°C, and where the medium may be an aggressive one, while the source may be subjected to considerable impact and vibration loads. Sources of betas and particularly of alphas must be very thin layers of an active substance firmly bound to a substrate and isolated by shielding material so that, on the other hand, maximum yield of particles will be obtained with minimum bremsstrahlung, and on the other hand, so that the purity of the source surface will be maintained. Thanks to the efforts of scientists, designers, and technologists, most of these problems have been successfully resolved.

The techniques of fabricating sources fall into three variants:

1) the use of active material in the form of wires, rods, etc. These include for the most part gamma sources of zinc, cobalt, and silver wire, also of cobalt rods pile-irradiated. Taking into account the greater propensity of radioactive materials to oxidation, only sources of low activity levels not exceeding several tenths or hundredths of milligram-equivalents of radium can be made in that form. In some cases (notably Tl^{204}), the active material is encapsulated in aluminum foil. Nevertheless, a certain amount of caution must be exercised in handling such sources, and it is well to have them completely isolated from the remaining parts of the instrument;

2) the use of encapsulated radioactive materials. This technique is resorted to mostly in fabricating medium-level and high-level gamma sources. The radioactive material is enclosed in either single or double capsules with carefully crimped lids (Co^{60}, Tm^{170}, Cs^{134}, Ir^{192}, etc.) or sealed in glass (Zn^{65}) or metal capsules (Cs^{137}, Cs^{134}).

3) preparation of surfaces by depositing an active layer on various substrates. This method is employed primarily in preparing sources from materials containing Sr^{90} and Pm^{147} isotopes, plutonium, and other materials. Active layers are electroplated-on or enameled.

Reliable and well recommended alpha, beta, and bremsstrahlung sources can be produced via these methods. To prevent mechanical injurty to the active layer, and also to produce bremsstrahlung where needed, the sources are placed in special containers in some instances.

Declassified and Approved For Release 2013/02/14 : CIA-RDP10-02196R000100060003-5

Declassified and Approved For Release 2013/02/14 : CIA-RDP10-02196R000100060003-5

At the present time, there are over 200 different types of radiation sources in mass production, representing 14 radioactive isotopes; these do not include the large number of radiation sources being produced on an experimental basis. Such a proliferation of sources in itself calls for some attempt at classification in order to standardize the sources being made available, and to facilitate a judicious selection of a source for any given application.

A moderate number of principles governing the nature of the interaction between nuclear radiations and the material of the test object underly the operation of all radioactive devices used in process control. Prominent among these basic principles are the attenuation of radiation on passing through matter, reflection of radiation from the boundaries of the media, and the ionizing power of the radiation emitted. It is obvious that all of these principles must also be considered in any standardization procedure.

In looking over the gamma-ray sources, one notes that their resultant spectrum may differ in some cases from the spectrum of the corresponding isotope (because of bremsstrahlung) and from the radiation associated with internal conversion, electron capture, and position annihilation. For example, the mean energy of the resultant spectrum of Tm^{170} sources is 80-200 kev (depending on the type of source) instead of the value of 84 kev taken from tabulated data; the mean energy of a Zn^{65} source is 0.35 Mev, instead of the tabular value 1.1 Mev, etc.

Eu^{155}, Se^{75}, Ce^{144}, and Zn^{65} sources must therefore be included among the soft emitters. These sources may be recommended for flaw detection of light alloys and metals, and thin layers of heavy metals, as well as for use in process control instruments based on recording reflected radiation from materials of low atomic number. The other sources mentioned are more fitted to such applications as flaw detection in thicker layers of ferrous metals.

A similar approach may be used in the choice of beta emitters for these or other applications. In reviewing the characteristics of beta-emitting sources available in large quantity at the present time, we might single out two groups of emitters:

1) "pure" beta emitters (Pm^{147}, Tl^{204}, Sr^{90} on plates and disks, and Ce^{144} on disks) which are suitable for removing electrostatic charges in product item counters, coating thickness meters, etc.;

2) sources with intense bremsstrahlung (Ce^{144} on plates of Ru^{106} and Sr^{90} in BI-type sources) which are suitable for use in devices based on the passage of radiation through matter.

The further development of nucleonic instrumentation depends on the successful solution of design and research problems associated with further improvements in existing devices and sources, and with new advances in the field.

The sessions of this panel section contributed to drawing up a tentative balance sheet of the progress registered to date, and highlighted the main avenues of further development in this field of instrument design.

BRIEF COMMUNICATIONS

USSR. The IV All-Union Conference on High-Energy Physics and Elementary Physics met at Erevan during June 1960. Representatives of physics research institutions of the Academies of the USSR, Georgia, Kazakhstan, and Armenia took part in the deliberations, along with representatives of the Joint Institute for Nuclear Studies and the Physics and Engineering Institutes of Leningrad and Kharkov.

Declassified and Approved For Release 2013/02/14 : CIA-RDP10-02196R000100060003-5

Declassified and Approved For Release 2013/02/14 : CIA-RDP10-02196R000100060003-5

BIBLIOGRAPHY

NEW LITERATURE

Books and Symposia

Yadernaya geofizika [Nuclear Geophysics]. A symposium of articles on the uses of radioactive isotopes and radiations in petroleum geology. Edited by F. A. Alekseev. Moscow, State Fuel Industry Press (Gostoptekhizdat), 1959. 372 pages, 12 rubles, 90 kopeks.

The book outlines materials on applications of radioisotopes and radiations in petroleum geology. Radiometric equipment for recording neutrons and gammas is described, and attention is given to the results of research using simulated rock strata, the basics of the induced-activity technique as applied to the analysis of borehole cuttings, etc.

Results from the use of the neutron method for quantitative determination of the porosity of a stratum are cited, and the use of this method and the induced-activity method to locate the oil-water interface in an oil pool are described.

The main problems encountered in studying radiometric logging measurements in oil wells are discussed. A new radiometric method for exploring oil fields, based on measurements of ground surface radioactivity in petroliferous areas, is described.

T. Kahan, M. Gauzy. Reactor Physics and Design. Translated from the French. Moscow, Atomizdat, 1960, 392 pages, 19 rubles, 40 kopeks.

This Russian translation is of the first volume of a three-volume treatise on nuclear engineering. The fundamentals of nuclear physics, radioactivity and the properties of nuclear radiations, nuclear fission processes, and chain reactions are among the subjects treated. Reactor steady-state theory and reactor dynamics are discussed. A description is given of methods for carrying out calculations for homogeneous and heterogeneous reactors. The text is illustrated with numerical examples and performance characteristics of existing reactor installations.

The book is written for students in the corresponding departments, and for engineering and technical workers in nuclear industry.

Promyshlennaya radiografiya [Industrial Radiography]. Translated from the English. Edited by A. S. Shtan', V. I. Sinitsyn. Moscow, Atomizdat, 1960. 330 pages, 14 rubles, 30 kopeks.

Applications of radioactive isotopes and nuclear radiations in various branches of industry, primarily in the metal working industry, are discussed. A description of various methods of nondestructive testing follows.

The book is written for engineering and technical workers in industry and for students in the field concerned.

V. I. Gerasimovskii. Mestorozhdeniya urana zarubezhnykh stran [Uranium Deposits Outside the USSR]. Moscow, published by the USSR Academy of Sciences, 1959. 144 pages, 4 rubles, 20 kopeks.

This book constitutes a short survey of foreign literature on uranium minerals and their principal deposits in foreign countries. It contains an account of numerous uranium minerals, their chemical composition, properties, and formation conditions. Deposits featuring large reserves of high-grade uranium-bearing ores and small payable deposits of industrial interest are described.

Atom ABC. [in German] Published by W. D. Müller. Düsseldorf, Econ-Verlag, 322 pages.

Declassified and Approved For Release 2013/02/14 : CIA-RDP10-02196R000100060003-5

Declassified and Approved For Release 2013/02/14 : CIA-RDP10-02196R000100060003-5

This item is a defining dictionary which explains in popular style many concepts encountered in the areas of nuclear physics, reactor engineering, and other fields offering applications for nucleonics: medicine, biology, agriculture, industry, etc. The book outlines the basic characteristics of research and test reactors, and gives an interpretation of the special terms, abbreviations, and definitions frequently encountered in the technical literature.

The dictionary was written for a broad readership interested in problems involving the use of atomic energy. It will also be found highly useful by specialists reading technical literature in German, as well as by translators and editors.

Articles from the Periodic Literature

I. NUCLEAR POWER PHYSICS

Neutron and reactor physics. Physics of Hot Plasmas and Thermonuclear Reactions. Physics of the Acceleration of Charged Particles

Vestnik akad. nauk SSSR No. 4 (1960)

Tsien, San-Tsiang, p. 121-24. Development of nuclear research in the Chinese Peoples Republic.

Dokl. akad. nauk Armyan. SSSR 29, No. 5 (1959)

S. A. Kheifets, pp. 211-13. A method for creating stability of vertical motion in an accelerator with magnetic field increasing radially.

S. M. Khzardzhan, pp. 215-221. Contribution to the theory of nonlinear plasma oscillations in a constant externally applied magnetic field.

Dokl. akad. nauk SSSR 131, No. 5 (1960)

S. R. Kholev, D. S. Poltavchenko, pp. 1060-63. Acceleration of a discharge plasma and production of intense shock waves in a chamber with coaxial electrodes.

Dokl. akad. nauk SSSR 131, No. 6 (1960)

A. Kh. Breger et al., pp. 1308-11. Absorption of gamma radiation from a point source in macroscopic systems

Zhur. éksptl. i teoret. fiz. 38, No. 5 (1960)

B. A. Bogachov et al., pp. 1374-80. Kinetic energy of U^{238}-photofission fragments.

M. D. Gabovich et al., pp. 1430-33. Detection of ion oscillations in a plasma.

G. N. Lovchikova, pp. 1434-5. Angular distribution of elastically scattered neutrons.

N. G. Koval'skii et al., pp. 1439-1445. Investigation of fast electrons in pulsed power discharges.

Yu. N. Barabanenkov, pp. 1512-14. Coulomb scattering of charges in a strong magnetic field.

V. V. Komarov, A. M. Popova, pp. 1559-63. Investigation of neutron spectra from the decay reaction of a deuteron acted upon by protons.

K. N. Stepanov, V. I. Pakhomov, pp. 1564-168. On synchrotron radiation in a confined plasma.

V. P. Silin, pp. 1577-83. On the electromagnetic properties of a relativistic plasma.

Declassified and Approved For Release 2013/02/14 : CIA-RDP10-02196R000100060003-5

Declassified and Approved For Release 2013/02/14 : CIA-RDP10-02196R000100060003-5

A. V. Gurevich, pp. 1597-1607. Contribution to the problem of the number of accelerated particles in an ionized gas in response to various acceleration mechanisms.

A. A. Zaitsev, M. Ya. Vasil'eva, pp. 1639-40. On the relation between oscillations and charged-particle loss in a low-pressure cylindrical plasma immersed in a longitudinal magnetic field.

I. F. Kvartskhava et al., pp. 1641-43. Instability of an induction pinch.

Izvestiya akad. nauk Armyan. SSR, seriya fiz.-matem. nauk 12, No. 5 (1959)

S. A. Kheifets, pp. 105-113. Excitation of phase oscillations of particles in an electron synchrotron by magnetic field noise, frequency noise, and accelerating-field voltage noise.

Izvestiya akad. nauk SSSR, seriya fiz. 24, No. 3 (1960)

B. S. Dzhelepov et al., pp. 258-260. Alphas from U^{233}.

Izvestiya vyssh. ucheb. zaved. Radiofizika. 3, No. 1 (1960)

V. V. Zheleznyanov, pp. 57-66. On the instability of a magnetoactive plasma relative to high-frequency electromagnetic disturbances. I.

B. N. Gershman, pp. 146-48. On the group velocity of plasma waves in the presence of a magnetic field.

Izvestiya vyssh. ucheb. zaved. Fizika No. 1 (1960)

V. G. Stepanov et al., pp. 104-114. Motion of a plasma in a flowing magnetic field.

V. N. Eponeshnikov et al., pp. 139-144. Dynamics of the effective sector angle in accelerators with rectilinear sections.

I. M. Ternov, V. S. Tumanov, pp. 155-162. Contribution to the problem of the flow of polarized electrons in a magnetic field.

V. N. Keesenikh, pp. 234-5. Coherent scattering in a plasma.

A. A. Vorob'ev, I. M. Ternov, pp. 236-241. International conference on high-energy particle accelerators and nuclear physics instrumentation, at Geneva, September 14-18, 1959.

V. N. Titov, pp. 241-243. Conference on electron accelerators.

Pribory i tekhnika éksperimenta No. 2 (1960)

Yu. G. Abov, pp. 3-14. Theory of neutron crystal monochromators.

G. A. Zeitlenok et al., pp. 16-20. A high-voltage power supply for the rotating plates of the ion-beam injection system for the 10 Gev proton synchrotron.

I. M. Samoilov, pp. 21-23. Injector for electron accelerators.

K. A. Petrzhak, R. V. Sedletskii, pp. 34-37. Counters for measuring weak activities.

T. I. Dmitrievskaya et al., pp. 38-40. Use of end-window counters to measure low-level beta radiation.

G. Ya. Pikus, pp. 104-106. Mass spectrometer with a high-vaccum mass analyzer.

N. N. Krasnov, pp. 148-150. A high-frequency cyclotron-type ion source.

Priroda 40, No. 5 (1960)

G. A. Kursanov, pp. 3-7. V. I. Lenin and the dialectics of the physical world.

Uspekhi fiz. nauk 70, No. 4 (1960)

G. M. Strakhovskii, N. V. Kravtsov. Strong magnetic fields.

Arkiv fys. 16, No. 5 (1960)

K. Singwi, pp. 385-411. The theory of diffusion cooling of neutrons in a solid moderator of finite dimensions.

Declassified and Approved For Release 2013/02/14 : CIA-RDP10-02196R000100060003-5

Declassified and Approved For Release 2013/02/14 : CIA-RDP10-02196R000100060003-5

Nucl. Energy 14, No. 145 (1960)

F. Paulsen, pp. 267-68. Investigations in the area of thermonuclear fusion, carried out by Euratom.

-- pp. 269-71. A neutron diffraction facility.

Nucl. Instrum. and Methods 7, No. 1 (1960)

W. Parker et al., pp. 22-36. Some methods in the preparation of radioactive materials for use in beta spectroscopy.

N. Mitrofanov, J. Van Loef, pp. 63-66. Detection of neutron and photon induced fusion by ZnS (Ag) mixed with uranium and thorium compounds.

H. Newson, R. Williamson, pp. 67-72. High-resolution neutron spectroscopy.

G. Henneberke, pp. 89-98. Electron accelerator in a pressurized tank from 3 ma beam current at 1,5 Mv direct voltage.

Nucl. Instrum. and Methods 7, No. 2 (1960)

R. Burman, A. Vavin, pp. 101-112. A multipurpose magnetic particle analyzer.

A. Deruytter, pp. 145-52. A 4π-fission detector.

E. Burke, L. Lowe, pp. 193-196. Derivation of thermal-neutron spectra from transmission data.

J. Butler, pp. 201-203. Neutron-absorbing bricks made from CaB_6.

Nucl. Sci. and Engng. 7, No. 4 (1960)

E. Gross, J. Marable, pp. 281-91. Static and dynamic multiplication factors, and their relation to the inhour equation.

T. Teichmann, pp. 292-94. Slowing down of neutrons.

W. Conkie, pp. 295-303. Velocity-dependent neutron transport theory.

W. Häfele, L. Dresner, pp. 304-12. Theory of the "softening" (diffusion cooling) of neutron spectra, for neutrons diffusing in homogeneous and heterogeneous media.

H. Russell, pp. 323-24. Isolation of carrier-free Mn^{54} and I^{125} from cyclotron targets.

P. Baker et al., pp. 325-26. Cyclotron targets using enriched stable isotopes.

F. Green, J. Martin, pp. 387-91. Maximizing production of radioisotopes in a cyclotron.

P. Aline et al., pp. 392-94. On the fast effect in beryllium.

Nucleonics 18, No. 6 (1960)

M. Thompson, pp. 133-40. How focusing collisions affect radiation damage.

Nukleonik 2, No. 3 (1960)

A. Özemre, pp. 100-105. Investigation of neutron beams created by introducing speed neutrons into a homogeneous breeding medium.

A. Kraut, pp. 105-128. Results of physical research on nuclear fission.

Nukleonika V, No. 1-2 (1960), Supplement 1

H. Niewodniczanski, J. Zakrzewski. Poland's first "big cyclotron."

Declassified and Approved For Release 2013/02/14 : CIA-RDP10-02196R000100060003-5

Declassified and Approved For Release 2013/02/14 : CIA-RDP10-02196R000100060003-5

II. NUCLEAR POWER ENGINEERING

Nuclear reactor theory and calculations. Reactor design. Performance of nuclear reactors and nuclear power stations.

Inzhener.-fiz. zhur. 3, No. 4 (1960)

V. S. Ermakov, pp. 127-31. Nonstationary temperature field in reactor fuel elements.

Inzhener. fiz. zhur. 3, No. 5 (1960)

O. I. Yaroshevich, pp. 81-85. Study of heat-transfer processes in fuel elements by hydraulic analog simulation.

V. S. Ermakov, pp. 115-18. Contribution to the question of a nonstationary temperature field in reactor fuel elements.

Tekhnol. sudostroeniya 1 (1960)

- - - - - - - - pp. 39-41. Building and launching of the icebreaker "Lenin."

A. K. Volkov, pp. 69-76. Contribution to the problem of steel weldments in atomic reactor design. (Survey of foreign literature).

V. P. Bogdanov, G. F. Kalashnikov, pp. 73-76. Nuclear-powdered shipbuilding economics. (Survey of the foreign literature).

Atomkernenergie V, No. 5 (1960)

H. Benzler, pp. 165-172. Reversal of coolant fuel in gas-cooled reactors.

Atomwirtschaft V, No. 5 (1960)

W. Finke, pp. 204-208. Contribution to the problem of nuclear fuel costs.

J. Armor et al., pp. 209-216. The "Latina," Italy's first nuclear electric power station.

Energia Nucleare 7, No. 5 (1960)

E. Torielli et al., pp. 333-41. Electronic analog for control of gas blowers in the Latina power station.

E. Diana et al., pp. 342-49. Calculating N^{16} formation in a "Latina" type reactor, by the Monte Carlo method.

Jaderná Energie VI, No. 6 (1960)

K. Barabas, pp. 188-191. On the economic feasibility of nuclear electric power stations.

V. Rýpar, pp. 192-99. Corrosion problems in CO_2-cooled power reactors.

Nucl. Energy 14, No. 145 (1960)

- - - - - - - - pp. 257-59. The PM-2A portable reactor designed for performance under Greenland arctic conditions.

C. Whelchel, C. Robbins, pp. 263-66. Use of rarefactions in nuclear power reactors.

Nucl. Engng. 5, No. 49 (1960)

B. Elthan, M. Cowper, pp. 243-44. Automatic shielding for a gas-cooled reactor.

A. Gray, pp. 245-48. Measurement of neutron flux at high temperatures.

- - - - - - pp. 264-65. Design of the Danish gas-cooled "Beta" reactor.

- - - - - - pp. 266-67. The American program for development of civilian nuclear reactors.

Declassified and Approved For Release 2013/02/14 : CIA-RDP10-02196R000100060003-5

Declassified and Approved For Release 2013/02/14 : CIA-RDP10-02196R000100060003-5

Nucl. Power 5, No. 50 (1960)

P. Bolt, pp. 97-99. Steam parameters for shipborne organic-moderated reactors.

----- pp. 116-17. Cleaning up heat-exchanger components.

R. Carstairs, M. Taylor, pp. 120-22. Behavior of a reactor radial eigenfunction.

Nucl. Sci. and Engng. 7, No. 4 (1960)

F. Hammitt, pp. 327-35. Problem of gaseous fission products in a circulating-fuel reactor.

K. Mochizuki, pp. 336-44. Analysis of neutron flux spatial oscillations resulting from xenon buildup in large power reactors.

D. Kottwitz, pp. 345-54. Thermal neutron spectrum in a medium with a temperature discontinuity.

G. Fischer, pp. 355-62. Measurements of neutron power spectrum in unmoderated assemblies.

H. Hummel, D. Meneghetti, pp. 363-68. Diffusion of intermediate-spectrum neutrons through a thick resonance absorber.

B. Finn, pp. 369-76. Relation between reactivity changes, buckling, and periods of a heavy-water reactor.

J. Newgard, M. Levoy, pp. 377-386. Nuclear rocket design.

Nucleonics 18, No. 6 (1960)

N. Palladino, H. Davis, pp. 85-116. Engineering design and power reactors in the USA.

E. Sowa, pp. 122-24. First TREAT results: meltdown tests of EBR-2 fuel.

Nukleonik 2, No. 3 (1960)

J. Engel, R. Schröder, pp. 88-90. Reactivity measurements in the Berlin BER reactor.

H. Märkl, pp. 90-100. Power and xenon concentration instability in a large heat power reactor.

Nukleonika IV, No. 6 (1959)

R. Pomerski, pp. 639-53. Perspectives for the development of nuclear power and possible changes in the cost of electric power generation.

Nukleonika V, No. 1-2 (1960)

E. Aleksandrowicz, pp. 1-21. The annual period of reactor performance, for the VVR-S type reactor in Poland (in Russian).

W. Frankowski, pp. 23-26. A facility for measuring burnup of fuel elements, without affecting the cladding.

III. NUCLEAR FUEL AND MATERIALS

Nuclear geology and primary ore technology. Nuclear metallurgy and secondary processing technology. Chemistry of nuclear materials.

Vestnik akad. nauk SSSR XXX, No. 5 (1960)

M. I. Yanovskii, G. A. Gaziev, pp. 27-31. A radiochromatograph for gases and liquids.

Geologiya rudnykh mestorozhdenii No. 2 (1960)

A. D. Kablukov, G. I. Vertepov, pp. 20-31. Scattering halos of elements near uraniferous ore bodies.

Declassified and Approved For Release 2013/02/14 : CIA-RDP10-02196R000100060003-5

Declassified and Approved For Release 2013/02/14 : CIA-RDP10-02196R000100060003-5

Geokhimiya No. 3 (1960)

E. S. Makarov et al., pp. 193-213. Crystal structure of uraninites and pitchblende.

G. B. Naumov, O. F. Mironova, pp. 241-246. Oxidation-reduction equilibrium in the uranium-iron system in a carbonate medium, and its significance in geochemistry.

Doklady akad. nauk SSSR 132, No. 2 (1960)

S. I. Danilevich, pp. 443-46. On the reliability of monazite ages determined by the uranium method.

Zhur. anal. khim. 15, No. 2 (1960)

V. F. Grigor'ev et al., pp. 184-190. Analytical chemistry of uranium. Bulletin No. 1. On the luminescent method of uranium determination.

Zhur. neorgan. khim. 5, No. 5 (1960)

L. P. Sokhina, A. D. Gel'man, pp. 1013-15. On the decomposition of oxalate complexes with plutonium bombarded by alpha radiation.

V. B. Shevchenko et al., pp. 1095-99. On a mechanism for the extraction of uranium VI from HCl solutions using tributyl phosphate.

Zapisy vsesoyuz. mineralog. obsh-va part 89, No. 2 (1960)

A. A. Chernikov et al., pp. 180-86. A uranium-bearing wulfenite.

Atomwirtschaft V, No. 5 (1960)

H. Ziehr, pp. 223-30. Helicopters in uranium prospecting.

Econ. Geol. 55, No. 3 (1960)

L. Hilpert, R. Moench, pp. 429-464. Uranium deposits in the south San Juan basin, New Mexico.

Energia Nucleare 7, No. 5 (1960)

E. Germagnoli, S. Granata, pp. 309-22. The behavior of vacancies in the lattice of pure metals.

L. Damiani et al., pp. 323-32. A pulsed liquid-extraction column. Part 1. Description and column performance.

E. Cerrai, F. Gazzarrini, pp. 358-360. Spectrophotometry of thorium and thoron in the presence of zirconium.

Jaderná Energie No. 6 (1960)

V. Zajíc, pp. 200-201. Specific heat and thermal conductivity of U_3O_8 powder.

Nucl. Energy 14, No. 145 (1960)

--- pp. 272-74. Fluorine compounds and nuclear energy. Part I. Production and applications of hydrogen fluoride.

--- pp. 276-82. Isotope production at Amersham.

Nucl. Engng. 5, No. 49 (1960)

G. Hanna et al., pp. 258-60. Beryllium processing in the laboratories of the Lucas Heights research center (Sydney, Australia).

--- pp. 261-63. Grenoble conference on plutonium metallurgy.

Nucl. Power 5, No. 50 (1960)

K. Saddington, pp. 92-96. Regeneration of fuel from civilian nuclear reactors.

E. Braithwaite, pp. 118-120. Colloidal graphitic lubricants.

A. Accary, P. Blum, pp. 122-23. Production and properties of uranium carbide.

Declassified and Approved For Release 2013/02/14 : CIA-RDP10-02196R000100060003-5

Declassified and Approved For Release 2013/02/14 : CIA-RDP10-02196R000100060003-5

Nucleonics 18, No. 6 (1960)

R. Flanders et al., pp. 126-27. Use of ammonium bifluoride as an etchant for Zircalloy.

Nukleonik 2, No. 3 (1960)

G. Eulitz, pp. 85-87. Separation of Pb, Ca, Sr, Ba, and Ra in a cation-exchange resin.

Nukleonika IV, No. 6 (1969)

W. Trzebiatowski et al., pp. 591-598. Reduction of uranium (IV) fluoride with molten aluminum in fused salts.

I. Złotowski, M. Zieliński, pp. 599-610. On some relationships between the mechanism of the $CO_{gas} \xrightarrow{I_2O_5} CO_2\ gas$ reaction and the kinetic isotope effect for C^{14}.

S. Zmysłowska, pp. 625-38. Use of a scintillation gamma spectrometer for the simultaneous determination of uranium, thorium, and potassium in rock and soil samples.

- - - pp. 665-681. VI congress of the Polish Chemical Society.

Nukleonika V, Nos. 1-2 (1960)

I. Złotowski, M. Zieliński, pp. 27-31. The isotope effect in the pyrolysis of $C^{14}H_3COONa$.

S. Minc, T. Bryl, pp. 33-45. Effect of light on the absorption spectrum of solutions of uranyl nitrate in tributyl phosphate.

S. Minc, W. Rafalski, pp. 47-53. Production of thorium metal by electrolysis from fused salts.

W. Korpak, K. Majchrzak, pp. 55-62. Uranium sorption from carbonate solutions, on the SM-x5 anion-exchange resin.

W. Korpak, Cz. Deptuła, pp. 63-71. The tri-n-butyl phosphate – solvent – HNO_3 – H_2O system.

W. Kołos, pp. 73-80. Reactivity of several ionized hydrocarbons.

IV. NUCLEAR RADIATION SHIELDING

Radiobiology and health physics. Shielding theory and shielding techniques. Instrumentation

Gigiena i sanitariya No. 4 (1960)

G. I. Bondarev, pp. 92-96. Foodstuffs irradiated by ionizing radiations, and their suitability for human consumption.

Izmerit. tekhnika No. 3 (1960)

B. Z. Votlokhin, pp. 38-39. Miniature radiometer with electric generator.

Inzhener.-fiz. zhur. 3, No. 4 (1960)

V. I. Kukhtevich et al., pp. 125-26. Dose characteristics of ionization chambers and scintillation crystals of large dimensions.

Med. radiologiya 5, No. 3 (1960)

V. S. Bubnov et al., pp. 61-64. Use of potassium bromide crystals in gamma dosimetry.

Declassified and Approved For Release 2013/02/14 : CIA-RDP10-02196R000100060003-5

Declassified and Approved For Release 2013/02/14 : CIA-RDP10-02196R000100060003-5

A. V. Terman, pp. 78-79. Use of radioactive tracers in health studies.

Priroda 49, No. 5 (1960)

L. P. Breslavets, Z. F. Mileshko, pp. 50-53. Shielding of plants from ionizing radiations.

Atomkernenergie V, No. 5 (1960)

U. Hagen, H. Langendorff, pp. 173-181. On the use of the "rem" unit of measurement in dosimetry.

D. Dunkel, pp. 183-87. On the use of ion-exchange resins to extract radioactive fission products from atmospheric fallout material.

Atomwirtschaft V, No. 5 (1960)

J. Seetzen, pp. 230-33. Nuclear reactor shielding.

H. Graf, pp. 235-38. International warning signs and symbols used in nuclear power operations.

Energia Nucleare 7, No. 5 (1960)

A. DeMatteis, P. Giacobbe, pp. 350-357. Use of the Monte Carlo method to study the physical characteristics of neutron detectors.

Industr. Health 21, No. 3 (1960)

C. Dunham, pp. 287-291. Ionizing radiations and industrial hygiene.

Jaderná Energie VI, No. 6 (1960)

F. Herčik, pp. 181-83. Biological action of radioactive carbon.

J. Čeřovsky, E. Malašek, pp. 184-187. Burial of contaminated laboratory equipment.

J. Walter Pollution Control Feder. 32, No. 2 (1960)

E. Tsivoglou et al., 262-87. Monitoring and radioactive contamination of the Animas River.

J. Walter Pollution Control Feder. 32, No. 5 (1960)

H. Krieger et al., pp. 495-504. Laboratory experiments on separation of fission products from nuclear fuel waste.

Nucl. Engng. 5, No. 49 (1960)

P. Barratt, pp. 251-254. Ionizing radiations and the design of electronic equipment.

P. Cavanagh, pp. 255-57. Direct-writing recorders for recording nuclear radiation pulses.

Nucl. Power 5, No. 50 (1960)

D. Taylor, pp. 110-114. Dosimetry instruments, 3.

--- p. 117. A new aluminum-base material for thermal neutron shielding.

Nucleonics 18, No. 6 (1960)

M. Campbell, pp. 118-19. Remote-controlled phase-separation bulb for radioactive sample analyses.

Nukleonika IV, No. 6 (1959)

T. Owczarski, pp. 655-63. Reliability of coincidence circuit arrangements in nuclear reactor scram systems.

Research XIII, No. 6 (1960)

P. White, S. Smith, pp. 228-233. Removal of radioactive particles from air.

Declassified and Approved For Release 2013/02/14 : CIA-RDP10-02196R000100060003-5

Declassified and Approved For Release 2013/02/14 : CIA-RDP10-02196R000100060003-5

V. RADIOACTIVE AND STABLE ISOTOPES

Tracer techniques. Use of radioactive radiations. Direct conversion of nuclear power to electric power

Doklady akad. nauk SSSR 131, No. 6 (1960)

A. N. Nesmeyanov, De Dyk Man, pp. 1383-85. Measurement of vapor pressure of solid chromium by the radioisotope method.

Izmerit. tekhnika No. 5 (1960)

M. I. Korsunskii et al., pp. 50-52. Use of radioisotopes to measure steam content.

Kauchuk i rezina No. 4 (1960)

A. Kh. Breger et al., pp. 17-22. Comparative estimate of the efficiency of various radiation sources for radiation vulcanization.

Narod. khoz. Kazakhstana No. 4 (1960)

R. Kaipov, pp. 85-87. Radioactive isotopes in the national economy of Kazakhstan.

Atomkernenergie V, No. 5 (1960)

H. Martin, pp. 187-201. Survey of recent Soviet research on the uses of radioactive isotopes.

Atomwirtschaft V, No. 5 (1960).

L. Wiesner, pp. 216-18. Use of nuclear physics techniques in oil prospecting and oil field exploitation.

Nucl. Power 5, No. 50 (1960)

B. Lindley, pp. 100-103. Direct conversion techniques.

Nucl. Sci. and Engng. 7, No. 4 (1960)

J. Gumbleton et al., pp. 313-319. Use of Fe^{59} to determine transient piston-ring wear in automotive engines.

F. Green, A. Somerville, pp. 320-322. Continuous count of gammas from hot radioactive liquids.

Nucleonics 18, No. 6 (1960)

C. Hill et al., pp. 130-33. Use of gamma absorption to measure barite content in a special lubricant.

D. Kniebes et al., pp. 142-47. Use of A^{41} to measure natural-gas flow.

Nukleonika IV, No. 6 (1959)

R. Broszkiewicz, pp. 611-24. Radioactive isotope applications in Poland during 1958.

Declassified and Approved For Release 2013/02/14 : CIA-RDP10-02196R000100060003-5

Declassified and Approved For Release 2013/02/14 : CIA-RDP10-02196R000100060003-5

2 outstanding new Soviet journals

KINETICS AND CATALYSIS

The first authoritative journal specifically designed for those interested (directly or indirectly) in kinetics and catalysis. This journal will carry original theoretical and experimental papers on the kinetics of chemical transformations in gases, solutions and solid phases; the study of intermediate active particles (radicals, ions); combustion; the mechanism of homogeneous and heterogeneous catalysis; the scientific grounds of catalyst selection; important practical catalytic processes; the effect of substance – and heat-transfer processes on the kinetics of chemical transformations; methods of calculating and modelling contact apparatus.

Reviews summarizing recent achievements in the highly important fields of catalysis and kinetics of chemical transformations will be printed, as well as reports on the proceedings of congresses, conferences and conventions. In addition to papers originating in the Soviet Union, KINETICS AND CATALYSIS will contain research of leading scientists from abroad.

Contents of the first issue include:

Molecular Structure and Reactivity in Catalysis. A. A. Balandin

The Role of the Electron Factor in Catalysis. S. Z. Roginskii

The Principles of the Electron Theory of Catalysis on Semiconductors. F. F. Vol'kenshtein

The Use of Electron Paramagnetic Resonance in Chemistry. V. V. Voevodskii

The Study of Chain and Molecular Reactions of Intermediate Substances in Oxidation of *n*-Decane. Z. K. Maizus, I. P. Skibida, N. M. Emanuél' and V. N. Yakovleva

The Mechanism of Oxidative Catalysis by Metal Oxides. V. A. Roiter

The Mechanism of Hydrogen-Isotope Exchange on Platinum Films. G. K. Boreskov and A. A. Vasilevich

Nature of the Change of Heat and Activation Energy of Adsorption with Increasing Filling Up of the Surface. N. P. Keier

Catalytic Function of Metal Ions in a Homogeneous Medium. L. A. Nikolaev

Determination of Adsorption Coefficient by Kinetic Method. I. Adsorption Coefficient of Water, Ether and Ethylene on Alumina. K. V. Topchieva and B. V. Romanovskii

The Chemical Activity of Intermediate Products in Form of Hydrocarbon Surface Radicals in Heterogeneous Catalysis with Carbon Monoxide and Olefins. Ya. T. Eidus

Contact Catalytic Oxidation of Organic Compounds in the Liquid Phase on Noble Metals. I. Oxidation of the Monophenyl Ether of Ethyleneglycol to Phenoxyacetic Acid. I. I. Ioffe, Yu. T. Nikolaev and M. S. Brodskii

Annual Subscription: $150.00

Six issues per year – approx. 1050 pages per volume

JOURNAL OF STRUCTURAL CHEMISTRY

This significant journal contains papers on all of the most important aspects of theoretical and practical structural chemistry, with an emphasis given to new physical methods and techniques. Review articles on special subjects in the field will cover published work not readily available in English.

The development of new techniques for investigating the structure of matter and the nature of the chemical bond has been no less rapid and spectacular in the USSR than in the West; the Soviet approach to the many problems of structural chemistry cannot fail to stimulate and enrich Western work in this field. Of special value to all chemists, physicists, geochemists, and biologists whose work is intimately linked with problems of the molecular structure of matter.

Contents of the first issue include:

Electron-Diffraction Investigation of the Structure of Nitric Acid and Anhydride Molecules in Vapors. P. A. Akishin, L. V. Vilkov and V. Ya. Rosolovskii

Effects of Ions on the Structure of Water. I. G. Mikhailov and Yu P. Syrnikov

Proton Relaxation in Aqueous Solutions of Diamagnetic Salts. I. Solutions of Nitrates of Group II Elements. V. M. Vdovenko and V. A. Shcherbakov

Oscillation Frequencies of Water Molecules in the First Coordination Layer of Ion in Aqueous Solutions. O. Ya. Samilov

Second Chapter of Silicate Crystallochemistry. N. V. Belov

Structure of Epididymite $NaBeSi_3O_7OH$. A New Form of Infinite Silicon–Oxygen Chain (band) $[Si_6O_{15}]$. E. A. Podedimskaya and N. V. Belov

Phases Formed in the System Chromium–Boron in the Boron-Rich Region. V. A. Épel'baum, N. G. Sevast'yanov, M. A. Gurevich and G. S. Zhdanov

Crystal Structure of the Ternary Phase in the Systems Mo(W)–Fe(Co,Ni)–Si. E. I. Gladyshevskii and Yu. B. Kyz'ma

Complex Compounds with Multiple Bonds in the Inner Sphere. G. B. Bokii

Quantitive Evaluation of the Maxima of Three-Dimensional Paterson Functions. V. V. Ilyukhin and S. V. Borisov

Application of Infrared Spectroscopy to Study of Structure of Silicates. I. Reflection Spectra of Crystalline Sodium Silicates in Region of 7.5-15μ. V. A. Florinskaya and R. S. Pechenkina

Use of Electron Paramagnetic Resonance for Investigating the Molecular Structure of Coals. N. N. Tikhomirova, I. V. Nikolaeva and V. V. Voevodskii

New Magnetic Properties of Macromolecular Compounds with Conjugated Double Bonds. L. A. Blyumenfel'd, A. A. Slinkin and A. E. Kalmanson

Annual Subscription: $80.00

Six issues per year – approx. 750 pages per volume

Publication in the USSR began with the May-June 1960 issues. Therefore, the 1960 volume will contain four issues. The first of these will be available in translation in April 1961.

(c/b) CONSULTANTS BUREAU 227 W. 17 ST., NEW YORK 11, N. Y.

Declassified and Approved For Release 2013/02/14 : CIA-RDP10-02196R000100060003-5

Declassified and Approved For Release 2013/02/14 : CIA-RDP10-02196R000100060003-5

RESEARCH by Soviet EXPERTS

Translated by Western Scientists

SPECTRA AND ANALYSIS

by A. A. Kharkevich

The first handbook directed toward acousticians and others working in those fields which require the analysis of oscillations—ultrasonics, electronics, shock and vibration engineering. This volume is devoted to the analysis of *spectral concepts* as they are applied to oscillations in acoustics and electronic engineering, and to a discussion of the methods of spectral analysis. Contents include KOTEL'NIKOV'S theorem for bounded spectra, the spectra and analysis of random processes, and (in connection with the latter) the statistical compression of spectra.

cloth **236 pages** **$8.75**

ULTRASONICS AND ITS INDUSTRIAL APPLICATIONS

by O. I. Babikov

This work is concerned with ultrasonic control methods which are applied in industry, and also with the action of high-intensity ultrasonic oscillations on various technological processes. Considerable attention is devoted to ultrasonic pulse methods of flaw detection and physicochemical research. It is an invaluable aid to scientific researchers, engineers, and technicians working in fields which make use of ultrasonic methods industrially, as well as being a convenient reference for a broad category of readers who might wish to become acquainted with the current state of ultrasonic instrumentation.

cloth **265 pages** **$9.75**

Tables of contents upon request

CONSULTANTS BUREAU

227 West 17th Street • New York 11, N.Y. • U.S.A.

Declassified and Approved For Release 2013/02/14 : CIA-RDP10-02196R000100060003-5